UNIVERSIDAD DISTRITAL
FRANCISCO JOSÉ DE CALDAS

Revista Ingeniería

Four-monthly scientific journal

2025

Volume 30 Issue 3 ISSN 0121-750X E-ISSN 2344-8393

REVISTA Ingeniería

Volume 30 • Issue 3 • Year 2025 • ISSN 0121-750X • E-ISSN 2344-8393

Four-monthly Scientific Journal

UNIVERSIDAD DISTRITAL
FRANCISCO JOSÉ DE CALDAS

Carrera 7 No. 40-53
Edificio Administrativo
Facultad de Ingeniería
Bogotá, Colombia
Correo revista:
revingenieria.ud@udistrital.edu.co

http://revistas.udistrital.edu.co/ojs/index.php/reving

Focus and Scope

The *Ingeniería* journal is an open-access academic-scientific online publication specialized in knowledge related to the fields of Engineering and Technology, according to the classification of scientific areas established by the Organization for Economic Cooperation and Development (OECD). Its main goal is to disseminate and promote debates about advances in research and development in the diverse areas of Engineering and Technology. We focus on disseminating original and unpublished articles in English that are relevant at both the national and international level. We seek to provide a platform to share knowledge and foster collaboration between researchers and professionals in the field. The journal does not request any Article Processing Charges (APC), as it is directly funded by Universidad Distrital Francisco José de Caldas. Moreover, the journal operates following a double-blind review process, thus ensuring the impartiality and quality of the published works. The journal is published in a continuous fashion and follows a quarterly numbering.

Open Access Policy

The *Ingeniería* journal provides free access to its content. This free access is granted under the principle of making research freely available to the public, which en-courages a greater exchange of global knowledge.

Article Processing Charges

No publication fees are charged to the authors or their institutions, nor are any payments made to expert peer reviewers or associate or adjunct editors. The *Ingeniería* journal is funded by Universidad Distrital Francisco José de Caldas, its Faculty of Engineering, and its Central Research Office.

Indexed in

Scopus
SciELO
Publindex Colombia Categoría B
Redalyc
Directorio Latindex
Fuente Académica Premier (EBSCO)
Applied Science & Technology Source Ultimate (EBSCO)
Emerging Sources Citation Index Bibliographic Bases (SC)
Fuente Académica Plus (EBSCO)
OpenAlex
Catálogo 2.0 Latindex
DOAJ
Dialnet
ROAD
Google Scholar Metrics
PKP Index
MIAR

Peer-reviewers in this issue

Braian Buitrago Uribe
Universidade do Minho, Portugal

Denis Moledo de Souza Abessa
Universidade Estadual Paulista, Brazil

Dibyendu Ghoshal
National Institute of Technology Agartala, India

Jesús Emilio Camporredondo-Saucedo
Universidad Autónoma de Coahuila, Mexico

Laura Bulgariu
Gheorghe Asachi Technical University of Iași, Romania

Maria Harja
Gheorghe Asachi Technical University of Iași, Romania

Mireia Faus
Universitat de València, Spain

Muhammad Luqman Hakim
Universitas Diponegoro, Indonesia

Nguyen Quoc Khanh Le
Taipei Medical University, Taiwan

Patrick A C Gane
Aalto University, Finland

Q. T. Doan
International Training Institute for Materials Science, Vietnam

Satyam Panchal
University of Waterloo, Canada

Song Ke
Wuhan University, China

Dewei Hu
University of Copenhagen, Denmark

Harikrishnan Ramiah
University of Malaya, Malaysia

Joon J. Song
Baylor University, United States

Luís M. O. Sousa
University of Trás-os-Montes and Alto Douro, Portugal

Mariya P. Aleksandrova
Technical University of Sofia, Bulgaria

Mohamad Shukri Zakaria
Universiti Teknikal Malaysia Melaka, Malaysia

Necati Alp Erilli
Sivas Cumhuriyet Üniversitesi, Turkey

Oscar Carranza
Instituto Politécnico Nacional, Mexico

Piotr Gorzelańczyk
Stanisław Staszic University of Applied Sciences in Piła, Poland

Sari Tuomikoski
University of Oulu, Finland

Socrates Basbas
Aristotle University of Thessaloniki, Greece

Verónica Pinos-Vélez
Universidad de Cuenca, Ecuador

Table of Contents

Editorial

Trends in Artificial Intelligence for Power Grid Automation from an Academic Viewpoint
José Guillermo Guarnizo Marín

Civil and Environmental Engineering

Analysis of Road Accidents in Colombia: Departmental Patterns and Trends from Vehicle Records
Karla Fernanda Mora Chacón, Cristian David Rosas López, Mariana Ulchur Ruíz

A Novel Rotational Limestone Treatment System for Effective Acid Mine Drainage Remediation
Cesar René Blanco Zúñiga, Laura Daniela Ulloa-Amador, Nicolás Rojas-Arias

Environmental Engineering

Use of Computational Tools in the Modeling of Columns for Cr(VI) Adsorption in Wastewater by Means of *Theobroma cacao L.*
Ángel D. González-Delgado, Ángel Villabona Ortiz , Candelaria Nahir Tejada Tovar

Mechanical Engineering

Two-Phase Mixture Numerical Study of Nanofluid Flow in a Lithium-Ion Battery Cooling System
Amina Benabderrahmane, Samir Laouedj

Electrical, Electronic and Telecommunications Engineering

Integration of Systemic and Participatory Approaches in Decision-Making for the Achievement of SDG 7 in Rural Areas
Diana Garcia Miranda, Francisco Santamaría Piedrahita, César Leonardo Trujillo Rodríguez, Marcel Castro Sitiriche

Experimental Performance of a Two-Stage Cross-Coupled MOS-Based Circuit in the Solar and Piezoelectric Energy Harvesting
JOYDEEP BANERJEE

Chemical, Food, and Environmental Engineering

Modeling a Fixed-Bed System with Coal Volatiles Post-Combustion for Ceramic Kiln Firing
Marco Antonio Ardila Barragán , Maria del Pilar Triviño Restrepo, Luis Fernando Lozano Gómez, Naren Natalia Ardila Otálora, Brigith Daniela Cruz Molina, Fabián Rolando Jiménez López, Alfonso López-Díaz, Jaime Alberto Riaño Villamizar

UNIVERSIDAD DISTRITAL
FRANCISCO JOSÉ DE CALDAS

Ingeniería

https://revistas.udistrital.edu.co/index.php/reving/issue/view/1295

DOI: https://doi.org/10.14483/23448393.24380

Editorial

Trends in Artificial Intelligence for Power Grid Automation from an Academic Viewpoint

José Guillermo Guarnizo Marín[1]*

[1] Assistant professor, Electronics Engineering Program, Universidad Distrital Francisco José de Caldas, Colombia. Researcher at the Alternative Energy Sources Research Laboratory (LIFAE). Electronic engineer, Master in Industrial Automation, PhD in Industrial Computing, Robotics, and Automation.

Electric power networks are interconnected systems entrusted with transforming, transmitting, and distributing electricity from generation points to the end user. Within this architecture, electrical substations perform the intermediate function of voltage transformation and help to ensure power quality through appropriate control and protection systems. Accordingly, they require automation technologies that enable the continuous monitoring, control, and protection of the infrastructure involved in these processes. Although there are international standards for grid-automation processes—most notably IEC 61850 for communications (1)—, current advances in artificial intelligence (AI) open a window of opportunity to enhance control responses to grid fluctuations.

From an academic perspective, these processes have undergone a notable evolution over the past four decades. In the 1990s, university research groups working on AI for the power sector focused on expert systems and fuzzy logic, aiming to build computational models that codified the empirical knowledge of substation technicians and other field personnel (2). The most common applications involved fault diagnosis, substation restoration, power control, and peak-load estimation in distribution systems.

In the 2000s, neural networks regained prominence and found varied applications in automation. Within power systems, they were trained on data from substations and grids for tasks such as load forecasting, fault diagnosis, and anomalous-event classification. This shift was enabled by the growing digitization of energy-infrastructure monitoring, which provided the necessary data to train detection and prediction models. For example, according to a report published by *Renewable Energy World* in September 2001, the number of projects involving automated meter reading installations in the United States grew by 40 % between 1999 and 2000 (3).

Editorial

* **Correspondence:** jgguarnizom@udistrital.edu.co

As of 2001, this translated into roughly 13.2 % of all meters served by AMR, with similar trends persisting throughout the decade.

Between 2010 and 2015, improvements in processing power and digital storage expanded data acquisition capabilities, increasing the volume of information available to train machine-learning models for power-sector applications. For example, in 2012, researchers at Columbia University presented a supervised learning approach to fault prediction using historical data from New York City (4). During this period, other studies focused on embedding neural networks into industrial controllers such as programmable logic controllers (PLCs), in order to enhance the on-device processing and interpretation of sensor data (5).

Building on the 2015 *Nature* article on deep learning by Yann LeCun, Yoshua Bengio, and Geoffrey Hinton (Nobel Prize in Physics, 2024) (6), researchers in the energy sector began exploring these methods in electric power grids. Notable lines of work included the optimal siting of electrical substations using aerial imagery, the training of high-capacity models for fault detection and anomalous-event classification, and intrusion detection in substation and grid communication networks.

Since 2021, and into the current decade, research on AI for the power sector has increasingly adopted hybrid models that fuse deep-learning techniques with physics-based or model-driven methods. Other lines of work combine multiple deep-learning architectures to enable real-time estimation, *e.g.*, inferring harmonic distortions from three-phase current and voltage measurements, as reported by researchers at the University of Johannesburg in 2023 (7). There has also been a marked rise in edge-computing approaches, wherein data are preprocessed locally before storage, monitoring, or cloud-level control, an evolution enabled by the broader deployment of smart meters. In the United States, the share of advanced meters rose from roughly 5 % in the late 2000s (≈4.7 % in 2007-2008) to 72.3 % in 2022, according to the Federal Energy Regulatory Commission's 2024 assessment.

AI continues to open meaningful avenues for improving automation across electric power networks by enhancing system-wide efficiency, reliability, and responsiveness. Key benefits include predictive maintenance, fault detection and diagnosis, and operations optimization, particularly at the substation level. However, widescale deployment still faces material hurdles: integration with existing—often legacy—systems, cybersecurity risks inherent to communications-connected infrastructures, and data quality and privacy constraints that affect both model training and dependable operation. These challenges create a timely opportunity for Colombian research groups in the energy sector to contribute from academia to the country's most ambitious objectives—most notably, a credible and sustained energy transition.

References

[1] M. Asim Aftab, S. Suhail Hussain, I. Al, and T. S. Ustun, "IEC 61850 based substation automation system: A survey," *Int. J. Elect. Power Energy Syst.*, vol. 120, art. 106008, 2020. https://doi.org/10.1016/j.ijepes.2020.106008 ↑1

[2] N. Mayadevi, S. VinodChandra, and S. Ushakumari, "A review on expert system applications in power plants," *Int. J. Elect. Comp. Eng. (IJECE)*, vol. 4, no. 1, pp. 116-126, 2014. http://dx.doi.org/10.11591/ijece.v4i1.5025 ↑1

[3] Clarion Energy Content Directors, "Electric utility AMR deployments on the rise," *Renewable Energy World*, September 1, 2001. [Online]. Available: https://www.renewableenergyworld.com/energy-storage/long-duration/electric-utility-amr-deployments-on-the-rise/ ↑1

[4] C. Rudin, D. Waltz, R. N. Anderson, A. Boulanger, A. Salleb-Aouissi, and M. Chow, "Machine learning for the New York City power grid," *IEEE Trans. Pattern Analysis Machine Intel.*, vol. 34, no. 2, pp. 328-345, 2012. http://hdl.handle.net/1721.1/68634 ↑2

[5] J. V. Fonseca and E. F. M. Ferreira, "Increase of PLC computability with neural network for recovery of faults in electrical distribution substation," presented at *IEEE Int. Instrum. Meas. Tech. Conf. (I2MTC)*, Minneapolis, MN, USA, 2013. https://doi.org/10.1109/I2MTC.2013.6555470 ↑2

[6] Y. LeCun, Y. Bengio, and G. Hinton, "Deep learning," *Nature*, vol. 521, pp. 436–444, 2015. https://doi.org/10.1038/nature14539 ↑2

[7] E. M. Kuyumani, A. N. Hasan, and T. Shongwe, "A hybrid model based on CNN-LSTM to detect and forecast harmonics: A case study of an Eskom substation in South Africa," *Elect. Power Comp. Syst.*, vol. 51, no. 8, pp. 746-760, 2023. https://doi.org/10.1080/15325008.2023.2181883 ↑2

UNIVERSIDAD DISTRITAL
FRANCISCO JOSÉ DE CALDAS

Ingeniería

https://revistas.udistrital.edu.co/index.php/reving/issue/view/1295

DOI: https://doi.org/10.14483/23448393.23475

Research

A Novel Rotational Limestone Treatment System for Effective Acid Mine Drainage Remediation

Un sistema novedoso de tratamiento rotacional de roca caliza para la remediación eficaz del drenaje ácido de minas

C.R. Blanco-Zúñiga[1], L.D. Ulloa-Amador[1], and N. Rojas-Arias[1,2,3]*,

[1]Universidad Pedagógica y Tecnológica de Colombia, Avenida Central del Norte 39-115 – PO Box 150001, Boyacá, Colombia
[2]School of Mechanical Engineering, University of Campinas, Rua Mendeley, 200, Campinas, SP, 13083-860, Brazil
[3]C.I. Hábitat a Vibe Company S.A.S. 110931, Bogotá, Colombia

Abstract

Context: The mining industry is the main culprit behind the generation of acid mine drainage (AMD). During coal extraction processes, sulfide minerals react with groundwater, releasing ions such as Fe^{2+} and Fe^{3+}, sulfates (SO_4^{-2}), and protonic acidity (H^+). The low pH of AMD can cause significant environmental damage. AMD remediation is usually achieved using alkaline systems, wherein the AMD passes through limestone to be neutralized. Nevertheless, this process requires prolonged treatment times and constant cleaning steps to remove the coating formed on the limestone, which reduces its effectiveness.
Method: This study evaluates a novel oxic-limestone rotational system for the treatment of AMD produced by the coal industry. The AMD collected was characterized in terms of pH, dissolved oxygen, Fe (Fe total, Fe^{2+}, and Fe^{3+}), and SO_4^{2-}.
Results: The results demonstrate the optimal efficiency of the proposed system, reducing the treatment time from 120 h in conventional systems to 1.5 h when applying a ratio of 0.25k g of limestone per liter of AMD.
Conclusions: The rotational system enables the superficial degradation of the limestone, maintaining an active contact area for longer periods. This allows for optimized AMD remediation efficiency, reducing operating costs and necessitating fewer system cleanup steps.

Keywords: coal mining, acid mine drainage, rotational system, superficial degradation

Article history

Received: Apr 10th, 2025

Modified: Jul 15th, 2025

Accepted: Sep 1st, 2025

Ing, vol. 30, no. 3, 2025, e23475

* **Correspondence:** nicolasr@unicamp.br

Resumen

Contexto: La industria minera es el principal responsable de la generación de drenaje ácido minero (DAM). Durante los procesos de extracción del carbón, los minerales sulfurados reaccionan con las aguas subterráneas, liberando iones como Fe^{2+} y Fe^{3+}, sulfatos (SO_4^{-2}), y acidez protónica (H^+). El bajo pH del DAM puede generar importantes daños medioambientales. La remediación del DAM generalmente se realiza a través de sistemas alcalinos, donde el DAM pasa a través de roca caliza para ser neutralizado. No obstante, este proceso requiere tiempos prolongados de tratamiento y etapas de limpieza constante para eliminar el recubrimiento formado en la roca, lo que reduce su eficacia.

Método: Este estudio evalúa un novedoso sistema rotacional de óxido-caliza para el tratamiento de DAM producido por la industria del carbón. El DAM recolectado se caracterizó en términos de pH, oxígeno disuelto, Fe (Fe total, Fe^{2+} y Fe^{3+}), y SO_4^{-2}.

Resultados: Los resultados demuestran la eficiencia óptima del sistema propuesto, que reduce el tiempo de tratamiento de 120 h con sistemas convencionales a 1.5 h al aplicar una relación de 0.25 kg de caliza por litro de DAM.

Conclusiones: El sistema rotacional facilita la degradación superficial de la caliza, manteniendo un área de contacto activa durante periodos más largos. Esto permite optimizar la eficiencia de remediación del DAM, reduciendo los costes de operación y las etapas de limpieza requeridas por el sistema.

Palabras clave: minería del carbón, drenaje ácido minero, sistema rotacional, degradación superficial

Table of contents

Page

1. Introduction 3
2. Experimentation 4
3. Static tests 4
   3.1. Dynamic tests using a rotational limestone system 4
4. Results 5
5. Discussion 6
6. Conclusion 11
7. Acknowledgments 11
8. Availability of data and materials 12
9. Declaration of competing interest 12
10. Author contributions 12
11. Use of artificial intelligence 12

Highlights

- A novel oxic limestone rotational drainage system for the treatment of AMD is proposed in this study.
- The rotational system promotes a superficial degradation of the limestone, increasing its activity for longer periods.

- The novel system improves the efficiency process, cutting AMD treatment time by 98.7 % over conventional static systems.

1. Introduction

The acid mine drainage (AMD) produced during mining activities is a polluting byproduct formed by the reaction between minerals, oxygen, and water (1). In the case of coal mining processes, AMD is characterized by a low pH and a high concentration of ions in the form of SO_4^{2-} , Fe^{2+}, and Fe^{3+}, produced by the oxidation of pyrite (FeS_2), in addition to other contaminating metal ions in lower proportions, such as Mn^{2+} and Al^{3+}, which are typical of AMD waste (2–5). The concentrations of these ions vary according to the geology of the area where the mining activity takes place (6).

In Colombia, the coal industry is one of the main mining activities, carried out mainly in the Boyacá region. This region contributes 38 % of the national coal production, which represents 3.087 million metric tons destined for use in the thermal and metallurgical sectors (7, 8). Coal mining operations in the area are not efficient, producing a high amount of pollutants that threaten nearby tributaries (9, 10). This problem is exacerbated by stormwater runoff, which can carry large amounts of AMD along with particulates and dissolved materials, substantially reducing the oxygen and nutrient content of the soil, as well as degrading aquatic systems and dependent biota (11, 12).

The application of systems such as aerobic wetlands and limestone drainage are potential alternatives that allow treating AMD (13, 14). The application of an active system (oxic) enables a higher rate of neutralization and removal of metal contaminants (15, 16). The high concentrations of SO_4^{2-} depend on the mineralogy of the place (17, 18), which makes water treatment difficult. Furthermore, the efficiency of open limestone channel (OLC) systems is compromised by the formation of gypsum ($CaSO_4 \cdot 2H_2O$) on the limestone surfaces, acting as a barrier that reduces its effectiveness during AMD treatment (19).

Similarly, optimal Fe removal values can be obtained using these systems (3). Nevertheless, these systems require continuous maintenance stages for their proper functioning, in addition to prolonged periods of fluid retention (20).

Considering the above, this study aims to evaluate the application of a novel rotational oxic limestone system to optimize AMD treatment processes. As a control mechanism, a non- moving device is used, called a *static system*. Tests were carried out in a controlled manner, using AMD samples collected from the area of interest. The authors did not find literature related to the evaluation of the effect of alkalization and the treatment of AMD using similar devices, which reinforces the novelty of this research.

2. Experimentation

The AMD used in this study was supplied by Cooperativa Agro-Minera (Coagromin Ltda.), located at Km 5 of the Paipa-Tunja road in Boyacá, Colombia. The AMD was later processed by adding limestone with a particle size between 1.27 and 2.54 cm. The limestone used was collected from Cantera Metrópolis, located at Km 6.6 of the Moniquirá-Arcabuco road (Boyacá). The limestone used in this study was analyzed via X-ray diffraction (XRD) in a Pananytical diffractometer (Co, $\lambda = 1.75$ Å). The analysis of the XRD pattern was carried out using the HighScore-Plus software, the Crystallography Open Database (COD), and the Inorganic Crystal Structure Database (ICSD).

3. Static tests

Static tests were performed on the system presented in Fig. **1**. The proposed system was isolated during the analysis period in order to avoid agitation, favoring a greater sedimentation and settling of the compounds that may be generated. The tests were conducted under controlled conditions, *i.e.*, at 2800 meters above sea level (m.a.s.l.), with a pressure of 740 hPa and an average temperature of 17 °C (21). The limestone:AMD ratio was 2.5:1 (in weight), ensuring the total coverage and reaction of the AMD. In this study, we evaluated the concentration of Fe ions (*i.e.*, Fe^{2+} and Fe^{3+}) and sulfates (SO_4^{2-}), considering that these are the main dissolved ions in AMD from coal mining processes due to the presence of pyrite (22). Therefore, other trace metals in AMD samples were not characterized. The tests were carried out until an optimal removal of Fe (total, Fe^{2+}, and Fe^{3+}) and SO_4^{2-} was achieved. Fe and sulfate measurements were taken using the FerroVer (iron reagent, Hach, USA) and SulfaVer IV (sulfate reagent, Hach, USA) reagents along with a DR6000 spectrophotometer (Hach, USA). The dissolved oxygen (DO) content was obtained from a Hach-Flexi HQ30d oximeter, and pH measurements were carried out using a SCOTT HandyLab pH11. Alkalinity was determined using 25 mL of undiluted AMD samples mixed with phenolphthalein and bromocresol green. The AMD sample was titrated with 0.02 N H_2SO_4 (*i.e.*, 10 mol·m^{-3}). Likewise, acidity was evaluated by adding phenolphthalein as an indicator solution. The mixture was also titrated with 0.02 N NaOH (*i.e.*, 20 mol·m^{-3}) (23).

3.1. Dynamic tests using a rotational limestone system

Dynamic tests were performed in a two-reactor rotational mechanical system. The vessel had an internal length of 30 cm and a diameter of 12 cm, containing a maximum volume of 3393 cm^3. The system was not operated at maximum capacity to preserve the functionality of the pressure gauges used to measure carbon dioxide (CO_2). We employed a vessel inclination of 6° and a rotation speed of 11 rpm. Although an angle of 10° is typically used, as has been reported by (3, 24, 25), we opted for a smaller inclination to ensure a greater retention of the liquid within the system. Fig. **1** shows a scheme of the devices used in this study. 0.25 kg of limestone were used for every 1 L of AMD (Limestone:AMD ratio of 0.25:1). The mixing process was carried out for 0.5, 1, and 1.5 h. pH. DO, alkalinity, acidity, Fe^{2+}, Fe^{3+}, and SO_4^{2-} measurements were made using the above-presented procedure.

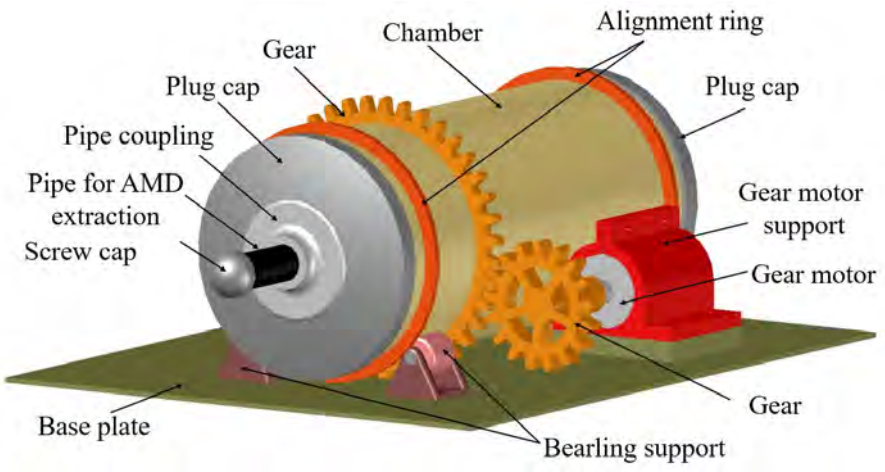

Figure 1. Schematic illustration of the AMD treatment device used in this study

4. Results

Fig. 2 shows the XRD pattern of the limestone used in this study. A semi-quantitative analysis, conducted using the Rietveld refinement method, revealed the presence of calcite—$CaCO_3$, space group $P_{121/c1}$ (14), ICSD 150 (26)—, which was the main mineralogical compound (73.2 %). Likewise, we observed the presence of dolomite—9.3 %, CaMg(CO3)2, $R\bar{3}H$ (148), ICSD 10404 (27)—, magnesite—0.5 %, $MgCO_3$, $R\bar{3}cH$ (167), ICSD 10264 (28)—, and silicates—17 %, mainly SiO_2, $P_{32}21$ (154), ICSD 16331 (29)—in a lower proportion. The composition of the limestone was similar to that found in other regions of Colombia, as reported by (30). A high content of carbonates in the limestone favors an optimal degree of alkalinity, as well as the limestone's ability to react with AMD (31). The presence of amorphous material can be observed in the first degrees of diffraction, which corresponds to organic material typical of sedimentary rocks.

Figs. 3 and 4 illustrate the behavior of the AMD when treated with a static and a rotational system, respectively. We followed the Colombian resolution no. 0631/2015 (32) to determine the efficacy of both systems. An initial characterization of the AMD is presented in Table I. Note that the values are outside the permissible values as per the aforementioned resolution, which was issued by the Colombian Ministry of the Environment and Sustainable Development.

Table I. Chemical characterization of the AMD sample used in this study and maximum permissible limit values for water resources linked to the extraction of coal and lignite according to Resolution 0631 of 2015 (32)

Parameter	Unit	This study	0631/2015 Legislation
pH	a.u.	2.5	6.0-9.0
DO	$mg{\cdot}L^{-1}$	7.09	-

Fe_{Total}	$mg{\cdot}L^{-1}$	228.75	2
Sulphates	$mg{\cdot}L^{-1}$	3300	1200
Acidity	$mg\ SO_4{\cdot}L^{-1}$	1180	analysis and report
Alkalinity	$mg\ CaCO_3{\cdot}L^{-1}$	0	analysis and report

5. Discussion

Limestone is an inexpensive, natural, and efficient raw material for the treatment of AMD from coal mining processes. Dolomitic limestone, *i.e.*, $CaMg(CO_3)_2$, is widely used within AMD systems due to its ease of reaction (33). Limestone reacts in the presence of hydrogen, enabling the release of carbonic acid, which can subsequently be converted into bicarbonate ions (3). The process is governed by the chemical reactions shown in Eqs. (1) and (2) (14,34). This dissociation generates a buffer effect within the system that maintains stable pH values during the formation of metal precipitates. The presence of bicarbonate ions and limestone also favors the removal of Fe, according to Eqs. (3) and (4) (35,36).

$$CaCO_3(s) + 2H^+ \leftrightarrow Ca^{2+} + H_2CO_3^0 \tag{1}$$

$$CaCO_3(s) + H_2CO_3 \leftrightarrow Ca^{2+} + 2HCO_3^- \tag{2}$$

$$Fe^{2+} + CaCO_3 \rightarrow Ca^{2+} + FeCO_3 \tag{3}$$

$$Fe^{2+} + HCO_3^- \rightarrow FeCO_3 + H^+ \tag{4}$$

A lower rate of acidity reduction in AMD after rotational treatment for 0.5 h may be due to the release of acidity (H^+) during the formation of siderite ($FeCO_3$). Nevertheless, part of the H+ produced can also react with the limestone, which generates CO_2, favoring carbonic acid formation (20,36).

$$2H^+ + CaCO_3 \rightarrow Ca^{2+} + H_2O + CO_2 \tag{5}$$

$$CO_2 + H_2O \leftrightarrow H_2CO_3 \tag{6}$$

Although the generation of acidity by hydrogen should lower the pH of the solution, it can also be slowed down when carbonic acids come into contact with the limestone, as shown in Eq. (1), as well as by the formation of CO_2 when reacting with part of the carbonic acids formed, *i.e.*,

$$HCO_3^- + H^+ \rightarrow CO_2 + H_2O \tag{7}$$

Likewise, the pH and alkalinity of the AMD can be leveled by the formation of passive layers of gypsum and siderite, which can be deposited on the surface of the limestone rock (Fig. 5). These precipitates act as a barrier that reduces the reactivity between the AMD and the rock (35,37). Calcium

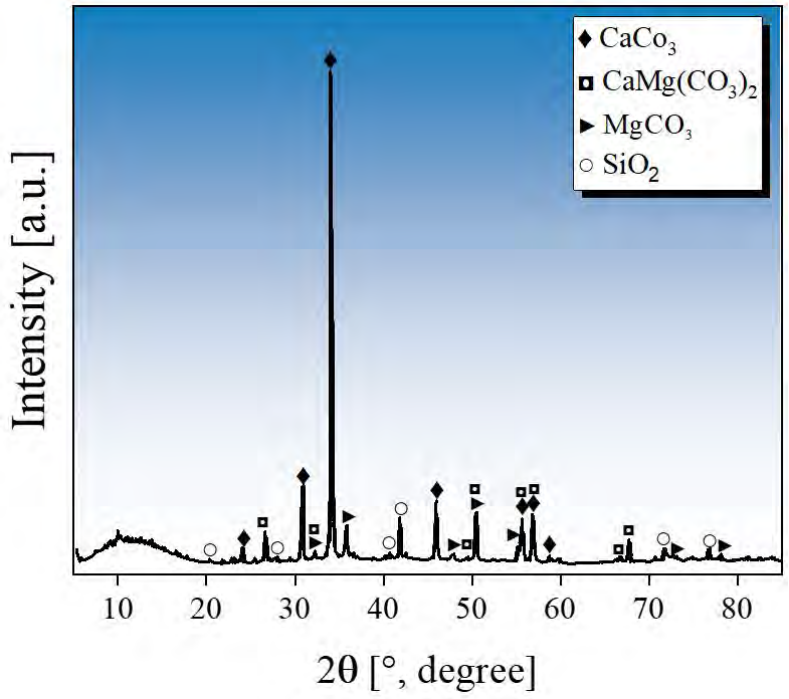

Figure 2. SXRD pattern of the limestone used in this study and collected in the region of Boyacá, Colombia

sulfate ($CaSO_4$) hydrates with two water molecules, forming gypsum ($CaSO_4{\cdot}2H_2O$). Based on a stoichiometric analysis, for every 136.14 g of anhydrite, 36.03 g of water are required to form 172.17 g of gypsum. Therefore, no significant reduction in the volume of water in the system is expected due to this reaction. The volume of gypsum formed may be regarded as negligible, since these are very thin layers deposited on the limestone, formed to mitigate the rock's activity.

$$CaCO_3 + SO_4^{2-} + 2H_2O \rightarrow CaSO_4 \cdot 2H_2O + CO_3^{2-} \tag{8}$$

$$CO_3^{2-} + Fe^{2+} \rightarrow FeCO_3 \tag{9}$$

The formation of these passive layers allows explaining the low efficiency of the AMD treatment when occurring in a static system, which is unable to remove the precipitates deposited on the limestone surface (35,38). Although the limestone:AMD ratio is ten times lower in the rotational system, the latter favors an autogenous grinding effect of the limestone (39), degrading the particles and removing the gypsum and siderite coatings.

The delay in Fe^{2+} removal may be due to the low reactivity of this ion to generate compounds other than siderite within the AMD, so it is highly dependent on their reactivity with limestone. A DO concentration greater than 0.5 $mg{\cdot}L^{-1}$ favors the reaction of Fe2+ ions with AMD (35,37,40). The difficulties in creating other compounds, *e.g.*, $Fe(OH)_2$, which is greenish, is impaired by the formation of limonite, $Fe(OH)_3$, from Fe^{3+}, which has a 5/8 10YR (Munsell Soil Color Chart (41)) color, as seen

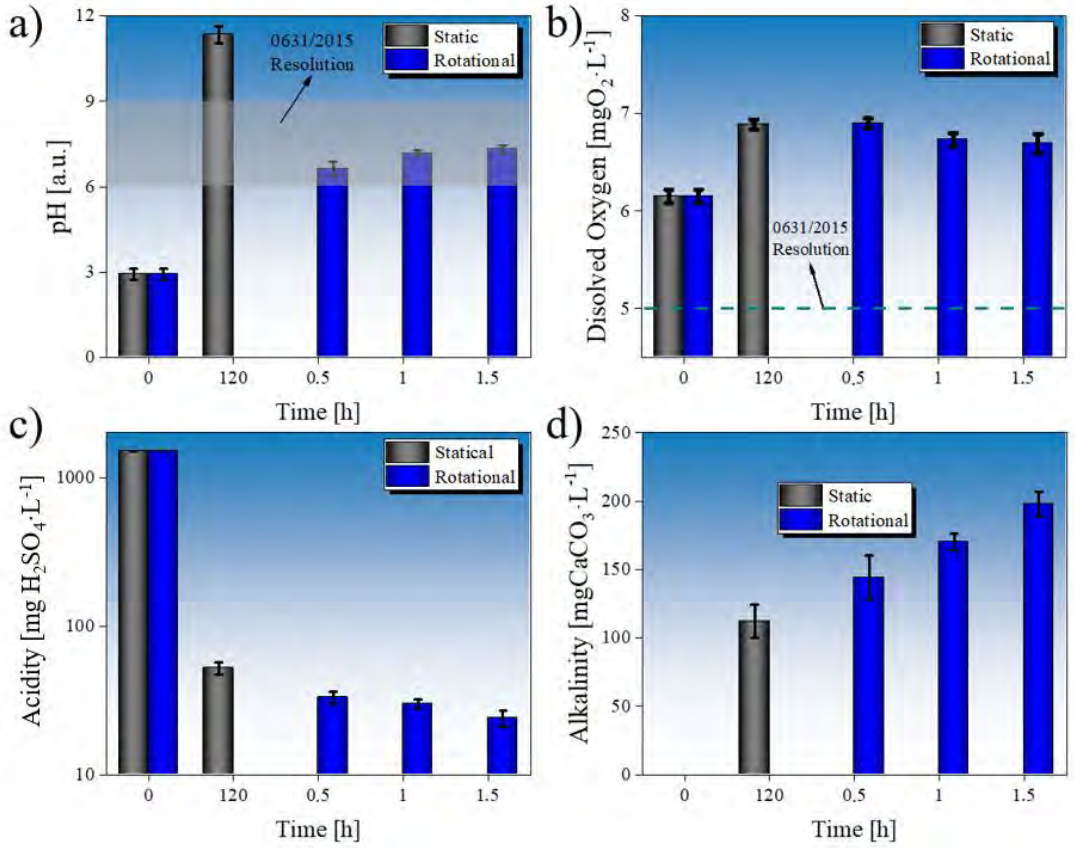

Figure 3. Values of a) pH, b) DO, c) acidity, and d) alkalinity for untreated and treated AMD in static and rotational systems. The pH and DO values obtained in this study were compared against those in resolution no. 0631/2015 for water quality (32)

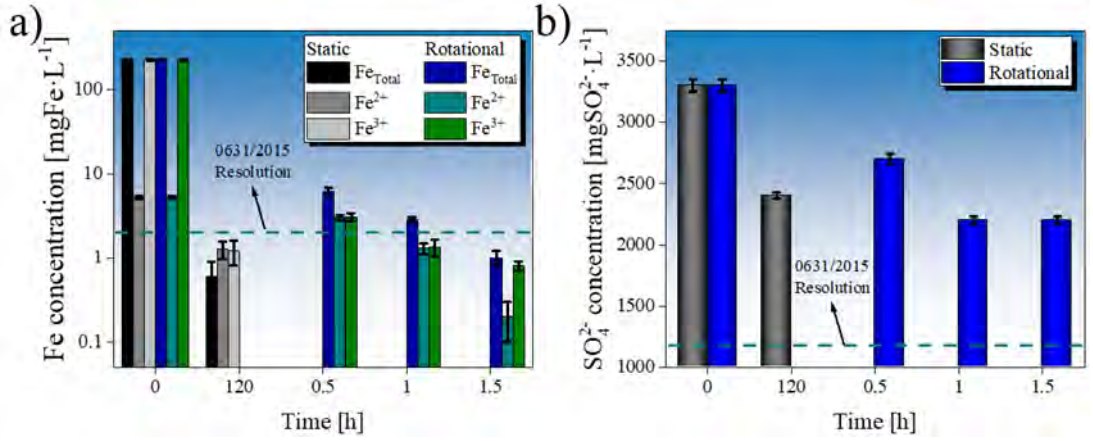

Figure 4. Concentration of a) Fe and b) sulfate ions in untreated and treated AMD after static and rotational treatment. The permissible values for pH and DO obtained in this study were compared against those in resolution no. 0631/2015 for water quality (32)

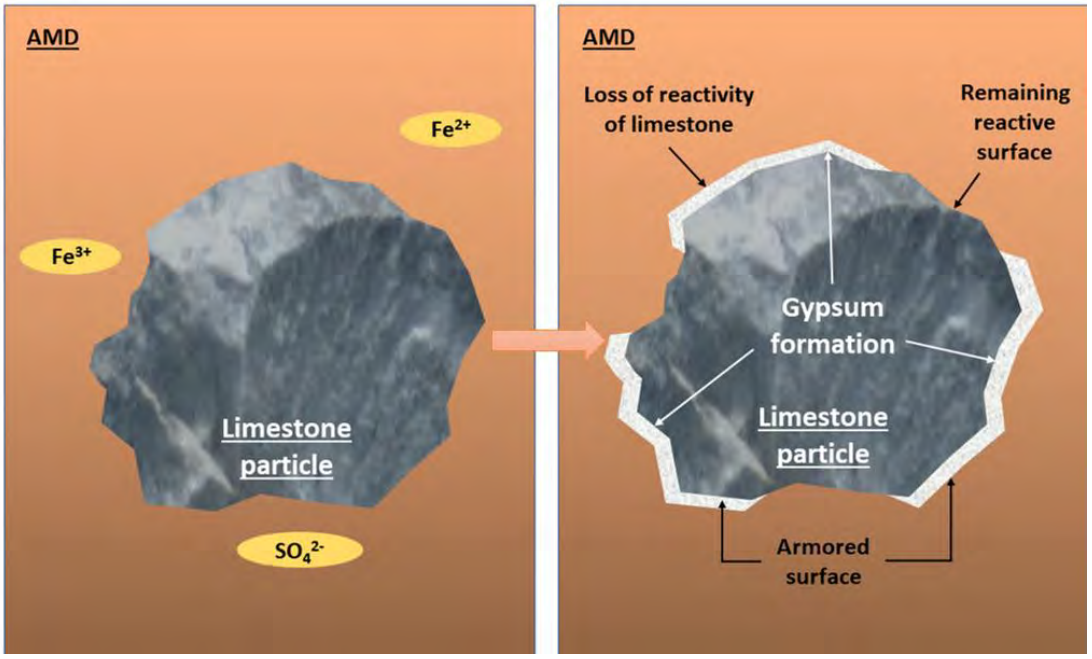

Figure 5. Schematic illustration of gypsum binder formation from the reaction between AMD and limestone

in Fig. 6. Likewise, the formation of $Fe(OH)_3$ is favored by pH values between 6.5 and 8 (42–45). Our measurement of the potential in the static and dynamic systems showed values between 0.1 and 0.15 V. As shown in Fig. 7, the final conditions obtained in this study favor the formation of the $Fe(OH)_3$ mineralogical phase.

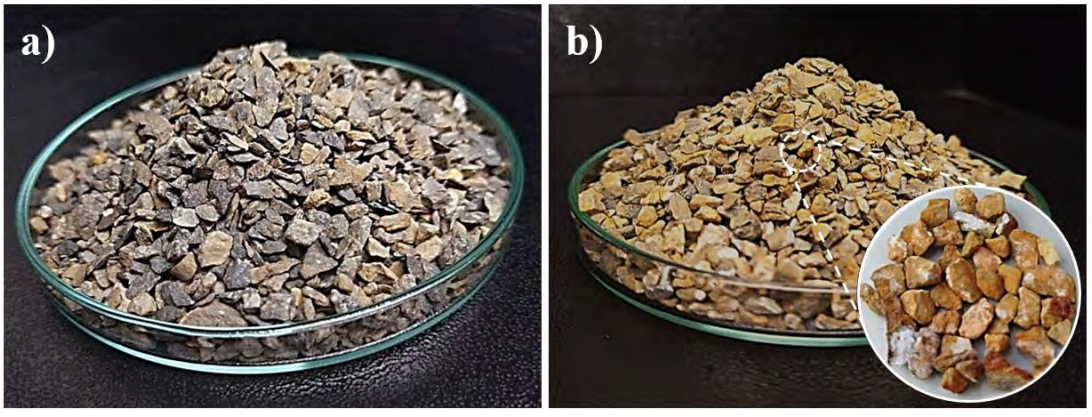

Figure 6. Photographs of the limestone samples used in this study a) before and b) after the AMD treatment. A change in the color of the limestone can be observed, which is due to the formation of precipitates on the rock surface

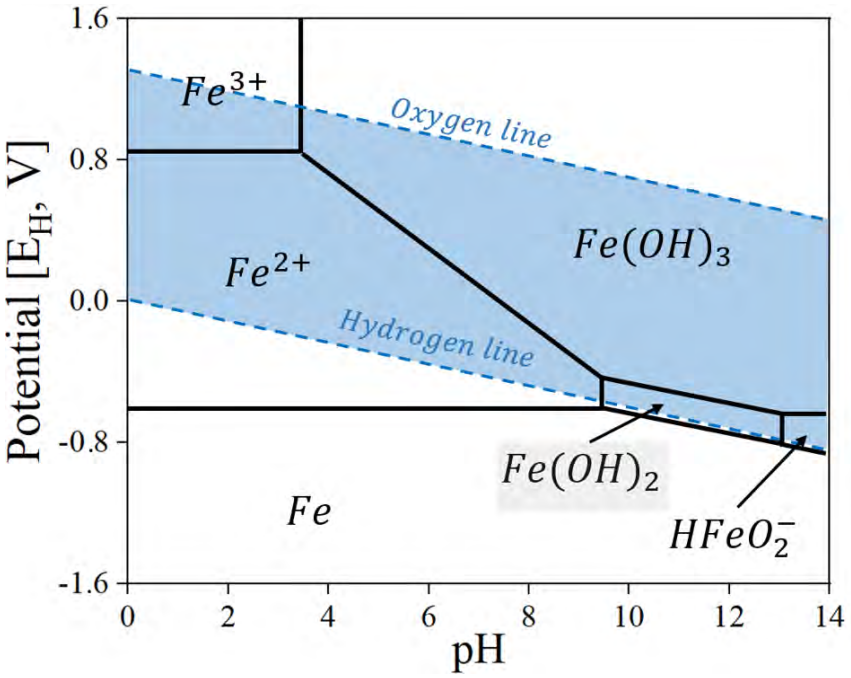

Figure 7. Generalized Pourbaix diagram for the Fe-H_2O system. The pH values obtained in this work show a greater tendency towards the formation of the $Fe(OH)_3$ phase

It has been reported that the Fe^{3+}/Fe^{2+} ratio present in leachate from coal minerals can favor biodesulfurization through the reaction of sulfate ions, allowing for the formation of pyrite and, subsequently, the iron (II) ($FeSO_4$) and iron (III) ($Fe_2(SO_4)_3$) sulfate phases (20, 46). A reduction of Fe^{3+} ions, in addition to the potential formation of gypsum precipitates adhered to the limestone surface, explains the blockage during sulfate removal from the AMD. Stagnation in the process of removing sulfate ions could be observed. This is because the increase in pH caused by the interaction between the limestone and the AMD inhibits the reactive capacity of the limestone particles with the sulfate and iron (II) ions, so their concentrations are generally not significantly affected (47). Although removal levels of 28 and 33 % were obtained for the samples treated in the static and rotational systems, respectively, it is necessary to apply secondary stages in order to comply with Colombian legislation. Even so, the application of a limestone system still exhibits an economic advantage compared to other technologies for the treatment of AMD and the removal of sulfates (35).

A system's operation must be evaluated based on its working time, as well as on the cost of the raw materials. The application of our rotational system in this affected region is facilitated by the ease of obtaining limestone. The authors express their motivation for the further development of this project, which can help to address the effects generated by mining activities in the region. The application of raw materials from the affected area and the construction of passive treatment systems allows for significant cost reductions.

While these systems can be used in other regions and for different types of AMD, it is necessary to consider that the effectiveness of the treatment depends on the characteristics and initial conditions of the raw materials, *i.e.*, the AMD and the limestone. In this study, the feasibility of this system was supported by the nearby availability of limestone. Therefore, when considering implementation in other affected areas, the costs of transporting limestone—as well as sustainability and logistical factors related to mining and transportation—must be considered.

During the AMD treatment, some residual materials were produced in the form of precipitates and clays. The chemical and toxic complexity of the waste generated currently precludes direct use in industrial activities due to the high risk of contamination associated with its release into the environment (48). The authors hope to conduct a feasibility analysis of the waste generated in subsequent studies, hoping to increase the sustainability of the proposal through new industrial products made from said waste.

6. Conclusion

This study evaluated the applicability of oxic-limestone drainage for the treatment of AMD and its effectiveness in the removal of Fe^{2+}, Fe^{3+} and SO_4^{2-} using a novel rotational system.

The application of a static system, which was used for comparison, required longer treatment times and yielded a lower ion removal efficiency compared to the rotational system. This was mainly due to the formation of precipitates that served as a barrier between the limestone and the AMD, hindering the system's ability to react due to a reduction in the active area of the limestone. This barrier cannot be directly removed within the static system. In contrast, the dynamic behavior of our proposed solution generates an autogenous grinding process that favors the removal, by wear, of the precipitates deposited in the limestone, thus maintaining a continuous active contact area between the limestone and the AMD. The inability to remove sulfate ions was due to the premature depletion of Fe^{2+} ions and the formation of precipitates adhering to the limestone surface, which slowed the chemical reactions generated during the treatment of the AMD.

The authors would like to express their interest in the application of this type of system for the treatment of AMD and other leachates generated during different industrial activities in the region, as well as in the application of new raw materials from the area that allow for optimized industrial water treatment.

7. Acknowledgments

The authors are grateful to the Engineering Department of Universidad Pedagógica y Tecnológica de Colombia and Cooperativa Agrominera Multiactiva de Paipa Ltda. (Cooagromin, Paipa-Boyacá, Colombia) for providing the raw material and resources necessary for the proper development of this

research. NRA would like to thank Conselho Nacional de Desenvolvimento Científico e Tecnológico do Brasil (CNPq, No. 408483/2022-9 and No. 383215/2024-2) for the financial support provided.

8. Availability of data and materials

Data presented in this study are available from the corresponding author upon reasonable request. Data is not publicly available because they pertain to ongoing research.

9. Declaration of competing interest

The authors declare that they have no known competing financial interests or personal relationships that could appear to have influenced the study reported in this paper.

10. Author contributions

C.R. Blanco-Zúñiga: conceptualization, methodology, validation, obtaining funds, writing (review and editing).
L. Ulloa-Amador: methodology, research, formal analysis, writing (review and editing).
N. Rojas-Arias: supervision, conceptualization, methodology, validation, writing (original draft, review, and editing).

11. Use of artificial intelligence

During this work, the authors did not employ any technologies associated with artificial intelligence.

References

[1] G. Naidu, S. Ryu, R. Thiruvenkatachari, Y. Choi, S. Jeong, and S. Vigneswaran, "A critical review on remediation, reuse, and resource recovery from acid mine drainage," *Environ. Poll.*, vol. 247, pp. 1110–1124, Apr. 2019. https://doi.org/10.1016/j.envpol.2019.01.085 ↑3

[2] H. E. Ben Ali, C. M. Neculita, J. W. Molson, A. Maqsoud, and G. J. Zagury, "Performance of passive systems for mine drainage treatment at low temperature and high salinity: A review," *Miner. Eng.*, vol. 134, pp. 325–344, Apr. 2019. https://doi.org/10.1016/j.mineng.2019.02.010 ↑3

[3] D. Silva, C. Weber, and C. Oliveira, "Neutralization and uptake of pollutant cations from acid mine drainage (amd) using limestones and zeolites in a pilot-scale passive treatment system," *Miner. Eng.*, vol. 170, art. 107000, Aug. 2021. https://doi.org/10.1016/j.mineng.2021.107000 ↑3, 4, 6

[4] J. S. Pozo-Antonio, I. Puente-Luna, S. L. López, and M. V. Ríos, "Tratamiento microbiano de aguas ácidas resultantes de la actividad minera: una revisión," *Tecno. Cien. Agua*, vol. 8, no. 3, pp. 75–91, 2017. https://doi.org/10.24850/j-tyca-2017-03-S05 ↑3

[5] I. Park *et al.*, "A review of recent strategies for acid mine drainage prevention and mine tailings recycling," *Chemosphere*, vol. 219, pp. 588–606, Mar. 2019. https://doi.org/10.1016/j.chemosphere.2018.11.053 ↑3

[6] I. Labastida, M. A. Armienta, R. H. Lara, R. Briones, I. González, and F. Romero, "Kinetic approach for the appropriate selection of indigenous limestones for acid mine drainage treatment with passive systems," *Sci. Total Environ.*, vol. 677, pp. 404–417, Aug. 2019. https://doi.org/10.1016/j.scitotenv.2019.04.373 ↑3

[7] D. M. Acosta-Bueno, "Impactos ambientales de la minería de carbón y su relación con los problemas de salud de la población del municipio de Samacá (Boyacá), según reportes ASIS 2005-2011," Specialization dissertation, Dept. Ed. Sci., Udistrital, Bogotá, Colombia, 2016. ↑3

[8] C. UPME, Ministerio de Minas y Energías, "Plan nacional de desarrollo minero con horizonte a 2025: Minería responsable con el territorio," 2017. [Online]. Available: https://www1.upme.gov.co/simco/PlaneacionSector/Documents/PNDM_Dic2017.pdf ↑3

[9] R. H. Garzón, "Minería del carbón en Boyacá: entre la informalidad minera, la crisis de un sector y su potencial para el desarrollo," *Zero*, vol. 33, no. 2344–8431, 2015. [Online]. Available: https://zero.uexternado.edu.co/mineria-del-carbon-en-boyaca-entre-la-informalidad-minera-la-crisis-de-un\-sector-y-su-potencial-para-el-desarrollo/ ↑3

[10] C. A. Agudelo Calderón, J. C. García-Ubaqie, R. Robledo Martínez, C. A. García-Ubaque, and L. Quiroz-Arcentales, "Evaluación de condiciones ambientales: aire, agua y suelos en áreas de actividad minera en Boyacá, Colombia," *Rev. Salud Púb.*, vol. 18, no. 1, pp. 50–60, Apr. 2016. https://doi.org/10.15446/rsap.v18n1.55384 ↑3

[11] A. L. Boyles *et al.*, "Systematic review of community health impacts of mountaintop removal mining," *Environ. Int.*, vol. 107, pp. 163–172, Oct. 2017. https://doi.org/10.1016/j.envint.2017.07.002 ↑3

[12] I. Moodley, C. M. Sheridan, U. Kappelmeyer, and A. Akcil, "Environmentally sustainable acid mine drainage remediation: Research developments with a focus on waste/by-products," *Miner. Eng.*, vol. 126, pp. 207–220, Sep. 2018. https://doi.org/10.1016/j.mineng.2017.08.008 ↑3

[13] L. E. Bertassello, P. S. C. Rao, J. Park, J. W. Jawitz, and G. Botter, "Stochastic modeling of wetland-groundwater systems," *Adv. Water Resour.*, vol. 112, pp. 214–223, Feb. 2018. https://doi.org/10.1016/j.advwatres.2017.12.007 ↑3

[14] C. Zipper, J. Skousen, and C. Jage, "Passive treatment of acid-mine drainage," Virgina Cooperative Extension, 2018. [Online]. Available: https://www.pubs.ext.vt.edu/content/dam/pubs_ext_vt_edu/460/460-133/CSES-216.pdf ↑3, 6

[15] H. L. Yadav and A. Jamal, "Removal of heavy metals from acid mine drainage: A review," *Int. J. New Technol. Sci. Eng.*, vol. 2, no. 3, pp. 77–84, 2015. ISSN 2349-0780. Available: https://www.ijntse.com/upload/1443503976hlyand%20ajamal%20sir%202015.pdf ↑3

[16] D. Bejan and N. J. Bunce, "Acid mine drainage: electrochemical approaches to prevention and remediation of acidity and toxic metals," *J. Appl. Electrochem.*, vol. 45, no. 12, pp. 1239–1254, Dec. 2015. https://doi.org/10.1007/s10800-015-0884-2 ↑3

[17] J. G. Skousen, P. F. Ziemkiewicz, and L. M. McDonald, "Acid mine drainage formation, control and treatment: Approaches and strategies," *Extr. Ind. Soc.*, vol. 6, no. 1, pp. 241–249, Jan. 2019. https://doi.org/10.1016/j.exis.2018.09.008 ↑3

[18] G. R. Watzlaf, K. T. Schroeder, and C. L. Kairies, "Long-term performance of anoxic limestone drains," *Mine Water Environ.*, vol. 19, no. 2, pp. 98–110, Sep. 2000. https://doi.org/10.1007/BF02687258 ↑3

[19] J. Skousen *et al.*, "Review of passive systems for acid mine drainage treatment," *Mine Water Environ.*, vol. 36, no. 1, pp. 133–153, Mar. 2017. https://doi.org/10.1007/s10230-016-0417-1 ↑3

[20] J. E. Santos Jallath, F. M. Romero, R. Iturbe Argüelles, A. Cervantes Macedo, and J. Goslinga Arenas, "Acid drainage neutralization and trace metals removal by a two-step system with carbonated rocks, Estado de Mexico, Mexico," *Environ. Earth Sci.*, vol. 77, no. 3, p. 86, Feb. 2018. https://doi.org/10.1007/s12665-018-7248-2 ↑3, 6, 10

[21] C. R. Blanco-Zuñiga, N. Rojas-Arias, L. Y. Peña-Pardo, M. E. Mendoza-Oliveros, and S. A. Martinez-Ovalle, "Study of the influence of clays on the transfer of dissolved oxygen in water," *Ingeniería*, vol. 26, no. 1, pp. 1–8, 2021. https://doi.org/10.14483/23448393.15846 ↑4

[22] Y. Bao, C. Guo, G. Lu, X. Yi, H. Wang, and Z. Dang, "Role of microbial activity in Fe(III) hydroxysulfate mineral transformations in an acid mine drainage-impacted site from the Dabaoshan Mine," *Sci. Total Environ.*, vol. 616–617, pp. 647–657, Mar. 2018. https://doi.org/10.1016/j.scitotenv.2017.10.273 ↑4

[23] E. W. Rice, R. B. Baird, and A. Eaton, *Standard methods for the examination of water and wastewater*, 23rd ed. Washington DC, USA: American Public Health Association, American Water Works Association, Water Environment Federation, 2017. https://yabesh.ir/wp-content/uploads/2018/02/Standard-Methods-23rd-Perv.pdf ↑4

[24] J. Skousen, A. Sexstone, K. Garbutt, and J. Sencindiver, "Wetlands for treating acid mine drainage," *Green Lands*, vol. 22, no. 4, pp. 31–39, 1992. ↑4

[25] P. F. Ziemkiewicz, J. G. Skousen, D. L. Brant, P. L. Sterner, and R. J. Lovett, "Acid mine drainage treatment with armored limestone in open limestone channels," *J. Environ. Qual.*, vol. 26, no. 4, pp. 1017–1024, Jul. 1997. https://doi.org/10.2134/jeq1997.00472425002600040013x ↑4

[26] L. Merrill and W. A. Bassett, "The crystal structure of CaCO3 (II), a high-pressure metastable phase of calcium carbonate," *Acta Crystallogr. B*, vol. 31, no. 2, pp. 343–349, Feb. 1975. https://doi.org/10.1107/S0567740875002774 ↑5

[27] P. L. Althoff, "Structural refinements of dolomite and a magnesian calcite and implications for dolomite formation in the marine environment," *Amer. Miner. J. Earth Planet. Mat.*, vol. 62, pp. 772–783, 1977. ↑5

[28] K. Dong, H. Morikawa, S. Iwai, and H. Aoki, "The crystal structure of magnesite," *Amer. Miner. J. Earth Planet. Mat.*, vol. 58, no. 11, pp. 1029–1033, 1973. ↑5

[29] H. d'Amour, W. Denner, and H. Schulz, "Structure determination of α-quartz up to 68 x 10$\hat{8}$ Pa," *Acta Crystallogr. B*, vol. 35, no. 3, pp. 550–555, Mar. 1979. https://doi.org/10.1107/S056774087900412X ↑5

[30] J. A. N. Carlos, B. Barrios, M. Lucia, M. Castro, and S. M. Arenas, "Prospectiva estratégica en los procesos de extracción y del beneficio de la roca caliza en el norte del Cesar, Colombia," *Rev. Agunkuya*, vol. 4, pp. 1–14, 2018. https://digitk.areandina.edu.co/server/api/core/bitstreams/d98c24ee-bd50-45b6-a541-cd80904882ce/content ↑5

[31] G. R. Watzlaf, K. T. Schroeder, and C. L. Kairies, "Long-term performance of anoxic limestone drains," *Mine Water Environ.*, vol. 19, no. 2, pp. 98–110, Sep. 2000. https://doi.org/10.1007/BF02687258 ↑5

[32] Ministerio de Ambiente y Desarrollo Sostenible, "Resolución 0631 De 2015. Diario Oficial No. 49.486 de 18 de abril de 2015," 2015. [Online]. Available: https://www.minambiente.gov.co/wp-content/uploads/2021/11/resolucion-631-de-2015.pdf ↑5, 8

[33] L. Bernier, M. Aubertin, A. M. Dagenais, B. Bussière, L. Bienvenu, and J. Cyr, "Limestone drain design criteria in AMD passive treatment: theory, practice and hydrogeochemistry monitoring at Lorraine Mine Site, Temiscamingue," CIM Minespace 2001 Québec, 2001. [Online]. Available: https://www.researchgate.net/profile/Louis-Bernier-3/publication/265411811_Limestone_Drain_Design_Criteria_in_AMD_Passive_Treatment_Theory_Practice_and_Hydrogeochemistry_Monitoring_at_Lorraine_Mine_Site_Temiscamingue/links/5757fc9e08aef6cbe3626507/Limestone-Drain-Design-Criteria-in-AMD-Passive-Treatment-Theory-Practice-\and-Hydrogeochemistry-Monitoring-at-Lorraine-Mine-Site-Temiscamingue.pdf ↑6

[34] L. N. Plummer, D. L. Parkhurst, and T. M. L. Wigley, "Critical review of the kinetics of calcite dissolution and precipitation," in *Chemical Modeling in Aqueous Systems*, New York, NY, USA: ACM, 1979, ACM Symposium Series, vol. 93, pp. 537–573. https://doi.org/10.1021/bk-1979-0093.ch025 ↑6

[35] W. A. M. Fernando, I. M. S. K. Ilankoon, T. H. Syed, and M. Yellishetty, "Challenges and opportunities in the removal of sulphate ions in contaminated mine water: A review," *Miner. Eng.*, vol. 117, pp. 74–90, Mar. 2018. https://doi.org/10.1016/j.mineng.2017.12.004 ↑6, 7, 10

[36] O. Aduvire, Drenaje acido de mina: generación y tratamiento. Madrid, Spain: Instituto Geológico y Minero de España Dirección de Recursos Minerales y Geoambiente, 2006. ↑6

[37] T. V. Rakotonimaro, C. M. Neculita, B. Bussière, T. Genty, and G. J. Zagury, "Performance assessment of laboratory and field-scale multi-step passive treatment of iron-rich acid mine drainage for design improvement," *Environ. Sci. Poll. Res.*, vol. 25, no. 18, pp. 17575–17589, Jun. 2018. https://doi.org/10.1007/s11356-018-1820-x ↑6, 7

[38] M. Jouini, T. V. Rakotonimaro, C. M. Neculita, T. Genty, and M. Benzaazoua, "Stability of metal-rich residues from laboratory multi-step treatment system for ferriferous acid mine drainage," *Environ. Sci. Poll. Res.*, vol. 26, no. 35, pp. 35588–35601, Dec. 2019. https://doi.org/10.1007/s11356-019-04608-1 ↑7

[39] B. A. Wills, "Grinding Mills," in *Mineral Processing Technology*, 4th ed. Amsterdam, Netherlands, Elsevier, International Series on Materials Science and Technology, 1988, ch. 7, pp. 253–308. https://doi.org/10.1016/B978-0-08-034937-4.50016-8 ↑7

[40] D. K. Nordstrom, D. W. Blowes, and C. J. Ptacek, "Hydrogeochemistry and microbiology of mine drainage: An update," *App. Geochem.*, vol. 57, pp. 3–16, Jun. 2015. https://doi.org/10.1016/j.apgeochem.2015.02.008 ↑7

[41] R. L. Pendleton and D. Nickerson, "Soil colors and special Munsell soil color charts," *Soil Sci.*, vol. 71, no. 1, pp. 35–44, 1951. ↑7

[42] E. Iakovleva, E. Mäkilä, J. Salonen, M. Sitarz, S. Wang, and M. Sillanpää, "Acid mine drainage (AMD) treatment: Neutralization and toxic elements removal with unmodified and modified limestone," *Ecol. Eng.*, vol. 81, pp. 30–40, Aug. 2015. https://doi.org/10.1016/j.ecoleng.2015.04.046 ↑9

[43] Y. Chai *et al.*, "Experimental study and application of dolomite aeration oxidation filter bed for the treatment of acid mine drainage," *Miner. Eng.*, vol. 157, art. 106560, Oct. 2020. https://doi.org/10.1016/j.mineng.2020.106560 ↑9

[44] J. Demchak, T. Morrow, and J. Skousen, "Treatment of acid mine drainage by four vertical flow wetlands in Pennsylvania," *Geochem. Explor. Environ. Analysis*, vol. 1, no. 1, pp. 71–80, Feb. 2001. https://doi.org/10.1144/geochem.1.1.71 ↑9

[45] F. Scholz and H. Kahlert, "The calculation of the solubility of metal hydroxides, oxide-hydroxides, and oxides, and their visualisation in logarithmic diagrams," *ChemTexts*, vol. 1, no. 1, p. 7, Mar. 2015. https://doi.org/10.1007/s40828-015-0006-0 ↑9

[46] H. A. Peláez Morales, M. C. Prada Fonseca, G. Caicedo Pineda, C. X. Moreno Herrera, and M. A. Márquez Godoy, "Influence of the initial relation of Fe3+/Fe2+ in the process of biodesulfuration of a coal sample solution," *Rev. Int. Cont. Amb.*, vol. 29, no. 2, pp. 2111–217, 2013. ISSN 0188-4999. Available: https://www.scielo.org.mx/pdf/rica/v29n2/v29n2a7.pdf ↑10

[47] C. A. Cravotta and G. R. Watzlaf, "Design and performance of limestone drains to increase pH and remove metals from acidic mine drainage," in *Handbook of Groundwater Remediation using Permeable Reactive Barriers*, Amsterdam, Netherlands: Elsevier, 2003, pp. 19–66. https://doi.org/10.1016/B978-012513563-4/50006-2 ↑10

[48] E. Azzali *et al.*, "Mineralogical and chemical variations of ochreous precipitates from acid sulphate waters (asw) at the Roşia Montană gold mine (Romania)," *Environ. Earth Sci.*, vol. 72, no. 9, pp. 3567–3584, Nov. 2014. https://doi.org/10.1007/s12665-014-3264-z ↑11

Cesar René Blanco Zúñiga, MSc.-Eng.

Civil engineer from Universidad Pedagógica y Tecnológica de Colombia, master's degree in engineering with an emphasis on the Environment (École de Technologie Supérieure, Montreal, Canada), Assistant Professor, School of Environmental Engineering, Universidad Pedagógica y Tecnológica de Colombia.
Email: cesar.blanco@uptc.edu.co

Laura Daniela Ulloa Amador, Eng. BSc

Environmental engineer from Universidad Tecnológica y Pedagógica de Colombia. She has worked on environmental impact assessment projects in the mining sector, promoting environmental awareness in

small-scale and subsistence mining. Her areas of interest include mining sustainability, the treatment of acid mine drainage, and the integration of renewable energies into environmental remediation processes.
Email: laura.ulloa@uptc.edu.co

Nicolás Rojas Arias, Dr.Techn.-Eng. BSc.

Metallurgical engineer and PhD in Science and Materials Engineering. Researcher specializing in mineral processing in extractive metallurgy—focusing on mining processes, radioactive source management, and process optimization—advanced manufacturing processes in the field of physical metallurgy, and materials design for engineering.
Email: nicolasr@unicamp.br

UNIVERSIDAD DISTRITAL
FRANCISCO JOSÉ DE CALDAS

Ingeniería

https://revistas.udistrital.edu.co/index.php/reving/issue/view/1295

DOI: https://doi.org/10.14483/23448393.23371

Research

Analysis of Road Accidents in Colombia: Departmental Patterns and Trends from Vehicle Records

Análisis de la siniestralidad vial en Colombia: patrones departamentales y tendencias a partir de registros vehiculares

Karla F. Mora Chacón[1], Cristian D. Rosas López[2]*, and Mariana Ulchur Ruíz[1]

[1]Civil Engineering, Universidad del Cauca, Colombia
[2]Professor of Department of Roads and Transportation, Universidad del Cauca, Colombia

Abstract

Context: The high rate of road accidents in Colombia constitutes a serious public health issue. This study seeks to identify spatial patterns in the occurrence of traffic accidents at the departmental level. Based on these data, the aim is to better understand the factors that influence road accidents in order to propose more effective prevention strategies.

Method: To this effect, a cluster analysis based on the K-means algorithm and binomial analysis was used. These statistical techniques allowed grouping Colombian departments according to their accident profile, considering variables such as geographical location, incidents, the validity of vehicle documents, and the presence of new road actors.

Results: The results of the analysis revealed three groups of departments with different accident rates: high, medium, and low. This classification makes it possible to identify regions with a higher risk of suffering road accidents and determine their associated factors, such as population density and road conditions. This study demonstrates the usefulness of cluster analysis to identify spatial patterns in road accidents at the departmental level.

Conclusions: The results obtained contribute to a better understanding of the factors that influence the occurrence of traffic accidents in Colombia, which enables the design of more focused and effective prevention strategies. Future research could delve into the analysis of the socioeconomic and cultural factors associated with road accidents, in addition to exploring the application of predictive models to anticipate the occurrence of accidents.

Keywords: accident rate, vehicles, traffic, binomial analysis, road safety, clusters

Article history

Received: Mar 20th, 2025

Modified: May 9th, 2025

Accepted: Aug 5th, 2025

Ing, vol. 30, no. 3, 2025, e23371

* **Correspondence:** cdrosas@unicauca.edu.co

Resumen

Contexto: La alta accidentalidad vial en Colombia constituye un serio problema de salud pública. Este estudio busca identificar patrones a nivel departamental en la ocurrencia de accidentes de tránsito. Con base en los datos de accidentalidad, se busca comprender mejor los factores que influyen en los sucesos para proponer estrategias de prevención más efectivas.

Método: Se utilizó un análisis de conglomerados basado en el algoritmo K-medias y un análisis binomial. Estas técnicas estadísticas permitieron agrupar los departamentos colombianos según su perfil de accidentalidad, considerando variables como: la ubicación geográfica, los incidentes, la validez de los documentos vehiculares y la presencia de actores viales.

Resultados: Los resultados del análisis mostraron tres grupos de departamentos con diferentes tasas de accidentalidad: alta, media y baja. Esta clasificación permite identificar las regiones con mayor riesgo de sufrir accidentes viales y determinar los factores asociados, como la densidad poblacional y el estado de las carreteras. Este estudio demuestra la utilidad del análisis de conglomerados para identificar patrones de comportamiento espacial en accidentalidad vial a nivel departamental.

Conclusiones: Los resultados obtenidos contribuyen a una mejor comprensión de los factores que influyen en la ocurrencia de accidentes de tránsito en Colombia, lo que permite diseñar estrategias de prevención específicas y eficaces. Futuras investigaciones podrían profundizar el análisis, con factores socioeconómicos y culturales asociados a los accidentes de tránsito. Además, de explorar la aplicación de modelos predictivos para anticipar la ocurrencia de accidentes.

Palabras clave: accidentalidad, vehículos, tráfico, análisis binomial, seguridad vial, conglomerados

Table of contents

Page

1. Introduction 2
2. Methodology 5
   - 2.1. Location 5
   - 2.2. Equations 8
3. Results 8
4. Discussion 15
5. Conclusions 18
6. Limitations of this work 19
7. Lines of research 19
8. Author contributions 20
9. Funding 20
10. Data availability 20
11. Conflicts of interest 20
12. Use of artificial intelligence 20

1. Introduction

According to the National Road Safety Agency (1), the main causes of traffic accidents in the country are excessive speed (42.91 %), failure to obey traffic signals (32.51 %), and driving under the influence of alcohol (4.94 %). These factors pose a significant risk to road safety and highlight the need to strengthen control and prevention strategies regarding mobility.

According to (2), five risk factors associated with traffic accidents have been identified, among which driving under the influence of alcohol, excessive speed, and the lack of protective systems (*e.g.*, helmets and seat belts) stand out. The same study reports that, in 2002, out of 6063 traffic-related deaths in Colombia, 39 % involved pedestrians, 19 % involved passengers, and 15 % involved motorcyclists. Additionally, 75 % of these accidents involved men, indicating that the male gender has been the most affected. This trend has remained consistent over time.

The analysis of accident rates in the context of risky and aggressive driving behaviors, as presented in the study by (3), reveals that factors such as age and gender significantly impact traffic accident rates. The results indicate that men and young drivers tend to exhibit riskier driving behaviors, which are associated with a higher likelihood of accidents. This study underscores the importance of identifying and addressing these behaviors to improve road safety.

In a different context, the study by (4) in Neiva, Colombia, examines the road infrastructure and its relationship with urban traffic accidents. The findings indicate that factors such as vehicle type, time of day, and road infrastructure characteristics play a crucial role in accident frequency, with motorcyclists being the most vulnerable victims. Combining these studies highlights the relevance of both driver behavior and road infrastructure in preventing traffic accidents, suggesting that improving road safety requires interventions targeting both driver conduct and infrastructure improvements.

Additional important factors, such as location, the lack of road safety systems for drivers, and road infrastructure conditions, contribute to a higher incidence of traffic accidents in certain areas (5). Likewise, studies such as that of the Colombian Safety Council (6) have shown that road conditions are a determining factor in the occurrence of accidents, as they influence both driver behavior and vehicle performance. In this context, geographic location and driving behavior play a significant role (7).

In an article on how black spots can significantly improve road safety, (8) argue that this is a key aspect in analyzing road safety. Addressing these areas, where most accidents occur, helps to reduce the likelihood of their recurrence. Moreover, in a broader sense, this approach could not only identify specific black spots, but also reveal 'black departments', or regions characterized by high accident rates. This may be influenced by multiple factors such as vehicle flow, the mandatory traffic accident insurance (SOAT), driver's licenses, and vehicle registrations, among other elements that contribute to this phenomenon. In 2023, the Colombian government implemented various initiatives aimed at strengthening driver capabilities and improving road safety. These actions align with the objectives of the Decade of Action for Road Safety. The Ministry of Transport's territorial programs (9) and the Global Plan for Road Safety 2021-2030 (10) prioritize the improvement of road infrastructure as a key measure to reduce traffic-related fatalities, with projections extending to the year 2030 (11).

Research in the field of road safety has advanced significantly due to the development of statistical models and machine learning techniques. Studies such as those by (12) and (13) have demonstrated the usefulness of these models in identifying patterns in accident data and assessing the impact of various

risk factors. By analyzing variables such as vehicle type, traffic flow, and road characteristics, these models enable the development of more effective strategies for accident prevention and road safety improvement.

The studies by (14) and (15) address issues related to traffic accidents in Colombian urban contexts, emphasizing the importance of identifying high-risk points to enhance road safety. In the case of Tunja, (14) applied spatial analysis, using geoprocessing techniques and kernel density estimation to identify risk-prone areas based on accident concentration while considering socio-spatial variables such as land use and traffic flows. This approach helps to delineate zones with a high probability of accidents, offering a useful framework for planning and managing road safety in urban areas. On the other hand, (15) focused on Ibagué, determining that, aside from factors such as mechanical failures and recklessness, decision-making errors at critical points like roundabouts significantly contribute to accident rates. Both studies agree on the need for an integrated approach to road risk management, incorporating both infrastructure and driver behavior to reduce accidents and improve public safety.

According to (16), the K-means and K-medoids algorithms are widely used in partition- based clustering techniques. These algorithms form clusters based on their centers, but they require the number of clusters (k) to be specified beforehand. To determine this optimal number, it is essential for the user to have adequate knowledge of the application dataset, as the value of k depends on the specific characteristics of the data. There are various methods for identifying the correct number of clusters, including the rule of thumb, cross-validation, the elbow method, information-based criteria, and the core matrix. However, most of these approaches require clustering beforehand in order to estimate the appropriate number of clusters.

According to the study by (17), which was conducted in a hospital in Metropolitan Lima during the COVID-19 pandemic, a significant increase in occupational accidents was observed during the pandemic. These included crush injuries, assaults, internal trauma, sprains, and fractures, notably impacting the lumbosacral region and fingers. This rise highlights the risks faced by healthcare workers during a public health crisis. In contrast, the work by (18) on the handling of traffic accident data in Brazil demonstrates how information can be effectively managed by integrating multiple databases. This process, implemented in five pilot capitals of the Vida no Transit project, enabled the creation of a unified victim list and the reclassification of accidents as severe or fatal. The results showed a significant increase in the number of recorded victims, emphasizing the importance of accurate data for planning and evaluating road safety actions. Although they address different contexts (occupational and traffic accidents), both studies agree on the importance of data collection and analysis to understand and mitigate risks in various domains. They suggest that improving safety requires integrating effective information systems and making decisions based on reliable data.

Furthermore, (19) analyzed factors affecting traffic accidents in Cartagena, Colombia, using a geographic information system (GIS) and a Bayesian approach. They identified 69 sections with a high propensity for accidents, noting that motorcycles have a higher accident rate than cars, and

that commercial areas experience more accidents due to the high presence of pedestrians. The study by (20) compared the adjusted traffic accident mortality rates (TAMR) in Colombia, Spain, and the United States, highlighting that Colombia has higher rates due to its lesser development in road safety. However, the European guidelines implemented by Spain have contributed to a reduction in mortality rates, whereas the United States demonstrates limited adherence to international guidelines, which also affects its TAMR.

As for developing countries, the analysis by (21) highlights Colombia's progress in adopting regulations to improve road safety. Nevertheless, despite recent legislative efforts, the country still faces significant challenges in enforcing and ensuring the effectiveness of these measures. This reflects the general situation in developing nations, where implementing road safety policies remains a priority.

After conducting a literature review, we determined that the factors with the most significant influence on road accidents are those provided by the National Road Safety Agency (ANSV). Therefore, this research aimed to find solutions to traffic safety problems by addressing questions such as: Do vehicle registration data influence accident rates? Is it possible to predict accidents based on the analysis of this data? and Is it feasible to classify accident-prone zones by department using this information? In line with these questions, the research objectives were firstly, to demonstrate the influence of vehicle registration records on road accident rates; secondly, to demonstrate the importance of analyzing variables in understanding road accidents and how they affect road behavior; and finally, to identify critical accident zones based on available information and analyze how these affect road safety in their corresponding regions.

2. Methodology

2.1. Location

Fig. **1** shows the geographical distribution of Colombia's 32 departments, serving as a fundamental reference for territorial and regional analysis. This spatial context is essential for identifying accident-prone areas and understanding regional differences regarding road safety. This map supports the examination of factors such as traffic flow, infrastructure, and administrative divisions. It provides the basis for targeted strategies aimed at reducing road accidents across the country.

The research methodology was structured in three main phases, as illustrated in Fig. **2**: database construction and segmentation, cluster center analysis, and the accident prediction model for improving road safety in Colombia. To conduct an analysis of accidentality based on a cluster distribution, various methods were employed to segment the data according to their characteristics and behavior. The criteria for segmentation were dictated by the distance between the data points. Grouping was executed using the K-means method, one of the most commonly utilized techniques for the specific purpose of data clustering (23).

Figure 1. Map with the 32 departments of Colombia

Source: (22)

This cluster analysis method aims to classify data related to a specific study, facilitating the formation of groups with a higher level of identification. This process is executed through the approximation of distance matrices, which are developed according to specific criteria (24). This method seeks to unite similar elements, providing solutions for addressing challenges related to pattern clustering, decision-making, data mining, and machine learning, among others. Conceptually, it deals with the representation of patterns, evaluates similarities, performs grouping, and ultimately aids in visualizing the resulting clusters (25).

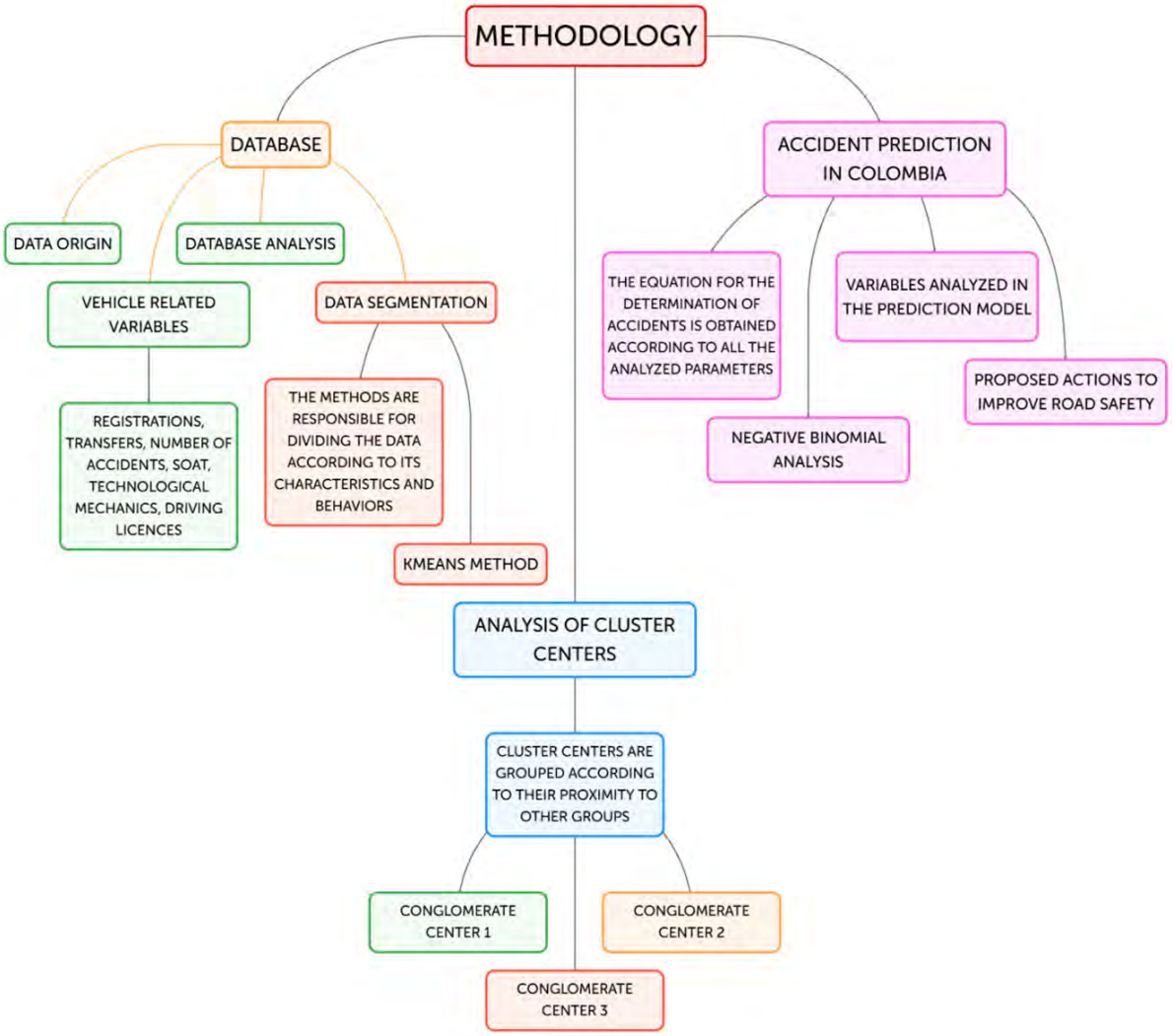

Figure 2. Methodology

The database utilized in this study was obtained from the National Single Traffic Registry (RUNT) and the ANSV. These data were essential for the efficient consolidation and distribution of vehicle-related variables, including registrations (the official identification records of vehicles, comprising a unique combination of letters and numbers), transfers (the formal process of transferring vehicle ownership), the number of fatal accidents (the total number of accidents resulting in the loss of human lives), the SOAT (the mandatory traffic accident insurance, covering medical expenses for victims), technical inspections (mandatory reviews ensuring compliance with safety and emissions standards), and driver's licenses (official documents authorizing individuals to operate vehicles on public roads after passing the required examinations). Based on these variables, an analysis was conducted in order to determine the distribution of the 32 departments in Colombia, following a data normalization process that incorporated population figures from the 2018 census conducted by the National Statistics Department (DANE).

2.2. Equations

To conduct this type of analysis, it is essential to determine the number of clusters into which the data will be divided. Consequently, it is necessary to normalize the data in order to ensure that all groups are on equal footing (26). In this work, the K-means method was employed for group separation (27). This method groups the data's spatial position and their distance to a random point within an iterative process directed by Eq. (2). The proposed process includes: (i) assigning a random position to each element (speed profile), (ii) calculating the distance of each element and grouping those with similar values according to Eq. (1), (iii) calculating the group center location using Eq. (2), and (iv) iterating between steps (iii) and (iv) until the sum of the distances of the elements is minimized, as evaluated via Eq. (3) (28).

$$\sum_{i=1}^{n} \left| D\big(X_{i+1}, C_j(k)\big) - D\big(X_i, C_j(k)\big) \right|^2 \tag{1}$$

$$C_j(r+1) = \frac{1}{n} X_i^{(j)} \tag{2}$$

$$E(r+1) = \sum_{i=1}^{k} \sum_{w \in W} |w - C_j(r+1)|^2 , \tag{3}$$

where n is the number of iterations, k the number of clusters, $C_j(n)$ the cluster center for $j = 1, 2, \ldots, k$; $D(X_{i+1}, C_j(k)$ the distance for $i = 1, 2, \ldots, k$; and Wj the cluster center. The result of this process assigns a value $(1, 2, 3, \ldots, n)$ to each analyzed speed profile, indicating the cluster to which it was assigned.

3. Results

This section provides a detailed overview of the results obtained from the analyzed methodological procedures.

Table I presents data related to the 32 departments of Colombia and their vehicular records, including registrations, transfers, SOAT, and technical-mechanical inspections. These descriptive statistics characterize the sample to facilitate grouping based on accidentality.

Table II presents the classification of the departments according to their population, which was normalized based on the analysis using the K-means method. This was complemented with a distribution selected through predefined criteria. Through this analysis, each department was assigned to one of three groups (1, 2, or 3). Subsequently, the incidence of accidents within each group was evaluated and classified as high, medium, or low, according to the criteria established in this study.

Fig. 3 presents the distribution of the 32 departments of Colombia, comprising three clusters based on the number of accidents for every 100 000 inhabitants in 2022 and 2023. The departments are represented by colored points, with each cluster identified by a specific color and number, providing an

overview of the spatial distribution of accidents in Colombia. Note that the departments with a higher number of accidents are concentrated in the central part of the country, while those with a lower number of accidents are located in peripheral regions.

Table I. Basic statistical description of the sample

REGISTRATIONS		TRANSFERS		SOAT		TECHNICAL-MECHANIC INSP.		LICENSES	
Min.	568	Min.	36	Min.	2002	Min.	117	Min.	0
1stQu	8669	1stQu	2708	1stQu	26152	1stQu	10 738	1stQu	3588
Median	15 532	Median	13 128	Median	122 279	Median	81 976	Median	15 174
Mean	26 167	Mean	41 227	Mean	283 017	Mean	196 864	Mean	27 607
3rdQu	26 668	3rdQu	28 189	3rdQu	225 378	3rdQu	156 080	3rdQu	26 500
Max.	167 566	Max.	310 006	Max.	1 911 332	Max.	1 478 598	Max.	197 663

A2022		A2023		A2024	
Min.	2	Min.	0	Min.	1
1stqQu	70.75	1stqQu	64.5	1stqQu	104
Median	158.5	Median	176	Median	237
Mean	187.1	Mean	192	Mean	258
3rdqQu	226.5	3rdQu	231	3rdQu	300.75
Max.	788	Max.	806	Max.	1093

Note: A2022 and A2023 correspond to accidents recorded in the years 2022 and 2023

Table II. Group distribution of the 32 departments of Colombia

DEPARTMENT	GROUP	POPULATION (DANE, normalized)	DEPARTMENT	GROUP	POPULATION (DANE, normalized)	DEPARTMENT	GROUP	POPULATION (DANE, normalized)
CUNDINAMARCA	1	2 792 877	BOLÍVAR	3	1 909 460	LA GUAJIRA	2	825 364
ANTIOQUIA	1	5 974 788	MAGDALENA	3	1 263 788	CHOCÓ	2	457 412
VALLE DEL CAUCA	1	3 789 874	CESAR	3	1 098 577	CAQUETÁ	2	359 602
BOGOTÁ D.C	1	7 181 469	CAUCA	3	1 243 503	GUAVIARE	2	73 081
HUILA	3	1 009 548	NARIÑO	3	1 335 521	PUTUMAYO	2	283 197
SANTANDER	3	2 008 841	META	3	919 129	AMAZONAS	2	66 056
NORTE DE SANTANDER	3	1 346 806	CALDAS	2	923 472	GUAINÍA	2	44 431
TOLIMA	3	1 228 763	SAN ANDRÉS Y PROVIDENCIA	2	48 299	CASANARE	2	379 892
BOYACÁ	3	1 135 698	RISARALDA	2	839 597	ARAUCA	2	239 503
ATLÁNTICO	3	2 342 265	QUINDÍO	2	509 640	VICHADA	2	76642
CÓRDOBA	3	1 555 596	SUCRE	2	864 036			

The center of cluster 1 includes the departments with the lowest number of accidents, with 24 to 25 accidents for every 100 000 inhabitants. The departments in this group are Cundinamarca, Antioquia, Valle del Cauca, and Bogotá DC. Cluster 2 comprises the departments with the highest number of accidents, with 14-15 accidents for every 100 000 inhabitants. The departments in this group include Huila, Santander, Norte de Santander, Tolima, Boyacá, Atlántico, Córdoba, Bolívar, Magdalena, Cesar, Cauca, Nariño, and Meta. Cluster 3 encompasses the departments with a moderate number of

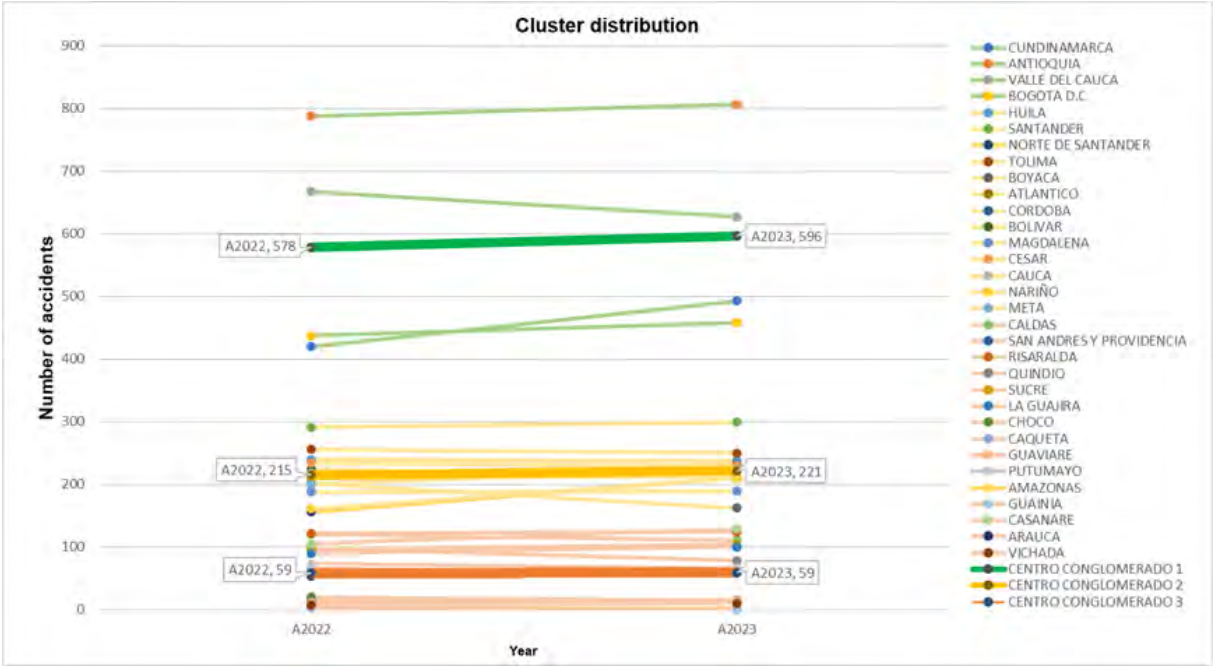

Figure 3. Cluster distribution

accidents, reporting 4 to 5 accidents for every 100 000 inhabitants. This group includes the remaining 19 departments, significantly influencing the overall distribution of accidents in the country.

However, departments with a higher number of accidents and a higher risk classification should be the central focus of road safety policies. Prioritizing these areas enhances decision-making processes and encourages the implementation of specific measures, such as contingency plans, road infrastructure and signage improvements, and awareness campaigns.

Fig. 4 presents a graphical analysis of the weighting of the cluster centers. It illustrates how they are grouped based on their proximity to other groups, identifying accidents that occurred in 2022 and 2023. This information could prove valuable in determining the areas of the country that require greater attention with regard to accident prevention. Here, the cluster with the lowest number of accidents is in black, the cluster with a moderate number of accidents is labeled green, and the cluster with the highest number of accidents is in red.

In the Cartesian plane, the X-axis quantifies the number of traffic accidents that occurred in 2023 (A2023), while the Y-axis represents the incidents recorded in 2022 (A2022). Each point on the graph corresponds to a department, and the color coding indicates cluster membership as defined through the K-means algorithm. Additionally, the asterisks represent the location of each group's centroid, which serves as the geometric center of each cluster within the analytical space. This facilitates the interpretation of regional trends in road accidentality, revealing marked regional differences that are associated with traffic density and the effectiveness of local road safety policies.

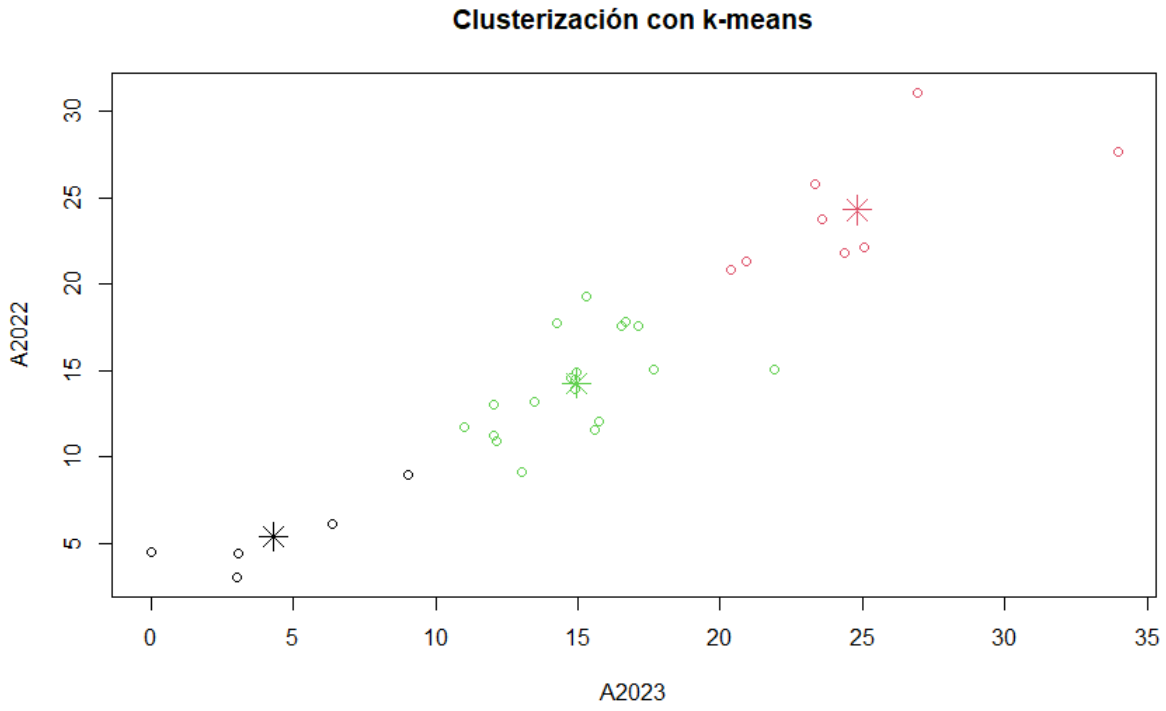

Figure 4. K-means clustering

The following three figures analyze the variation in the percentage of accidents by department for the years 2022 and 2023. This analysis is based on the classification of cluster centers 1, 2, and 3, which enables a deeper understanding of the distribution and behavior of accidents in the country. The main objective is to identify patterns and trends at the departmental level. This information is crucial for decision-making regarding road safety.

This article sought to analyze the departments with the highest and lowest percentage of accidents, the trends in accidents, and the impact of socioeconomic factors in this regard. The results have important implications for the design of public policies and academic research in the field of road safety. Although there are limitations in relation to the availability and quality of the data, we expect that this analysis will serve to understand and address the issue of road accidents in Colombia.

Fig. 5 shows the results of the classification performed using cluster analysis, which identified territorial groupings with similar characteristics in terms of variables associated with the occurrence of road accidents. In the specific case of cluster 1, corresponding to the areas or departments with the highest incidence of accidents, a direct relationship is evident between this classification and key variables such as the number of registered vehicles, population density, and vehicular activity. This is observed in Bogotá, as it belongs to this cluster 1 and represents the lowest percentage of accidents in this classification, accounting for approximately 5 % of the total number of recorded accidents. This

allows inferring and highlighting the importance of this city, combined with its high population density and level of road activity, reinforcing and consolidating its position within this group. Based on the above, this classification not only responds to the absolute number of accidents; it is also influenced by the behavior of the variables considered in this work, which show greater intensity and correlation in this group when compared to clusters 2 and 3. Therefore, the results suggest that the grouping of these departments is strongly determined by structural and dynamic factors of vehicular traffic, which provides a consolidated technical criterion for interpreting and prioritizing road safety intervention within the analyzed areas.

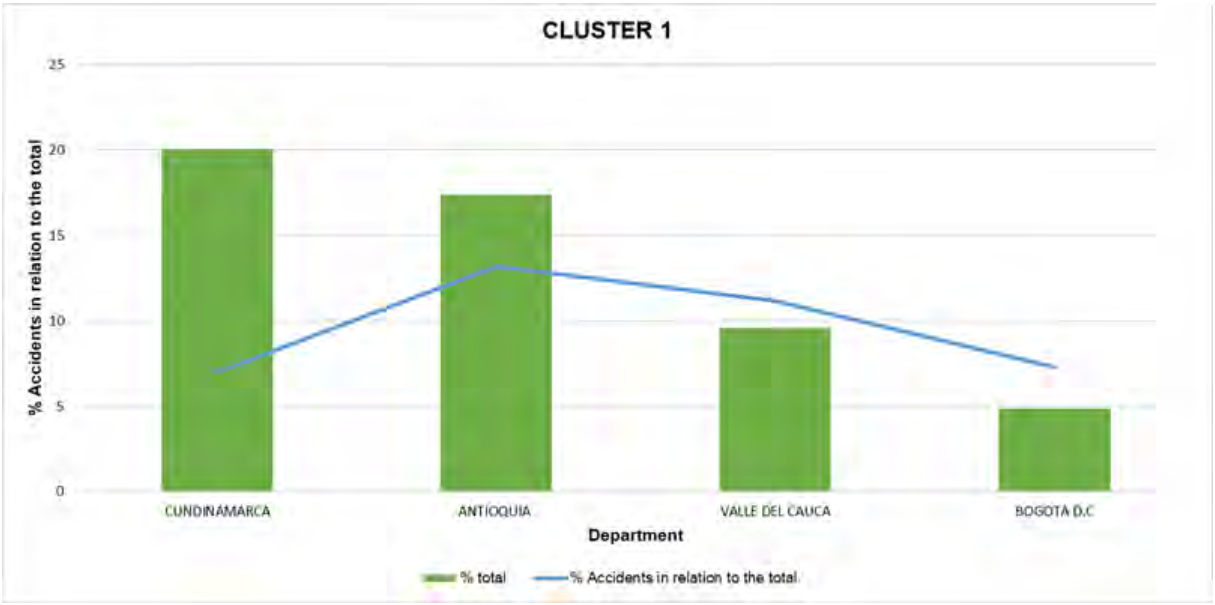

Figure 5. Cluster 1

Fig. 6 presents a comparative representation of the total percentage of records and the percentage of accidents with respect to the total number of registered vehicles for each of the departments in cluster 2. We evidenced a heterogeneous distribution of accidents concerning the proportion of each department within the group. Some departments, such as Santander and Norte de Santander, exhibit higher accident percentages than the cluster average, highlighting that, despite having similar relationships with the total records, their road accident rates are higher in comparison with others in the same group. In contrast, departments such as Boyacá and Tolima show a lower proportion of accidents in relation to their total representation, which suggests a more favorable behavior in terms of relative road safety.

Fig. 7, representing cluster 3, shows the departments with the lowest levels of road accidents in Colombia. This cluster is particularly notable for its low population density, lower volume of registered vehicles, and lower traffic volumes, which reflects its low percentages regarding both the absolute number of accidents and its relative incidence within the country. Some departments, such as Guainía, Vaupés, Amazonas, and Vichada, have near-zero percentages in both variables, suggesting a rather limited road exposure, attributed to their geographic location. Departments such as Putumayo,

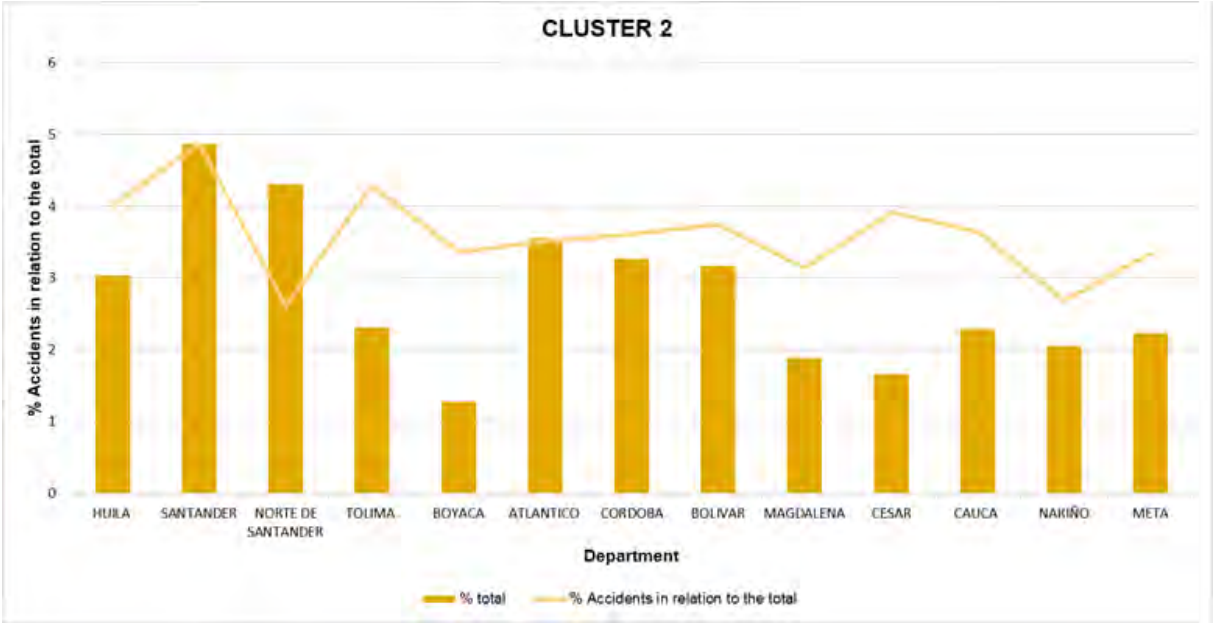

Figure 6. Cluster 2

Guaviare, and Caquetá also have higher proportions within the cluster, although their percentages are lower than 2 %, which is consistent with the classification. Considering that this cluster corresponds to a low accident rate, its analysis is vital, as the presence of specific events or future territorial growth can alter these conditions, especially in departments with emerging development dynamics. Finally, an approximate prediction of accident behavior was generated through a negative binomial analysis, which initially utilized the analyzed variables. The aim was to consolidate and adjust this analysis by examining the strength of the variables in the prediction.

Eq. (4) presents the initial model, which was based on accident data from the year 2022. In contrast, Eq. (5) represents an updated version of the model that incorporates data from 2023 in order to generate an accident prediction for 2024.

$$Accidents = \exp\big(A + REGISTRATIONS * B + TRANSFERS * C + SOAT * D + TECHNICAL{-}MECHANICAL\ INSPECTIONS * E + LICENSES * F + A2022 * G\big) \quad (4)$$

$$Accidents = \exp\big(A + REGISTRATIONS * B + TRANSFERS * C + SOAT * D + TECHNICAL{-}MECHANICAL\ INSPECTIONS * E + LICENSES * F + A2023 * G\big) \quad (5)$$

According to Table **III**, we analyzed each of the constants in the mathematical model related to accident prediction. Each constant (A-G) indicates the influence of a variable on the number of accidents. Constant A represents the baseline level of accidents when all other variables are zero. Coefficient B shows that a higher number of registered license plates increases the number of accidents. Conversely, coefficient C indicates that more transfers are associated with fewer accidents, possibly due to vehicle renewal. Coefficient D (SOAT) also shows a slight inverse relationship, suggesting that greater insurance

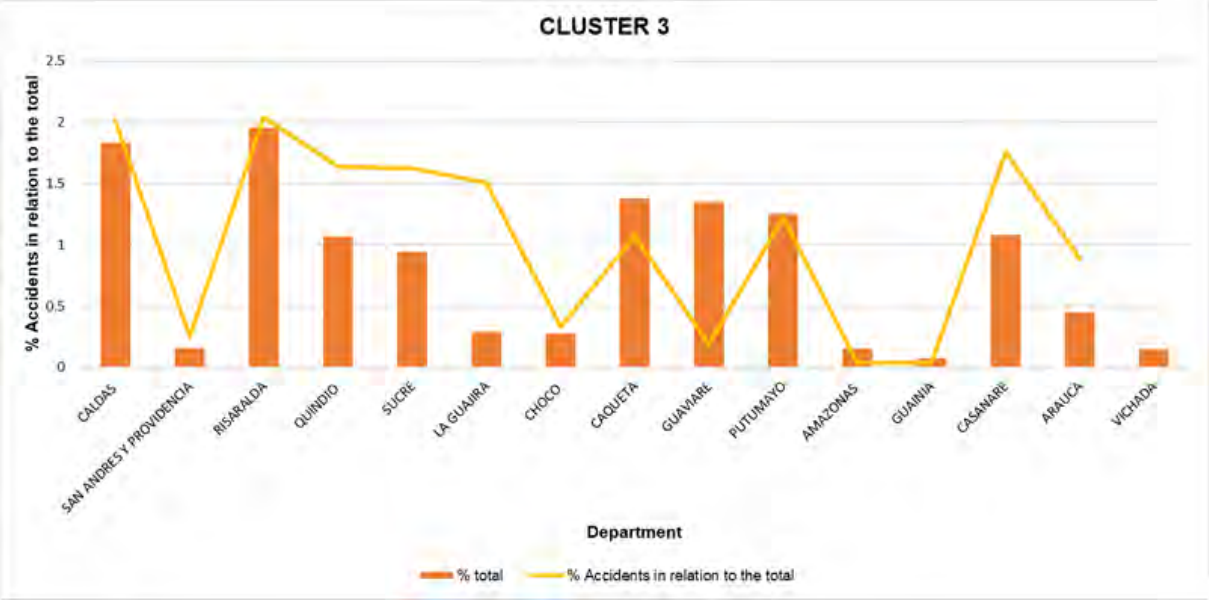

Figure 7. Cluster 3

compliance may slightly reduce accidents. The technical-mechanical inspection variable has a positive effect, perhaps because more inspections reflect a greater number of vehicles in circulation. Coefficient F indicates that more licenses mean more drivers and, therefore, a higher risk of accidents. Finally, coefficient G (accidents in 2022) has the greatest influence, showing that accident rates tend to remain similar from one year to the next.

Table III. Accident prediction by department of Colombia

Constants					
		Estimate	**Std.**	**Error**	**p-value**
(Intercept)	A	4.13E+00	2.89E-02	142.888	2.00E-16
REGISTRATIONS	B	1.47E-05	1.01E-06	14.607	2.00E-16
TRANSFERS	C	-2.22E-05	1.25E-06	-17.778	2.00E-16
SOAT	D	-1.32E-06	3.40E-07	-3.877	0.000106
TECHNICAL-MECHANICAL INSP.	E	2.02E-06	5.15E-07	3.929	8.53E-05
LICENSES	F	3.44E-05	2.65E-06	12.984	2.00E-16
A2022	G	2.11E-03	1.51E-04	14.024	2.00E-16

The p-value indicates whether the estimated effect of each variable on accidents is statistically significant. When the p-value is less than 0.05, there is sufficient evidence to indicate that the variable has a real effect on accidents. For example, variables such as transfers, licenses, and A2022 have extremely low p-values (2.00E-16), indicating a high statistical significance. The SOAT variable, although it has a very small coefficient, has a p-value of 0.000106 (also less than 0.05), so its effect, although weak,

is statistically significant. It should be noted that a low p-value does not necessarily imply that the variable has a large impact on the equation but rather highlights that its effect is consistent.

Considering the above, it should be highlighted that the prediction model uses the exponential function through a regression equation, as the variables to be analyzed are related to the number of accidents. This ensures that the predictions are always positive values.

4. Discussion

In order to improve road safety, policies aimed at reducing accidents must be designed based on the identification of patterns regarding the factors that influence accident records, driver behavior, and vehicle conditions. With this information, both the Ministry of Health and the Ministry of Transportation, in collaboration with the ANSV, will be able to identify how various variables influence the occurrence of traffic accidents. Key variables to consider include vehicle registration, the number of licenses, technical-mechanical inspections, and the SOAT. This not only optimizes the control of road safety but also contributes to a more efficient and equitable management in the distribution of preventive measures, especially in departments with high accident rates. This allows for policies focusing on specific areas and creates a more robust structure for accident reduction.

In this sense, one possible strategy could be the creation of point-based license types, which would incentivize responsible driving and reduce accidents. With a more effective license allocation system, adapted to the needs of each driver according to their history and performance, which considers and understands the impact of these variables on accidents, public policies can be formulated in order to mitigate the occurrence of accidents in high-risk and critical areas through improvements in the registration and regulation of licenses, the SOAT, and technical-mechanical inspections.

Table IV presents the public policies considered in this work, as well as their proposed aims, penalties, and requirements.

Table IV. Public policies analyzed in this work

Category	Aims	Penalties	Requirements
SOAT (mandatory traffic accident insurance)	To ensure that vehicles are insured and covered	Monetary fine for not having a valid SOAT	One-year validity
	To guarantee medical attention in case of a traffic accident	Vehicle immobilization	Availability of sales points

Technical-mechanical inspection	To ensure that vehicles are in safe conditions to circulate	Fines for not passing the inspection	Inspections to be conducted at authorized centers (CDA)
	To identify mechanical failures	Vehicle immobilization Prohibition to circulate	Annual inspection for vehicles over six years old
Vehicle ownership transfers	To regulate the change of ownership of vehicles	Legal issues if the vehicle is reported as stolen	Complete and updated documentation: SOAT, technical-mechanical inspection, ID card
	To ensure that transfers are legal and properly registered		Verification of tax payments
Driver's licenses	To regulate and certify trained drivers	Fines for driving without a license	Theoretical, practical, and medical exams
	To conduct medical, theoretical, and practical exams	Fines for driving with an expired license	Compliance with age and health requirements
	To issue driving licenses	Vehicle immobilization	Updated knowledge on road safety

Our model for accident prediction by department in Colombia was tested in Cundinamarca, Cauca, and Tolima, based on data from 167 566 vehicle registrations, 158 595 ownership transfers, 1 242 294 vehicles with SOAT and 795 736 with technical-mechanical inspection, 639 590 driver's licenses, and 420 accidents during 2022—as well as 493 in 2023 for the department of Cundinamarca. Using these data, the model demonstrated high accuracy. It predicted 458 accidents, and 493 actually occurred in 2023; there was a difference of only 35 accidents compared to the initial figures based on 2022 data.

This analysis validated the robustness of the model and its ability to anticipate the number of accidents with a minimal margin of error. The early prediction of accidents allows authorities and road safety agencies to design and implement more effective prevention and mitigation strategies, as it enables the identification of patterns, trends, and risk factors associated with accidents. With this advance information, resources can be optimized, efforts can be focused on critical areas, and awareness campaigns aimed at reducing the incidence of accidents in each department can be promoted.

Based on the above, Tables **V** and **VI** present a summary of the departments and the years analyzed, confirming the accuracy obtained with respect to an update made for the year 2024. This demonstrates that the prediction model continues to function correctly, as the estimated values closely match the observed data.

Table V. Accident prediction for 2023

PREDICTION FOR 2023	ACCIDENTS IN 2023	DEPARTMENT
420	493	CUNDINAMARCA
299	213	CAUCA
324	250	TOLIMA

Table VI. Accident prediction for 2024

PREDICTION FOR 2024	ACCIDENTS IN 2024	DEPARTMENT
534	664	CUNDINAMARCA
306	262	CAUCA
320	318	TOLIMA

It is essential to highlight that this study presents an initial analysis, whose purpose is to establish a baseline for understanding the observed conditions. In addition, it incorporates data from the previous year, which makes it easier to identify key trends for a correct interpretation. According to (29), traffic accidents are a major public health issue and the second leading cause of death for individuals aged five to 29. This study examines the application of geosimulation as a means to prevent these accidents. Through computational models that integrate geospatial data and traffic variables, it is possible to simulate various scenarios and evaluate the impact of factors such as road infrastructure and driver behavior. This approach enables the identification of high-risk areas and the planning of more effective interventions to enhance road safety.

The use of advanced tools such as GIS, neural networks, and agent-based models is significantly transforming the analysis and prevention of traffic accidents. These technologies offer a more dynamic and detailed approach, allowing for a deeper understanding of the conditions that contribute to these events and facilitating the design of specific strategies to mitigate them. GIS, for instance, are essential for creating maps that identify areas with the highest incidence of accidents. Moreover, they enable the integration of key information, such as traffic volume, weather conditions, and proximity to high-risk locations. These comprehensive analytical capabilities provide traffic management authorities with a more complete understanding of the factors associated with accidents, thereby facilitating the planning of targeted interventions for each problematic area.

In this research, however, we were unable to apply this method due to its reliance on specific variables such as traffic density, vehicle speed, road characteristics (including geometry and pavement conditions), and driver behavior, all focused on a specific study area. Instead, our data were gathered on a global scale using information from the RUNT and the ANSV, covering all 32 departments of Colombia. Nonetheless, in a more detailed study, it would be feasible to combine these approaches and replicate the method to achieve more accurate results.

A study conducted in Kazakhstan applied K-means clustering analysis to vehicle liability insurance data, classifying claims based on their frequency and severity. This technique allowed insurers to optimize premium pricing and improve risk detection. Although the study was carried out in a different context, the results could be applicable to systems such as the SOAT in Colombia, using equivalent variables to identify accident patterns among policyholders (30).

Similarly, in the city of Medellín, Colombia, a geospatial K-means clustering model was implemented to analyze high-risk areas associated with traffic accidents, grouping zones according to the type of incident (*e.g.*, collisions, pedestrian runovers, *etc.*). This approach enabled the identification of accident patterns related to specific environmental features, such as proximity to bars or parks. Although the study did not include variables like driver's licenses or technical-mechanical inspections, it demonstrated that spatial clustering techniques are useful for identifying high-accident zones based on environmental characteristics (31).

In developed countries such as Switzerland and other European nations, latent class clustering (LCC) techniques have been applied for analyzing the severity of pedestrian accidents using contextual and geographic variables. This methodology has allowed researchers to identify specific factors influencing accident severity. By employing LCC, more adaptive and accurate predictive models have been developed to enhance prevention strategies and improve road safety by integrating various factors that affect accident occurrence (32).

Furthermore, studies conducted in the United States and Ethiopia have combined the use of K-means methods with classification algorithms such as random forests and naïve Bayes to improve accident severity predictions. This process involves grouping incidents by shared characteristics and then applying classification models within each group to determine severity levels (33).

Finally, in Italy, researchers have explored the integration of geographic information—such as climate, land use, and points of interest—through machine learning techniques. This combination has significantly improved the prediction of accident risk by considering multiple environmental factors (**?**).

It should be highlighted that these studies were mostly conducted in highly developed countries, which allows them to rely on advanced road intelligence systems and robust databases. In contrast, developing countries like Colombia are beginning to adopt integrated techniques that combine clustering and classification, although they still face significant challenges related to data availability, quality, and standardization.

5. Conclusions

In summary, this work confirmed the viability of the classification of groups using the K-means method based on the incidence of accidents from current data. Three clusters were identified: high, medium, and low accident rates. We acknowledge the potential to improve the results through the

expansion of the database provided by the RUNT and the ANSV. The inclusion of additional data, especially those related to vehicle records, could significantly enrich the analysis and enhance the accuracy of the initial accident prediction model. This approach could offer valuable insights for traffic safety management by providing a more comprehensive and detailed understanding of the factors contributing to accident incidence.

After identifying the departments with high accident rates based on various records (vehicle registrations, SOAT, and technical-mechanical inspections, among others), the actions to be implemented by the ANSV and other government entities could be more precisely focused. Additionally, by assessing the influence of factors such as driving licenses and technical-mechanical inspections on accident prediction, it can be concluded that increasing the number of issued licenses and improving the review process for said inspections will lead to significant improvements in road safety. These actions can be implemented through educational, preventive, and punitive campaigns.

Moreover, an initial accident prediction model was developed in this work, which, as previously mentioned, considers vehicle parameters such as vehicle registration, SOAT, and ownership transfers, among others. These aspects are essential for enhancing the accuracy and effectiveness of the analysis, as they facilitate targeted actions aimed at establishing sustainable and long-lasting mechanisms for improving road safety and designing safer roadways. Ultimately, it is emphasized that cluster analysis is a tool with significant potential in the field of road engineering, although it has not received the necessary attention, as there are limited references on the subject. This type of analysis can be employed to understand and improve various aspects, such as road safety to prevent traffic accidents, human factors, simulation, and traffic flow on highways. It is also crucial to have a database derived from real information.

6. Limitations of this work

The study faced several limitations, including limited data availability, as the analysis was constrained by the scarcity of available data; the lack of temporal continuity, since there were no continuous data series, particularly because the study involved future predictions; evaluation at the macrozone level, as the study focused on a broad territory without reaching the level of specific zones, which limited the thoroughness of the analysis; and the absence of an average daily traffic analysis due to the scope and magnitude of the data used.

7. Lines of research

Future research directions include access to complementary variables, where including additional variables and more specific data on accidents would enrich the analysis and improve the model's accuracy; international comparison, aimed at evaluating the applicability of the model in countries with similar conditions, which would help validate its robustness and adaptability; and the exploration

of new statistical methods, which could enhance both the prediction and the identification of clustering patterns in accident data.

Finally, as future studies, the analysis of underdeveloped countries that have this type of records will allow verifying the usefulness of the method in identifying regions with high accident rates, thus contributing to improving road safety in these areas.

8. Author contributions

Karla Fernanda Mora Chacón: conceptualization, formal analysis, investigation, methodology, resources, validation, visualization, writing (original draft, review, and editing).
Cristian David Rosas López: conceptualization, formal analysis, investigation, methodology, resources, validation, visualization, writing (original draft, review, and editing).
Mariana Ulchur Ruiz: conceptualization, formal analysis, investigation, methodology, resources, validation, visualization, writing (original draft, review, and editing).

9. Funding

This research received no external funding.

10. Data availability

The data will be made available upon request.

11. Conflicts of interest

The authors declare no conflict of interest.

12. Use of artificial intelligence

During this work, the authors did not employ any technologies associated with artificial intelligence.

References

[1] National Road Safety Agency, "Anuario nacional de siniestralidad vial – Colombia 2023," 2023. [Online]. Available: https://ansv.gov.co/es/observatorio/publicaciones/anuario-nacional-de-siniestralidad-vial-colombia-2023 ↑2

[2] J. I. Ruiz and A. N. Herrera, "Accidentes de tránsito con heridos en Colombia según fuentes de información: caracterización general y tipologías de accidentes," *Revista CES Psicol.*, vol. 9, no.1, pp. 32-56, 2016. http://www.scielo.org.co/pdf/cesp/v9n1/v9n1a04.pdf ↑3

[3] D. Herrero-Fernández, M. Oliva-Macías, and P. Parada-Fernández, "Prediction of accident rate from risky and aggressive behavior behind the wheel: Differences by age and gender," *Rev. Psicopatol. Psicol. Clin.*, vol. 24, no. 3, pp. 159–169, 2019. https://doi.org/10.5944/rppc.23370 ↑3

[4] J. D. Parra-Quintero, J. A. Barrera-Cardozo, and P. Ramírez-Soto, "Factorial analysis of road infrastructure related to traffic accidents occurred in Neiva in the years 2017–2018," *Dyna*, vol. 91, no. 231, pp. 99–107, 2024. https://doi.org/10.15446/dyna.v91n231.110396 ↑3

[5] R. Mejia, E. Quinteros, and A. Ribo Arnau, "Áreas geográficas con mayor concentración de accidentes de tránsito en San Salvador, El Salvador: un análisis espacial del periodo 2014-2018," *Rev. Peru. Med. Exp. Salud Publica*, vol. 40, no. 4, pp. 413–425, 2023. https://doi.org/10.17843/rpmesp.2023.404.12963 ↑3

[6] Consejo Colombiano de Seguridad, "Cómo afecta el mal estado de las carreteras a la seguridad en el vehículo," Oct. 12, 2023. [Online]. Available: https://ccs.org.co/como-afecta-el-mal-estado-de-las-carreteras-a-la-seguridad-en-el-vehiculo/ ↑3

[7] AASHTO, *Highway safety manual*, 1st ed. Washington, DC, USA: American Association of State Highway and Transportation Officials, 2010. ↑3

[8] I. Karamanlis, A. Nikiforiadis, G. Botzoris, A. Kokkalis, and S. Basbas, "Towards sustainable transportation: The role of black spot analysis in improving road safety," *Sustainability*, vol. 15, no. 19, art. 14478, 2023. https://doi.org/10.3390/SU151914478 ↑3

[9] Ministerio de Transporte, "La Agencia Nacional de Seguridad Vial, ANSV, avanza con sus programas en los territorios del país," 2023. [Online]. Available: https://mintransporte.gov.co/publicaciones/11348/la-agencia-nacional-de-seguridad-vial-ansv-avanza-con-sus-programas-en-los\-territorios-del-pais/ ↑3

[10] Ministerio de Transporte, *Plan Nacional de Seguridad Vial 2022-2031*. Bogotá, Colombia: Ministerio de Transporte, 2022. ↑3

[11] Observatorio Vial Argentina, "Infraestructura vial: factor de riesgo de la seguridad vial," 2020. [Online]. Available: https://www.argentina.gob.ar/seguridadvial/observatoriovialnacional/infraestructura-vial-factor-de-riesgo-de-la-seguridad-vial ↑3

[12] J. Qiu, H. Wang, R. Jiang, W. Xiao, H. Chang, and S. Zhu, "Identification and analysis of serious conflicts in expressway transition areas," *China Safety Sc.i J.*, vol. 32, no. 2, pp. 184–191, 2022. https://doi.org/10.16265/j.cnki.issn1003-3033.2022.02.025 ↑3

[13] C.-W. Choe, S. Lim, D. J. Kim, and H.-C. Park, "Development of Spatial Clustering Method and Probabilistic Prediction Model for Maritime Accidents," *Appl. Ocean Res*, vol. 154, art. 104317, 2025. https://doi.org/10.1016/j.apor.2024.104317 ↑3

[14] F. Á. C. Escobar, G. P. Buitrago, and F. A. Guío B., "Spatial analysis with weighted kernel groupings to determine risk sectors due to traffic accidents in urban area. Tunja analysis, Colombia," *Cuad. Geogr. Rev. Colomb. Geogr*, vol. 62, no. 1, pp. 45–58, 2023. https://doi.org/10.30827/cuadgeo.v62i1.18025 ↑4

[15] J. L. Montealegre Quijano and J. A. Garzón Quiroga, "Critical points of traffic accidents in Ibagué, Colombia," *Estud. Demogr. Urbanos*, vol. 36, no. 4, pp. 298–312, 2021. https://doi.org/10.24201/edu.v36i2.2035 ↑4

[16] S. Chatti, G. Rama Krishna, S. Krishna Mohan Rao, and P. Venketeswa Rao, "A method to find optimum number of clusters based on fuzzy silhouette on dynamic data set," *Procedia Comput. Sci*, vol. 46, pp. 346–353, 2015. https://doi.org/10.1016/j.procs.2015.02.030 ↑4

[17] Y. H. Caña, R. Gomero-Cuadra, R. P. Llerena, J. Armada, and C. R. Mejía, "Work-related accident rates at a metropolitan Lima hospital during the COVID-19 pandemic: A behavioral analysis," *Rev. Asoc. Esp. Espec. Med. Trab.*, vol. 32, no. 4, pp. 297–307, 2023. https://scielo.isciii.es/scielo.php?script=sci_arttext&pid=S3020-11602023000400004 ↑4

[18] A. B. Silva and M. C. Oliveira, "Data integration process: An information management model for multiple databases on traffic accidents in Brazil," *Epidemiol. Serv. Saude*, vol. 27, no. 2, p. e201800218, 2018.2024. https://doi.org/10.5123/S1679-49742018000200018 ↑4

[19] V. Cantillo, P. Garcés, and L. Márquez, "Factors influencing the occurrence of traffic accidents in urban roads: A combined GIS-empirical Bayesian approach," *Rev. Ing.*, vol. 40, no. 2, pp. 123–135, 2024. https://doi.org/10.15446/dyna.v83n195.47229 ↑4

[20] J. D. Alarcón, I. Gich Saladich, L. Vallejo Cuéllar, A. M. Ríos Gallardo, C. Montalvo Arce, and X. Bonfill Cosp, "Mortalidad por accidentes de tráfico en Colombia. Estudio comparativo con otros países," *Rev. Esp. Salud Pública*, vol. 92, art. e201807040, 2018. https://pubmed.ncbi.nlm.nih.gov/29967318/ ↑5

[21] G. Lozano Pérez, D. Muñoz Torres, and V. Villalba Vimos, "Road safety perspective in developing countries - Colombia," *Rev. Espacios*, vol. 39, no. 42, pp. 11-23, 2018. https://www.revistaespacios.com/a18v39n42/18394211.html ↑5

[22] DANE, "Mapas Nacionales | GEOPORTAL." [Online]. Available: https://geoportal.dane.gov.co/ ↑6

[23] L. Yue, C. Xiaoquan, D. Tian, and J. Feng , "Customer segmentation using K-means clustering and the adaptive particle swarm optimization algorithm,' *Appl. Soft Comput.*, vol. 113, art. 107924, 2021. https://doi.org/10.1016/j.asoc.2021.107924 ↑5

[24] A. Baíllo y A. Grané, *100 problemas resueltos de estadística multivariante*. Madrid, Spain: Delta Publicaciones Universitarias, 2007. ↑6

[25] A. Jain, M. Murty, and P. Flynn, "Data Clustering: A Review," *ACM Comput. Surv.*, vol. 31, nº 3, pp. 264–323, 1999. https://doi.org/10.1145/331499.331504 ↑6

[26] J. L. Devore, *Probability and statistics for engineering and the sciences*, 8th ed. Boston, MA, USA: Brooks/Cole, Cengage Learning, 2012. ↑8

[27] C. Rosas, C. Gaviria, and C. Calero, "Classification of Driver Behavior in Horizontal Curves of Two-Lane Rural Roads," *Rev. Fac. Ing.*, vol. 30, no. 57, art. e13410, 2021. https://doi.org/10.19053/01211129.v30.n57.2021.13410 ↑8

[28] H. Taherdoost and M. Madanchian, "A Comprehensive Overview of the ELECTRE Method in Multi Criteria Decision-Making," *J. Manage. Sci. Eng. Res.*, vol. 6, no. 2, pp. 5–16, 2023. https://doi.org/10.30564/jmser.v6i2.5637 ↑8

[29] F. Castro, "The geosimulation, a tool for the prevention of traffic accident," *Ing.Inv. Tecnol.*, vol. 19, no. 2, pp. 135–145, 2018. https://doi.org/10.22201/fi.25940732e.2018.19n2.012 ↑17

[30] A. C. Yeo, K. A. Smith, R. J. Willis, and M. Brooks, "Clustering technique for risk classification and prediction of claim costs in the automobile insurance industry," *Intell. Syst. Account. Finance Manage.*, vol. 10, no. 1, pp. 39–50, 2001. https://doi.org/10.1002/ISAF.196 ↑18

[31] D. Wang, Y. Huang, and Z. Cai, "A two-phase clustering approach for traffic accident black spots identification: integrated GIS-based processing and HDBSCAN model," *Int. J. Inj. Control Saf. Promot.*, vol. 30, no. 2, pp. 270–281, 2023. https://doi.org/10.1080/17457300.2022.2164309 ↑18

[32] B. Sui, N. Lubbe, and J. Bärgman, "A clustering approach to developing car-to-two-wheeler test scenarios for the assessment of Automated Emergency Braking in China using in-depth Chinese crash data," *Accid. Anal. Prev.*, vol. 132, art. 105242, 2019. https://doi.org/10.1016/j.aap.2019.07.018 ↑18

[33] S. S. Yassin and Pooja, "Road accident prediction and model interpretation using a hybrid K-means and random forest algorithm approach," *SN Appl. Sci.*, vol. 2, no. 9, 2020. https://doi.org/10.1007/s42452-020-3125-1 ↑18

Karla Fernanda Mora Chacón

Civil engineer from the Universidad del Cauca, she has a solid background in her field, complemented by skills in engineering and information systems. She is distinguished by her strong sense of responsibility and commitment to fulfilling her duties. Karla actively participates in the Roads and Transportation Research Group.

Email: kamora@unicauca.edu.co

Cristian David Rosas López

Civil engineer from Universidad del Cauca (2012), with a specialization (2022) and a Master's degree (2022) in Roadway Engineering from the same institution. He has professional and academic competencies in the areas of topography, road consulting, research, and teaching at the secondary and university levels.

Email: cdrosas@unicauca.edu.co

Mariana Ulchur Ruíz

Civil engineer from Universidad del Cauca (2025), with a valid professional license. She has a comprehensive background in planning, coordinating, supervising, and managing infrastructure projects, as well as in risk analysis and in the formulation of technical solutions focused on community service and environmental protection.

Email: mulchur@unicauca.edu.co

UNIVERSIDAD DISTRITAL
FRANCISCO JOSÉ DE CALDAS

Ingeniería

https://revistas.udistrital.edu.co/index.php/reving/issue/view/1295

DOI: https://doi.org/10.14483/23448393.23141

Research

Use of Computational Tools in the Modeling of Columns for Cr(VI) Adsorption in Wastewater by Means of *Theobroma cacao* L.

Uso de herramientas computacionales en el modelado de columnas para la adsorción de Cr(VI) en aguas residuales utilizando *Theobroma cacao* L.

Ángel D. González-Delgado[1], Ángel Villabona-Ortiz[1], and Candelaria Tejada-Tovar[1]*

[1] Department of Chemical Engineering, Universidad de Cartagena, Cartagena de Indias, 130015 Colombia

Abstract

Context: Industrial growth and various anthropogenic activities have generated multiple pollutants, including heavy metals such as hexavalent chromium, or Cr(VI), which pose a major threat to both humans and the environment, as their characteristics make them persistent, bioaccumulative, and non-biodegradable.

Method: In this paper, computer-aided process engineering (CAPE) was used to simulate an industrial-scale adsorption column packed with a biomass based on cocoa husk residues for the removal of Cr(VI) in solution. A parametric sensitivity analysis was conducted, using Aspen Adsorption as a simulation tool to analyze different column configurations.

Results: The Freundlich isothermal model, in combination with the linear driving force (LDF) kinetic model, yielded efficient results in removing Cr(VI) via adsorption, with values of up to 97.1 %. The best operating conditions included an initial concentration of 5000 mg/L, a bed height of 5 m, and an inlet flow rate of 100 m^3/day.

Conclusions: This study demonstrates that the use of computational assistance holds great potential for predicting the performance of an adsorption column packed with agro-industrial waste, which constitutes a safe and cost-effective alternative for the design and modeling of industrial-scale columns.

Keywords: waste biomass, adsorption column, chromium (VI), simulation, water treatment, wastewater treatment

Article history

Received: Dec 30th, 2024

Modified: Jul 8th, 2025

Accepted: Aug 10th, 2025

Ing, vol. 30, no. 3, 2025, e23141

* **Correspondence:** ctejadat@unicartagena.edu.co

Resumen

Contexto: El crecimiento industrial y diversas actividades antropogénicas han generado múltiples contaminantes, entre los que se encuentran metales pesados como el cromo hexavalente, o Cr(VI), los cuales representan una amenaza significativa tanto para el medio ambiente como para el ser humano, pues sus características los hacen persistentes, bioacumulativos y no biodegradables.
Método: En este artículo se empleó la ingeniería de procesos asistida por ordenador (CAPE) para simular una columna de adsorción a escala industrial llena de biomasa a base de residuos de cáscara de cacao para la eliminación de Cr(VI) en solución. Se realizó un análisis de sensibilidad paramétrica, utilizando Aspen Adsorption como herramienta de simulación para analizar diferentes configuraciones de la columna.
Resultados: El modelo isotérmico de Freundlich, junto con el modelo cinético de fuerza motriz lineal (LDF) arrojó resultados eficientes en la remoción de Cr(VI) mediante adsorción, con valores de hasta 97.1 %. Las mejores condiciones de operación incluyeron una concentración inicial de 5000 mg/l, una altura del lecho de 5 m y un caudal de entrada de 100 m^3/día.
Conclusiones: Este estudio demuestra que el uso de la asistencia computacional tiene gran potencial para predecir el rendimiento de una columna de adsorción llena de residuos agroindustriales, constituyéndose en una alternativa segura y rentable para el diseño y modelado de columnas a escala industrial.

Palabras clave: biomasa residual, columna de adsorción, cromo (VI), simulación, tratamiento de agua, tratamiento de aguas residuales

Table of contents

Page

1. **Introduction** 3
2. **Materials and methods** 5
   - 2.1. Parameterization and modeling . . 5
   - 2.2. Mathematical fundamentals 6
     - 2.2.1. Mass balance 6
     - 2.2.2. Freundlich isothermal model 7
     - 2.2.3. LDF kinetic model 7
3. **Results and discussion** 7
   - 3.1. Evaluating the mathematical models using Aspen Adsorption . . . 7
   - 3.2. Influence of the inlet flow rate . . . 7
   - 3.3. Influence of initial concentration . 7
   - 3.4. Influence of bed height 9
   - 3.5. Comparison with other results in the literature 10
4. **Conclusions** 11
5. **Acknowledgements** 11
6. **Author contributions** 12
7. **Funding** 12
8. **Data availability** 12
9. **Conflicts of interest** 12
10. **Use of artificial intelligence** 12

Nomenclature

C_e	Pollutant concentration in solution at equilibrium $(\mathrm{mg/L})$
n	Effect of initial concentration on adsorption capacity
k_f	Freundlich's constant indicating adsorption capacity $\left(\frac{\mathrm{mg}}{\mathrm{g}}\right)\left(\frac{\mathrm{Lm}}{\mathrm{g}}\right)^n$
MTC	Global mass transfer coefficient $\left(\frac{\mathrm{m}}{\mathrm{s}}\right)$
$\frac{C_f}{C_o}$	Efficiency
w_k	Instantaneous equilibrium adsorbate loading on the adsorbent $\left(\frac{\mathrm{mg}}{\mathrm{g}}\right)$
z	Distance along the bed (m)
Q_i	Quantity of metal ions adsorbed by the adsorbent (mg/g)
C_i	Concentration of cadmium ions in the liquid phase (mg/L)
ρ_s	Bulk density ($\mathrm{g/cm^3}$)
t	Time (min)
ε	Bed porosity
u_o	Fluid velocity (m/s)

1. Introduction

Water sources play an essential role in human life due to their great usefulness and versatility in different activities, *e.g.*, industrial processes, agricultural and livestock activities, hospitals, shopping centers, rural areas, and domestic households, among others (1). Using this resource generates different types of wastewater that are loaded with pollutants. A large portion of this water, which originates from industrial activity, is considered to be of great concern due to its properties, as is the case with the toxic substances it contains (2, 3). This toxicity depends on various factors such as chemical composition, which varies from sector to sector, making the elimination of these substances a challenge, as each effluent contains unique pollutants that require customized treatment (4,5). Among the various pollutants present in industrial wastewater are heavy metals, a worldwide concern due to their high toxicity, their detrimental impact on both the environment and human health, and their high strength and non-biodegradability (6).

Despite being an essential metal, chromium is considered to be one of the 16 main toxic pollutants with adverse effects on human health. This metal, which can be ingested, inhaled, or absorbed through the skin (7), is used in various manufacturing sectors, such as the metallurgy, tanning, cement, textile, and dyeing industries. These sectors represent major sources of pollution (8). Chromium ranks second in abundance among the heavy metal pollutants, surpassed only by lead. It is naturally found in three

forms: metallic, trivalent, and hexavalent, with the latter, Cr(IV), being the toxic one. This form has a variety of detrimental health effects, such as digestive, urinary, reproductive, and immune system dysfunctions. Therefore, it is necessary to treat any water sources contaminated with Cr(IV) that are discharged into the environment (9). In Colombia, the limit for chromium in drinking water, as dictated by Law 0631 of 2015, is 0.5 mg/L (10), while the World Health Organization's permitted level is 0.05 mg/L for Cr (11).

Adsorption is an effective method for removing unwanted pollutants, given its feasibility and easy scalability. This method is also able to effectively remove various inorganic chemicals that affect the adsorption system (12). This technique has several advantages that make it a very attractive method for use in water treatment. Among these advantages are its efficiency in removing various types of pollutants, including heavy metals, dyes, emerging contaminants, and other types of substances (13); its applicability at low temperature and pressure, since, compared to other water treatment processes, it does not require extreme conditions; its versatility in dealing with pollutants in both gaseous and liquid form (14); the regenerative capacity of the materials used in the adsorption process, which allows reusing biomaterials multiple times depending on the type of biomass employed and its characteristics (15); the speed at which this technique removes pollutants, allowing for effective and fast processes; and its versatility in enabling a modular and scalable design of the adsorption process in the form of columns or adsorbent beds, modeled on a small or a large scale as required (16).

This technique may involve one of two different adsorption methods: *physisorption*, wherein adsorption stems from the presence of weak attractions between the pollutant and the adsorbent material, generated by short-range electrostatic forces (*i.e.*, van der Waals forces) (17); and *chemisorption*, where adsorption takes place due to the presence of chemical bonds between the adsorbate and the adsorbent, causing a stronger and more selective interaction. This process is less reversible than physisorption and requires considerably more energy for the desorption of the adsorbed species (18). The adsorption process can be carried out in two ways: in batches or in columns (19).

This technique has been recognized as one of the simplest and most economical strategies due to its remarkable ability for heavy metal removal (20, 21). Different biomaterials have been developed and used to this effect, such as *Ulva flexuosa*, a species of algae (22); babano shell (23); rapeseed (*Brassica napus*) (24); and coconut (25), among others. Cocoa (*Theobroma cacao L.*) is a widely cultivated product in Colombia, and it generates a large amount of residual biomass, comprising the husk of the cob, the husk of the bean, and the pulp. Among the different byproducts of this plant, the husk is a promising material for the production of adsorbent materials, given its abundance, low cost, and renewable nature. The cocoa husk is composed of cellulose, hemicellulose, and lignin, and it offers a high adsorption capacity, which makes it a sustainable alternative for the elimination of pollutants in aqueous media, *e.g.*, heavy metals (26). Most adsorption studies have been conducted at the laboratory level under simple conditions and on small scales. This is due to different limiting factors, such as resource, space, and time availability, among others. In light of the above, several computational tools like Aspen Plus (27) or ChemCAD (28), have been developed for modeling processes on a larger scale, but scaling to solids

in adsorption towers is still in its early stages. Therefore, researchers have searched for new ways to scale their proposals under the existing limitations. Among them, the Aspen Adsorption software has proven to be a tool for adsorption columns. This tool allows modeling multi-scale adsorption columns by simulating key phenomena such as mass transfer, adsorption equilibrium, and fluid dynamics. It allows predicting performance at the laboratory, pilot, and industrial scales, optimizing system design and operation based an experimental data. Its use in treating chromium-contaminated water also demonstrates its ability to respond to various operating conditions, improving process efficiency and supporting scaling from laboratory-level to industrial applications. This tool constitutes an advantage for a broader exploration of different parameters or operating variables such as flow, bed height, and pollutant concentration, among others, facilitating the optimization of the process before designing a pilot or building industrial plant.

A study published by (29) delved into the performance of dolochar as a Cd(II) adsorbent, using Aspen Adsorption to simulate a large-scale process. The results, obtained via the response surface methodology, show that, with optimal bed height, inlet concentration, flow rate, and fixed biosorbent mass values, the CD(II) ion adsorption capacity and depletion time of the packed dolochar bed are 1.85 mg/g and 11.39 hours, respectively.

Using Aspen Adsorption V11, the study by (30) simulated the adsorption of Pb(II) on tire-based activated carbon (TAC) and commercial activated carbon (CAC) in a fixed-bed column while considering different concentration ranges, bed heights, and flow rates. The optimal conditions found in this study included a concentration of 500 mg/L, a bed height of 0.6 m, and a flow rate of 9.88×10^{-4} m^3/s, which yielded breakthrough times of 488 and 23 s for TAC and CAC, respectively, with removal capacities of 114.26 and 7.72 mg/g.

In light of the above, the objective of this study was to model an industrial column packed with *Theobroma cacao* L. for the adsorption of Cr(VI) in solution, using Aspen Adsorption to conduct a parametric sensitivity analysis and evaluate the performance of the system by altering key parameters. Our work demonstrates the potential of computational tools for predicting the performance of adsorption columns and provides a solid basis for the design and simulation of large-scale adsorption systems that employ agro-industrial materials for water treatment.

2. Materials and methods

2.1. Parameterization and modeling

In this study, we used Aspen Adsorption V12.1 to simulate an adsorption column packed with *Theobroma cacao* L. for the removal of Cr(VI) in an industrial stream. A parametric study was carried out regarding the inlet flow rate, the initial concentration, and the column height, with the aim of determining the extent to which modifying these factors affects adsorption performance. We also conducted a sensitivity analysis that considered the breakthrough profile. Different parameter ranges

were used to evaluate the performance of the adsorption system. For the inlet flow rate, values of 250, 200, 150, 100, and 50 m3/day were employed; for the bed height, we established values of 3, 4, and 5 m[30]; and, finally, for the initial concentration of Cr(VI), 5000, 3500, 2000, and 1000 mg/L were considered (31,32).

To design our proposal, studies on the use of columns for the removal of heavy metals from industrial wastewater were used as a basis, considering the different parameters required to simulate the process in Aspen Adsorption. In this vein, we established a bed diameter of 1 m (33), a bulk density of 0.0365 g/cm^3 for the biomaterial (34), a bed porosity of 0.67 (m^3 of voids per m^3 of bed), a total vacuum porosity of 0.4 (35,36), and a constant mass transfer coefficient of 1.37×10^{-4} s^{-1} (37).

To understand the behavior caused by the interactions between the adsorbate and the adsorbent during the process, we employed the Freundlich isothermal model (38), while the linear driving force (LDF) kinetic model was used to determine the rate at which the adsorption occurred (39). Fig. **1** presents the simulation flowchart for the column.

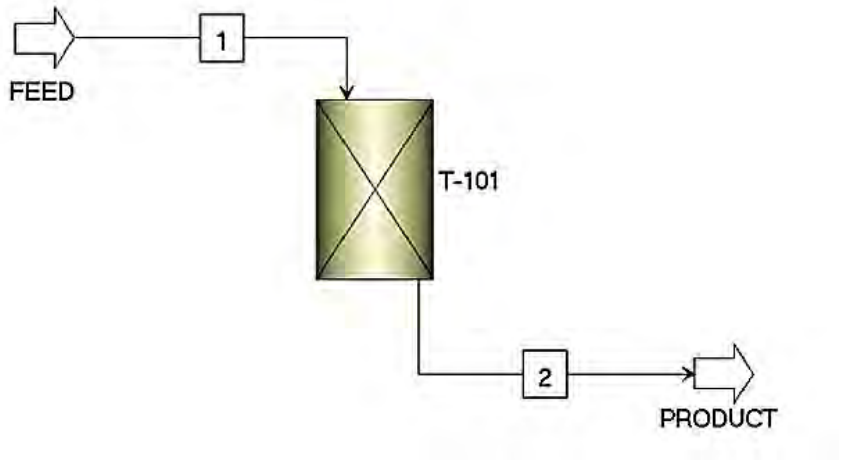

Figure 1. Simulation flowchart for the adsorption column

2.2. Mathematical fundamentals

2.2.1. Mass balance

The equation used by Aspen Adsorption for the mass balance of the adsorption column is presented below:

$$u_0\varepsilon\frac{\partial C_i}{\partial z}+\varepsilon\frac{\partial C_i}{\partial t}+\rho_s\frac{\partial Q_i}{\partial t}=0 \quad (1)$$

2.2.2. Freundlich isothermal model

The Freundlich model considers a multilayer adsorption on a heterogeneous surface, where the distribution of the components depends on the time and energy of the secured sites (40, 41). This model is described by Eq. 2.

$$q_e = k_f C_e^{1/n} \tag{2}$$

2.2.3. LDF kinetic model

The LDF kinetic model implies that the driving force for the mass transfer of components is a linear function of the concentration of the component in the liquid or solid phase (42, 43). This model is presented in Eq. 3.

$$\frac{\partial w_k}{\partial t} = MTC_{sk}\left(w_k^* - w_k\right) \tag{3}$$

3. Results and discussion

3.1. Evaluating the mathematical models using Aspen Adsorption

The Freundlich isothermal model and the LDF kinetic model were evaluated while considering the above-presented parameters and ranges. The results indicated that, by reducing the height of the column and increasing the flow rate, the break and saturation times can be reduced. This is due to the fact that, with a low bed height and a high flow rate, the fluid passes through the bed more quickly, which results in reduced process times. The results for the break time (TR) and the saturation time (TS) are shown in Table **II**.

3.2. Influence of the inlet flow rate

By means of a parametric sensitivity analysis, the influence of the inlet flow rate on the performance of the adsorption column was evaluated. To this effect, inlet flow rates of 250, 200, 150, 100, and 50 m^3/day were considered. Fig. **2** shows the breakthrough profiles obtained from the Freundlich-LDF model. Note that the efficiency increases with the flow rate, but the breakthrough and saturation times are reduced. This behavior is due to the fact that a high inflow rate has a positive effect on mass transfer, causing a faster accumulation of the pollutant and decreasing the number of available active sites, which leads to reduced times. This behavior is also evident in the efficiency values obtained: 95.2 % for 250 m^3/day, 94 % for 200 m^3/day, 92.1 % for 150 m^3/day, 88.4 % for 100 m^3/day, and 78.1 % for 50 m^3/day (44, 45).

3.3. Influence of initial concentration

For the parametric sensitivity analysis of the initial Cr(VI) concentration, values of 5000, 3500, 2000, and 1000 mg/L were considered. Fig. **3** shows the breakthrough profiles obtained from the simulation of the Freundlich-LDF model. Note that, when this parameter is increased or decreased, the rupture times

Table II. Results obtained for the analyzed models

Freundlich -LDF		Flow rate (m^3/day)														
		250			200			150			100			50		
		Bed height (m)														
Concentration (mg/L)	Results	3	4	5	3	4	5	3	4	5	3	4	5	3	4	5
5000	TR (min)	105	144	184	135	184	233	184	250	315	282	381	480	579	778	978
	TS (min)	1194	1540	1884	1449	1884	2294	1884	2440	2978	2708	3499	4264	5014	6429	7792
3500	TR (min)	112	153	195	143	195	247	195	264	334	299	403	507	612	822	1032
	TS (min)	1161	1494	1820	1409	1820	2231	1820	2361	2880	2678	3394	4129	4830	6187	7475
2000	TR (min)	124	169	214	157	214	271	214	289	365	327	441	555	669	898	1129
	TS (min)	1100	1422	1732	1341	1732	2111	1732	2234	2731	2480	3201	3885	4545	5783	6967
1000	TR (min)	141	192	242	179	242	306	242	327	412	370	498	626	755	1013	1272
	TS (min)	1037	1331	1620	1254	1620	1969	1620	2081	2518	2307	2950	3555	4146	5240	6239

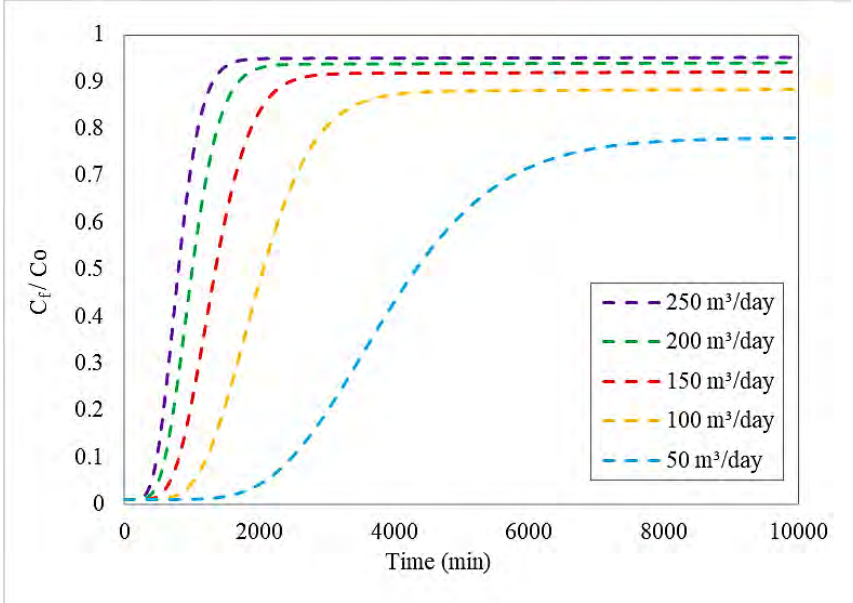

Figure 2. Breakthrough curve for a bed height of 5 m and an initial concentration of 500 mg/L at different flow rates

(TR) and saturation times (TS) obtained for each column configuration are very close to each other. Similarly, the efficiencies achieved show a similar trend, indicating that, under these conditions, the influence of concentration on the difference between TR, TS, and the overall system performance is limited. This phenomenon is due to the high presence of Cr(VI) in the flow, which causes an early break in the curve—this behavior is also observed at different times. Nevertheless, varying this parameter does not affect the adsorption performance, as the observed difference was less than 1 %. This can be attributed to different factors, such as the number of active sites available in the adsorbent, the strong affinity between the adsorbent and the adsorbate (which allows quickly reaching adsorption equilibrium), and the operating conditions considered, among others (46).

3.4. Influence of bed height

We also analyzed the influence of bed height on the performance of the adsorption column used for the removal of Cr(VI) in aqueous solution. The values considered in this analysis were 3, 4, and 5 m. Fig. 4 shows the breakthrough profiles obtained from the simulation of the Freundlich-LDF model. The breakthrough and saturation times increase with bed height, whereas efficiency is reduced. This is due to the fact that, with a larger adsorption surface, the fluid entering the column takes longer to exit. In addition, there are more active sites available, which extends the useful life of the adsorbent material, since it does not saturate as quickly, resulting in increased process times. On the other hand, the efficiency values obtained after the simulation were 92.9 % for 3 m, 90.6 % for 4 m, and 88.4 % for 5 m (47).

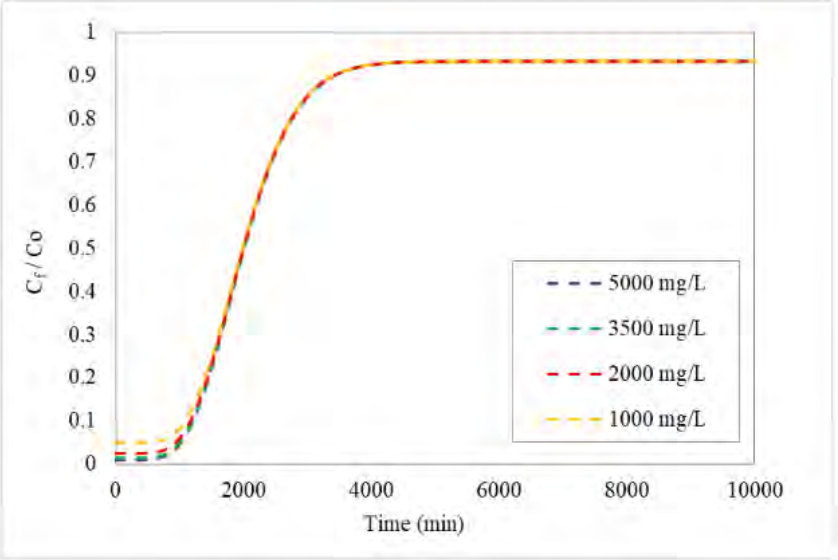

Figure 3. Breakthrough profiles for a column height of 5 m and an inlet flow rate of 100 m^3/day at various Cr(IV) concentrations

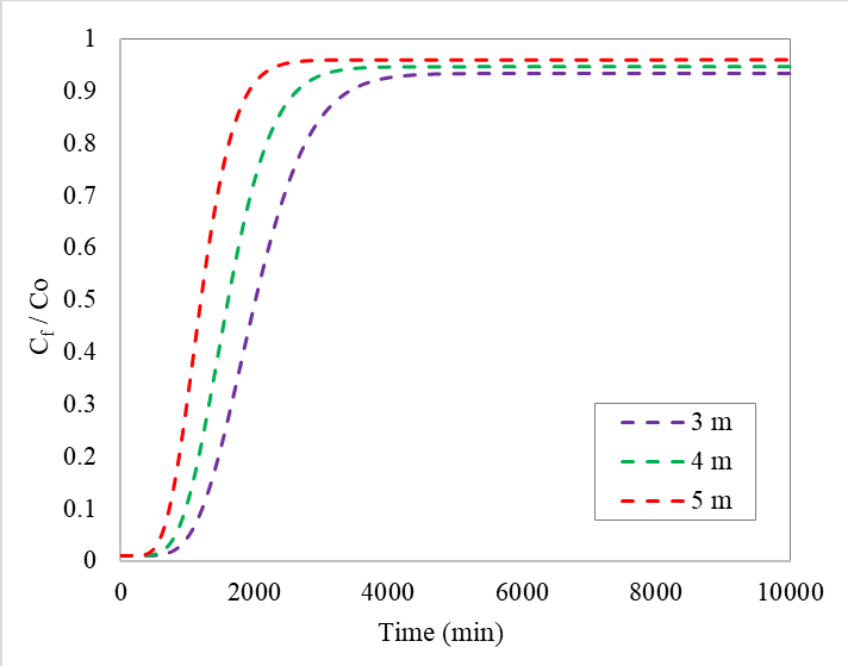

Figure 4. Breakthrough profiles for an initial concentration of 5000 mg/L and a flow rate of 100 m^3/day at different bed heights

3.5. Comparison with other results in the literature

The data obtained after conducting various simulations of the industrial cocoa-packed adsorption column were compared against the results of studies published in the specialized literature. It should

be noted that this comparison has relative value, since each study was carried out under different inlet flow rate, initial concentration, bed height, and biomaterial conditions. The results of this work indicate that *Theobroma cacao* L. offers an acceptable in Cr(VI) removal. Table III shows de aforementioned comparison.

Table III. Comparison with literature-reported results

Contaminant	Adsorbent	Parameters	Results	Source
Pb(II)	Activated alumina	Initial concentration: 0.1 mg/L Inlet flow rate: 54.52 m^3/day Bed height: 1.459 m	Rupture time: 40 320 min	(48)
Pb(II)	*Bambusa* spp.	Initial concentration: 20 mg/L Inlet flow rate: 1.728 m^3/day Bed height: 1 m	Rupture time: 52 min	(49)
Cr(VI)	*Theobroma cacao* L.	Initial concentration: 5000 mg/L Inlet flow rate: 100 m^3/day Bed height: 5 m	Rupture time: 480 min Saturation time: 4264 min	This study

4. Conclusions

This study presented an innovative approach to modeling and simulating large-scale adsorption columns using agro-industrial waste (cocoa residues in this case) to remove heavy metals such as Cr(VI) from water systems. This work provides valuable quantitative data that contribute to the development and understanding of industrial adsorption processes. A parametric sensitivity analysis allowed evaluating the effect of varying the column's bed height, inlet flow rate, and initial pollutant concentration on the efficiency of the process. The results that increasing the bed height increases the break and saturation times but reduces the adsorption efficiency. On the other hand, high inlet flows improve the adsorption efficiency but decrease the biomaterial's saturation times. It is also noteworthy that the initial concentration does not have a significant effect on adsorption efficiency. These results constitute a robust technical basis for the design and optimization of industrial effluent treatment systems, as they allow anticipating the behavior of the system prior to its full-scale implementation.

5. Acknowledgements

The authors would like to thank Universidad de Cartagena for providing equipment, reagents, and technical and financial support for the project approved via Resolution no. 01385 and Minute no. 093 of 2021.

6. Author contributions

Ángel González Delgado: contextualization, software, formal analysis, writing (review and editing), visualization.
Ángel Villabona Ortiz: project administration, contextualization, methodology, software, validation, formal analysis, research, resources, data curation, writing (original draft).
Candelaria Tejada Tovar: methodology, validation, research, data curation, writing (original draft), visualization, supervision.

7. Funding

This research received no external funding.

8. Data availability

The data will be made available upon request.

9. Conflicts of interest

The authors declare no conflict of interest.

10. Use of artificial intelligence

During this work, the authors did not employ any technologies associated with artificial intelligence.

References

[1] S. Bochynska *et al.*, "The impact of water pollution on the health of older people," *Maturitas*, vol. 185, art. 107981, Jul. 2024. https://doi.org/10.1016/J.MATURITAS.2024.107981 ↑3

[2] Rozirwan *et al.*, "Ecological risk assessment of heavy metal contamination in water, sediment, and polychaeta (*Neoleanira tetragona*) from coastal areas affected by aquaculture, urban rivers, and ports in south Sumatra," *J. Ecol. Eng.*, vol. 25, no. 1, pp. 303–319, 2024. https://doi.org/10.12911/22998993/175365 ↑3

[3] A. R. Amal Raj, P. Mylsamy, V. Sivasankar, B. S. Kumar, K. Omine, and T. G. Sunitha, "Heavy metal pollution of river water and eco-friendly remediation using potent microalgal species," *Water Sci. Eng.*, vol. 17, no. 1, pp. 41–50, Mar. 2024. https://doi.org/10.1016/J.WSE.2023.04.001 ↑3

[4] S. Naik and S. E. Jujjavarapu, "Self-powered and reusable microbial fuel cell biosensor for toxicity detection in heavy metal polluted water," *J Environ. Chem. Eng.*, vol. 9, no. 4, art. 105318, Aug. 2021. https://doi.org/10.1016/J.JECE.2021.105318 ↑3

[5] G. Crini and E. Lichtfouse, "Advantages and disadvantages of techniques used for wastewater treatment," *Environ. Chem. Lett.*, vol. 17, no. 1, pp. 145–155, Mar. 2019. https://doi.org/10.1007/S10311-018-0785-9/METRICS ↑3

[6] Z. Wang *et al.*, "Overview assessment of risk evaluation and treatment technologies for heavy metal pollution of water and soil," *J. Clean. Prod.*, vol. 379, art. 134043, Dec. 2022. https://doi.org/10.1016/J.JCLEPRO.2022.134043 ↑3

[7] N. Zulfiqar, M. Shariatipour, and F. Inam, "Sequestration of chromium(vi) and nickel(ii) heavy metals from unhygienic water via sustainable and innovative magnetic nanotechnology," *Nanoscale Adv.*, vol. 6, no. 1, pp. 287–301, Dec. 2023. https://doi.org/10.1039/D3NA00923H ↑3

[8] A. Ayele and Y. G. Godeto, "Bioremediation of Chromium by Microorganisms and Its Mechanisms Related to Functional Groups," *J Chem*, vol. 2021, no. 1, p. 7694157, Jan. 2021. https://doi.org/10.1155/2021/7694157 ↑3

[9] J. Jiang *et al.*, "Utilizing adsorption of wood and its derivatives as an emerging strategy for the treatment of heavy metal-contaminated wastewater," *Environ. Poll.*, vol. 340, art. 122830, Jan. 2024. https://doi.org/10.1016/J.ENVPOL.2023.122830 ↑4

[10] Ministerio de Ambiente y Desarrollo Sostenible, "Resolucion 631 de 2015 vertimientos," 2015. [Online]. Available: https://www.minambiente.gov.co/wp-content/uploads/2021/11/resolucion-631-de-2015.pdf ↑4

[11] B. Gupta, A. Mishra, R. Singh, and I. S. Thakur, "Fabrication of calcite based biocomposites for catalytic removal of heavy metals from electroplating industrial effluent," *Environ. Technol. Innov.*, vol. 21, art. 101278, Feb. 2021. https://doi.org/10.1016/J.ETI.2020.101278 ↑4

[12] Y. Wang *et al.*, "Research status, trends, and mechanisms of biochar adsorption for wastewater treatment: A scientometric review," *Environ. Sci. Eur.*, vol. 36, no. 1, pp. 1–17, Feb. 2024. https://doi.org/10.1186/S12302-024-00859-Z ↑4

[13] F. Younas *et al.*, "Current and emerging adsorbent technologies for wastewater treatment: Trends, limitations, and environmental implications," *Water*, vol. 13, no. 2, art. 215, Jan. 2021. https://doi.org/10.3390/W13020215 ↑4

[14] S. Satyam and S. Patra, "Innovations and challenges in adsorption-based wastewater remediation: A comprehensive review," *Heliyon*, vol. 10, no. 9, art. e29573, May 2024. https://doi.org/10.1016/J.HELIYON.2024.E29573 ↑4

[15] R. Yousef, H. Qiblawey, and M. H. El-Naas, "Adsorption as a process for produced water treatment: A review," *Processes*, vol. 8, no. 12, art. 1657, Dec. 2020. https://doi.org/10.3390/PR8121657 ↑4

[16] M. Ince and O. Kaplan Ince, "An overview of adsorption technique for heavy metal removal from water/wastewater: A critical review," *Int. J. Pure Appl. Sci.*, vol. 3, no. 2, pp. 10–19, 2017. https://doi.org/doi.org/10.29132/ijpas.358199 ↑4

[17] A. F. Taiwo and N. J. Chinyere, "Sorption characteristics for multiple adsorption of heavy metal ions using activated carbon from Nigerian bamboo," *J. Mater. Sci. Chem. Eng.*, vol. 04, no. 04, pp. 39–48, 2016. https://doi.org/10.4236/MSCE.2016.44005 ↑4

[18] H. Sukmana, N. Bellahsen, F. Pantoja, and C. Hodur, "Adsorption and coagulation in wastewater treatment – Review," *Prog. Agri. Eng. Sci.*, vol. 17, no. 1, pp. 49–68, Nov. 2021. https://doi.org/10.1556/446.2021.00029 ↑4

[19] K. Erattemparambil, L. Mohan, N. Gnanasundaram, and R. Krishnamoorthy, "Insights into adsorption theory of phenol removal using a circulating fluidized bed system," *Arab. J. Chem.*, vol. 16, no. 6, art. 104750, 2023. https://doi.org/10.1016/j.arabjc.2023.104750 ↑4

[20] W. Liu *et al.*, "Adsorption-based post-combustion carbon capture assisted by synergetic heating and cooling," *Renew. Sust. Energy Rev.*, vol. 191, art. 114141, 2024. https://doi.org/10.1016/j.rser.2023.114141 ↑4

[21] Y. Gao *et al.*, "Interpretation of the adsorption process of toxic Cd2+ removal by modified sweet potato residue," *RSC Adv.*, vol. 14, no. 1, pp. 433–444, 2024. https://doi.org/10.1039/d3ra06855b ↑4

[22] R. Lekshmi *et al.*, "Adsorption of heavy metals from the aqueous solution using activated biomass from Ulva flexuosa," *Chemosphere*, vol. 306, p. 135479, Nov. 2022. https://doi.org/10.1016/J.CHEMOSPHERE.2022.135479 ↑4

[23] R. M. Mohamed *et al.*, "Adsorption of heavy metals on banana peel bioadsorbent," *J. Phys. Conf. Ser.*, vol. 1532, no. 1, art. 012014, Jun. 2020. https://doi.org/10.1088/1742-6596/1532/1/012014 ↑4

[24] T. Arsenie, I. G. Cara, M. C. Popescu, I. Motrescu, and L. Bulgariu, "Evaluation of the adsorptive performances of rapeseed waste in the removal of toxic metal ions in aqueous media," *Water*, vol. 14, no. 24, art. 4108, Dec. 2022. https://doi.org/10.3390/W14244108 ↑4

[25] B. Siriweera and S. Jayathilake, "Modifications of coconut waste as an adsorbent for the removal of heavy metals and dyes from wastewater," *Int. J. Environ. Eng.*, vol. 10, no. 4, art. 329, 2020. https://doi.org/10.1504/IJEE.2020.110458 ↑4

[26] C. T. Tovar, Á. V. Ortiz, and M. J. Villadiego, "Remoción de cromo hexavalente sobre residuos de cacao pretratados químicamente," *Rev. UDCA Act. & Div. Cient.*, vol. 20, no. 1, pp. 139–147, 2017. https://doi.org/10.31910/rudca.v20.n1.2017.71 ↑4

[27] V. Marcantonio, E. Bocci, J. P. Ouweltjes, L. Del Zotto, and D. Monarca, "Evaluation of sorbents for high temperature removal of tars, hydrogen sulphide, hydrogen chloride and ammonia from biomass-derived syngas by using Aspen Plus," *Int. J. Hydrogen Energy*, vol. 45, no. 11, pp. 6651–6662, 2020. https://doi.org/10.1016/j.ijhydene.2019.12.142 ↑4

[28] A. P. Sánchez, E. J. P. Sánchez, and R. M. S. Silva, "Simulation of the acrylic acid production process through catalytic oxidation of gaseous propylene using ChemCAD® simulator," *Ingeniare*, vol. 27, no. 1, pp. 142–150, 2019. https://doi.org/10.4067/S0718-33052019000100142 ↑4

[29] U. Upadhyay, S. Gupta, A. Agarwal, I. Sreedhar, and K. Latitha, "Process optimization at an industrial scale in the adsorptive removal of Cd2 + ions using dolochar via response surface methodology," *Environ. Sci. Poll. Res.*, pp. 0–27, 2021. https://doi.org/10.21203/rs.3.rs-811892/v1 ↑5

[30] A. Hameed, B. H. Hameed, F. A. Almomani, M. Usman, M. M. Ba-Abbad, and M. Khraisheh, "Dynamic simulation of lead(II) metal adsorption from water on activated carbons in a packed-bed column," *Biomass Convers. Biorefin.*, vol. 14, no. 7, pp. 8283–8292, Apr. 2024. https://doi.org/10.1007/S13399-022-03079-8/TABLES/3 ↑5

[31] D. Mohan and C. U. Pittman, "Activated carbons and low cost adsorbents for remediation of tri- and hexavalent chromium from water," *J. Hazard. Mater.*, vol. 137, no. 2, pp. 762–811, Sep. 2006. https://doi.org/10.1016/J.JHAZMAT.2006.06.060 ↑6

[32] B. Hemambika and V. R. Kannan, "Intrinsic characteristics of Cr6+-resistant bacteria isolated from an electroplating industry polluted soils for plant growth-promoting activities," *Appl. Biochem. Biotechnol.*, vol. 167, no. 6, pp. 1653–1667, Jul. 2012. https://doi.org/10.1007/S12010-012-9606-Y/METRICS ↑6

[33] A. Agarwal, U. Upadhyay, I. Sreedhar, and K. L. Anitha, "Simulation studies of Cu(II) removal from aqueous solution using olive stone," *Clean. Mater.*, vol. 5, art. 100128, 2022. https://doi.org/10.1016/j.clema.2022.100128 ↑6

[34] J. Lara, C. Tejada, Á. Villabona, A. Arrieta, and C. Granados Conde, "Adsorción de plomo y cadmio en sistema continuo de lecho fijo sobre residuos de cacao," *Rev. ION*, vol. 29, no. 2, pp. 113–124, Jan. 2016. https://doi.org/10.18273/REVION.V29N2-2016009 ↑6

[35] F. Benyahia and K. E. O'Neill, "Enhanced voidage correlations for packed beds of various particle shapes and sizes," *Part. Sci. Tech.*, vol. 23, no. 2, pp. 169–177, 2005. https://doi.org/10.1080/02726350590922242 ↑6

[36] A. G. Dixon, "Correlations for wall and particle shape effects on fixed bed bulk voidage," *Can. J. Chem. Eng.*, vol. 66, no. 5, pp. 705–708, 1988. https://doi.org/10.1002/cjce.5450660501 ↑6

[37] B. K. Koua, P. M. E. Koffi, and P. Gbaha, "Evolution of shrinkage, real density, porosity, heat and mass transfer coefficients during indirect solar drying of cocoa beans," *J. Saudi Soc. Agri. Sci.*, vol. 18, no. 1, pp. 72–82, 2019. https://doi.org/10.1016/j.jssas.2017.01.002 ↑6

[38] R. Ragadhita, A. Bayu, and D. Nandiyanto, "Curcumin adsorption on zinc imidazole framework-8 particles: Isotherm adsorption using Langmuir, Freundlich, Temkin, And Dubinin-Radushkevich models," *J. Eng. Sci. Tech.*, vol. 17, no. 2, pp. 1078–1089, 2022. https://jestec.taylors.edu.my/Vol%2017%20Issue%202%20April%20%202022/17_2_19.pdf ↑6

[39] S. Nikam, D. Mandal, and P. Dabhade, "LDF based parametric optimization to model fluidized bed adsorption of trichloroethylene on activated carbon particles," *Particuology*, vol. 65, pp. 72–92, 2022. https://doi.org/10.1016/j.partic.2021.05.012 ↑6

[40] M. R. Fouad, "Physical characteristics and Freundlich model of adsorption and desorption isotherm for fipronil in six types of Egyptian soil," *Curr. Chem. Lett.*, vol. 12, no. 1, pp. 207–216, 2023. https://doi.org/10.5267/J.CCL.2022.8.003 ↑7

[41] J. G. Amrutha, C. R. Girish, B. Prabhu, and K. Mayer, "Multi-component Adsorption Isotherms: Review and Modeling Studies," *Environ. Proc.*, vol. 10, no. 2, pp. 1–52, Jun. 2023. https://doi.org/10.1007/S40710-023-00631-0/FIGURES/2 ↑7

[42] T. Ahmad *et al.*, "Enhanced adsorption of bisphenol-A from water through the application of isocyanurate based hyper crosslinked resin," *J. Mol. Liq.*, vol. 395, art. 123861, Feb. 2024. https://doi.org/10.1016/J.MOLLIQ.2023.123861 ↑7

[43] S. Nikam, D. Mandal, and P. Dabhade, "LDF based parametric optimization to model fluidized bed adsorption of trichloroethylene on activated carbon particles," *Particuology*, vol. 65, pp. 72–92, Jun. 2022. https://doi.org/10.1016/J.PARTIC.2021.05.012 ↑7

[44] R. Fran Mansa, A. Osong Patrick, S. Kumaresan, and T. Ming Ling, "Simulation of lead removal using palm kernel shell activated carbon in a packed bed column," 2021. [Online]. Available: https://easychair.org/publications/preprint/GZFQ ↑7

[45] D. C. D. Caldeira, C. M. Silva, F. de Ávila Rodrigues, and A. J. V. Zanuncio, "Aspen Plus simulation for effluent reuse in thermomechanical pulp mills," *Water Sci. Tech.*, vol. 88, no. 3, pp. 751–762, Aug. 2023. https://doi.org/10.2166/WST.2023.242 ↑7

[46] A. Bringas, E. Bringas, R. Ibañez, and M. F. San-Román, "Fixed-bed columns mathematical modeling for selective nickel and copper recovery from industrial spent acids by chelating resins," *Sep. Purif. Tech.*, vol. 313, art. 123457, May 2023. https://doi.org/10.1016/J.SEPPUR.2023.123457 ↑9

[47] H. Patel, "Batch and continuous fixed bed adsorption of heavy metals removal using activated charcoal from neem (Azadirachta indica) leaf powder," *Sci. Rep.*, vol. 10, no. 1, pp. 1–12, 2020. https://doi.org/10.1038/s41598-020-72583-6 ↑9

[48] M. Hardyianto Vai Bahrun, Z. Kamin, S. M. Anisuzzaman, A. Bono, and M. H. V Bahrun, "Assessment of adsorbent for removing lead (pb) ion in an industrial-scaled packed bed column," *J. Eng. Sci. Tech.*, vol. 16, no. 2, pp. 1213–1231, 2021. https://jestec.taylors.edu.my/Vol%2016%20issue%202%20April%202021/16_2_23.pdf ↑11

[49] M. L. R. M. Lubiano, C. V. L. Manacup, A. N. Soriano, and R. V. C. Rubi, "Continuous biosorption of Pb2+ with bamboo shoots (Bambusa spp.) using aspen adsorption process simulation software," *ASEAN J. Chem. Eng.*, vol. 23, no. 2, pp. 153–166, 2023. https://doi.org/10.22146/AJCHE.77314 ↑11

Ángel Darío González-Delgado

Chemical engineer with a PhD in Chemical Engineering. A professor of Chemical Engineering at Universidad de Cartagena, he is versed in areas related to process optimization, biorefineries, biotechnology, biofuels, nanotechnology, and computer-aided process engineering.

Email: agonzalezd1@unicartagena.edu.co

Ángel Villabona-Ortiz

Chemical engineer with a Master's degree in Environmental Engineering. A professor of Chemical Engineering at Universidad de Cartagena, he is knowledgeable in areas related to waste biomass utilization, biofuels, corrosion, industrial wastewater bioremediation, and process simulation.

Email: avillabonao@unicartagena.edu.co

Candelaria Nahir Tejada-Tovar

Chemical engineer with a Master's degree in Education and Environmental Engineering, professor of Chemical

Engineering at Universidad de Cartagena, and academic coordinator of the Master's Program in Chemical Engineering. Her areas of knowledge include waste biomass utilization, biofuels, corrosion, industrial wastewater bioremediation, and process simulation.
Email: ctejadat@unicartagena.edu.co

UNIVERSIDAD DISTRITAL
FRANCISCO JOSÉ DE CALDAS

Ingeniería

https://revistas.udistrital.edu.co/index.php/reving/issue/view/1295

DOI: https://doi.org/10.14483/23448393.22822

Research

Two-Phase Mixture Numerical Study of Nanofluid Flow in a Lithium-Ion Battery Cooling System

Estudio numérico de mezcla bifásica del flujo de nanofluidos en un sistema de enfriamiento para una batería de iones de litio

Amina Benabderrahmane[1] and Samir Laouedj[2]

[1] University of Mustapha Stambouli (Mascara, Algeria)
[2]University Djilali Liabes (Sidi bel abbes, Algeria).

Abstract

Context: The cooling performance of a thermal battery plays a critical role in its efficiency, lifespan, and safety. This importance stems from the heat generated during charging and discharging processes. As temperatures rise, key battery characteristics are significantly affected.

Method: Using the ANSYS Fluent computational fluid dynamics software, a 2D numerical simulation was conducted to study the cooling of a lithium-ion battery in the presence of nanofluids. The flow of nanofluids was analyzed using the multiphase mixture model.

Results: It was found that the coolant inlet velocity significantly impacts the module's temperature distribution and the maximum temperature difference, where the temperature differences almost stabilize for inlet velocities exceeding 0.3 m/s. The effect of using nanofluids was studied with three different types of nanoparticles (alumina, copper, and fullerene) dispersed in water as the base fluid. The results show that the temperature difference in the module varies depending on the nature and volume fraction of the nanoparticles. The incorporation of nanofluids leads to a significant reduction in module temperatures. Fullerene nanoparticles were found to exhibit superior cooling performance compared to other nanoparticle types. On the other hand, a nanoparticle volume fraction exceeding 2 % yields a nearly uniform temperature distribution within the module, as well as reduced cell temperatures.

Conclusions: Nanofluids have an important effect on battery cooling. Optimizing nanoparticle concentration and flow dynamics can effectively improve thermal management strategies for lithium-ion battery systems.

Keywords: computational fluid dynamics, lithium-ion battery, cooling, nanofluids, mixture, battery thermal management

Article history

Received: Oct 24th, 2024

Modified: Jun 16th, 2025

Accepted: Sep 1st, 2025

Ing, vol. 30, no. 3, 2025, e22822

* **Correspondence:** amina.benabderrahmane@univ-mascara.dz

Resumen

Contexto: El rendimiento de refrigeración de una batería térmica desempeña un papel fundamental en su eficiencia, vida útil y seguridad. Esta importancia se debe al calor generado durante los procesos de carga y descarga. A medida que aumentan las temperaturas, las características clave de la batería se ven significativamente afectadas.
Método: Utilizando el *software* de dinámica de fluidos computacional ANSYS Fluent, se realizó una simulación numérica 2D para estudiar el enfriamiento de una batería de iones de litio en presencia de nanofluidos. El flujo de nanofluidos se analizó utilizando el modelo de mezcla multifásica.
Resultados: Se observó que la velocidad de entrada del refrigerante afecta significativamente la distribución de temperatura del módulo y la diferencia máxima de temperatura, donde las diferencias de temperatura prácticamente se estabilizan para velocidades de entrada superiores a 0.3 m/s. Se estudió el efecto del uso de nanofluidos con tres tipos diferentes de nanopartículas (alúmina, cobre y fullereno) dispersas en agua como fluido base. Los resultados muestran que la diferencia de temperatura en el módulo varía según la naturaleza y la fracción de volumen de las nanopartículas. La incorporación de nanofluidos produce una reducción significativa en la temperatura del módulo. Se observó que las nanopartículas de fullereno presentan un rendimiento de refrigeración superior al de otros tipos de nanopartículas. Por otro lado, una fracción de volumen de nanopartículas superior al 2 % da como resultado una distribución de temperatura prácticamente uniforme dentro del módulo, así como una reducción en la temperatura de la celda.
Conclusiones: Los nanofluidos tienen un efecto importante en la refrigeración de las baterías. Optimizar la concentración de nanopartículas y la dinámica del flujo puede mejorar eficazmente las estrategias de gestión térmica de los sistemas de baterías de iones de litio.

Palabras clave: dinámica de fluidos computacional, batería de iones de litio, refrigeración, nanofluidos, mezcla, gestión térmica de la batería.

Table of contents

Page

1. **Introduction** 3
2. **Physical model** 5
3. **Boundary conditions** 6
4. **Governing equations** 7
5. **Mesh independence study** 8
6. **Results and interpretations** 9
   - 6.1. Effect of velocity inlet on cell temperature distribution 9
   - 6.2. Effect of nanofluids on temperature distribution 9
   - 6.3. Effect of nanofluids on heat transfer 11
   - 6.4. Effect of nanoparticle volume fraction on temperature distribution 13
7. **Conclusion** 15
8. **Author contributions** 16
9. **Funding** 16
10. **Data availability** 16
11. **Conflicts of interest** 16
12. **Use of artificial intelligence** 16

Nomenclature

Symbols

C	Specific heat, J/kg·K
Nu	Nusselt number
p	Pressure, Pa
Q	Heat
Re	Reynolds number
T	Temperature, K
t	Time, s
V	Velocity, m/s

Greek Symbols

ρ	Density, kg/m^3
μ	Dynamic viscosity, Pa·s
λ	Thermal conductivity, W/m·K
ϕ	Nanoparticles volume fraction

Subscripts

b	Battery
dr,k	Drift velocity of the k-th phases
k	Number of phases
m	Mixture
p	Particles
w	Water

Acronyms

BTMS	Battery thermal management system
CFD	Computational fluid dynamics
CPCM	Composite phase change material
EV	Electrical vehicle
LIB	Lithium-ion battery
PCM	Phase change material
SOC	State of charge
TEC	Thermoelectric cooling

1. Introduction

Lithium-ion (Li-ion) batteries play an essential role in many modern applications, including electric vehicles, portable electronic devices, and renewable energy storage. The rapid development of this technology has led to a growing demand for efficient cooling systems to maintain batteries' optimum operating temperature. Inadequate battery cooling can lead to reduced efficiency, a shorter lifespan,

and even safety risks, such as overheating and fire. In response to these challenges, extensive research has focused on the use of nanofluids to improve battery cooling processes.

Most researchers have investigated the impact of improved heat transfer on battery performance through experimental, theoretical, and numerical studies. Experimental studies are frequently used to validate numerical results in practical cases, but they are generally more costly than other types of investigations.

(1) proposed an optimization method for the architecture of battery sensor systems based on an online sensing method to capture global electrothermal profiles in large-scale battery packs. Their results demonstrate that the double-layered technique can capture more information in a single step.

(2) experimentally studied the heat generation parameters of battery modules using three electrothermal models: Model A (constant resistance), Model B (resistance varying with depth of discharge), and Model C (resistance varying with both depth of discharge and temperature). They found that model C offers the best results for improving Li-ion battery performance and safety.

(3) numerically investigated the thermal performance of a battery thermal management system (BTMS) using phase change material (PCM) with three different mesh types. Their results demonstrated that the hexahedral mesh performs the closest to the experimental values.

(4) conducted a numerical investigation of the interaction between various fin configurations (namely sinusoidal and positive/negative straight fins) and local oscillation within a finned rectangular enclosure. They found that negative rectangular fins offer higher thermal performance, and that the effectiveness of oscillation decreases when localized between fins.

(5) examined the performance characteristics of Samsung li-ion batteries, *i.e.*, a INR21700 30T high-power (HP) cell and a INR21700 50E high-energy (HE) cell. According to their results, the HP cell had a greater rate capability, retaining 93.8 % of its capacity at 2C discharge, whereas the HE cell did the same at 1.6C.

In another work, the impact of using a thermoelectric cooler (TEC) to cool a Li-ion plate battery was numerically simulated using the COMSOL software (6). The heated part of the TEC was cooled by a heat sink, while the cold part was mounted on the battery. Three main types of heat sink were used. In addition, a non-Newtonian hybrid nanofluid served as the working fluid. For nanofluids with volume fractions of 0.05, 0.25, and 0.5 %, the heat sink temperature, the battery temperature, and the TEC's hot end temperature were calculated by varying the inlet Reynolds number (Re) between 200 and 800. The results showed that the application of Model C resulted in higher TEC temperatures. Models A and B kept the battery and heat sink temperatures low during periods of both low and high Re. As Re increased, the battery, TEC, and heat sink temperatures decreased, while the amount of ΔP increased. The highest and lowest ΔP values were found in Models C and A, respectively. The addition

of nanoparticles increased the ΔP by 267 and ≈ 95 % at Re = 200 and 800, respectively. (7) created electrochemical-thermal combination models for Li-ion cell modules arranged in series, investigating a unique mixed thermal management system comprising (PCM) and liquid cooling via a thermally conductive structure. The hybrid cooling system was initially tuned using this method, studying the impact of cell separation and incoming liquid velocity on electrical, chemical, and thermal efficiencies. As spacing increased, the highest temperature and the selection temperature difference decreased, but once the gap reached around 4 mm, the rate of decrease almost disappeared. The main reason for the discharge imbalance between cells in the battery module was diffusion polarization in the electrolyte, which can be corrected by the proposed hybrid cooling system, according to a theoretical calculation used to assess and quantify unequal discharge.

(8) studied a liquid cooling BTMS for 18650 Li-ion batteries. Nanofluids with high thermal conductivity were used as coolants to improve thermal performance. Various nanofluids were compared against water in order to evaluate their cooling effectiveness. The best-performing solution was a Cu water-based nanofluid, which reduced the maximum temperature difference between the battery and the water by 1.066 K and 12.6 %, respectively. The results show that, although the volume percentage and the displacement velocity of the nanofluids increased simultaneously with the pressure drop, the maximum temperature difference and the maximum battery temperature decreased.

(9) investigated a dual cooling method combining forced convection cooling and convergent channels with composite phase-change material (CPCM). The results showed that, when hybrid cooling is used, the unit temperature drops below the safety limit. In addition, higher temperature uniformity and improved thermal performance are achieved when the CPCM surrounds the battery cell rather than being sandwiched between the cold plates and the battery cell.

Furthermore, a unique liquid cooling system, with stepped and zigzag channels consisting of alumina nanofluid and copper coating, was numerically investigated to improve the cooling capacity and temperature distribution of battery thermal control systems during discharge and charge processes (10). The results suggest that the maximum temperature and the temperature non-uniformity of the battery module were significantly reduced when a cooling alumina nanofluid with a volume fraction of 2 % was added. Various studies using numerical, experimental, and mathematical methods have been conducted to examine the impact of different cooling systems and various coolants on the electrical and thermal performance of many engineering systems (11–26).

2. Physical model

A 2D numerical simulation was conducted in order to study the cooling of a Li-ion battery in the presence of nanofluids. This was done using the ANSYS Fluent computational fluid dynamics (CFD) software. The battery module consisted of 90 cylindrical Li-ion cells with nominal specifications of 54 V/13.2 Ah. The cooling plates, made from aluminum, were sandwiched between two rows of cells. The gaps between two adjacent cells in the x- and y-axes measured 2 and 4 mm, respectively, with air filling

the space between adjacent cells in the x-axis. A detailed schematic diagram of the battery module is shown in Fig. 1.

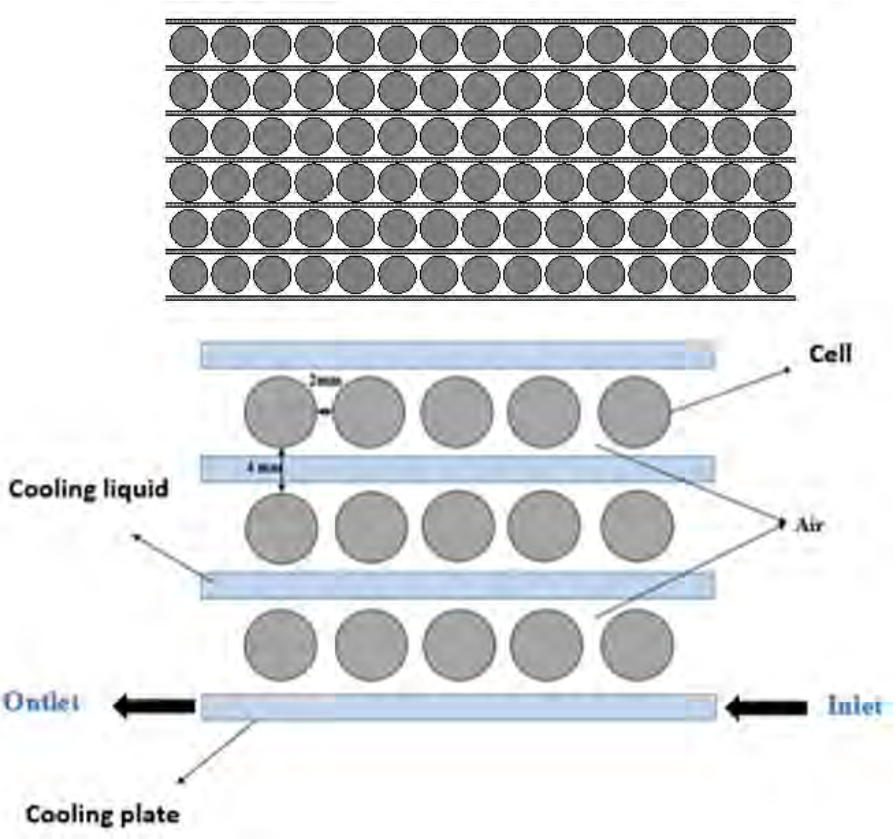

Figure 1. Schematic diagram of the battery module

The key technical specifications of an actual Li-ion battery cell typically include a nominal voltage of 3.7 V and a maximum voltage of around 4.2 V. The lowest voltage that the cell can reach before discharging becomes detrimental is usually around 3.0 V (27). The C-rate is commonly used to represent the charge/discharge rate. It is calculated by dividing the charge/discharge current by the nominal capacity. The cathode is constructed from a lithium cobalt oxide (LCO), and the anode is from graphite. A lithium salt dissolved in an ethylene carbonate is generally used as the electrolyte, which facilitates the movement of lithium ions between the electrodes during the operation of the battery. During discharge, lithium ions move from the anode to the cathode through the electrolyte, and, during charging, the process is reversed.

3. Boundary conditions

The boundary conditions for the inlet and outlet of the liquid cooling system were defined as the velocity inlet and the pressure outlet, respectively (Fig. 1). All surfaces inside the battery module were set as adiabatic boundary conditions. The initial liquid inlet and cell temperatures were set at 25 and 31 °C. The flow was considered to be laminar. In all studies, the Reynolds number was set between 700

and 1800. Three type of nanoparticles were employed in this work: alumina, copper, and fullerene. The thermophysical properties of the materials and nanoparticles are shown in Tables I and II.

Table I. Thermo-physical properties of the battery module materials (27)

	ρ (kg/m^3)	C_p (J/ kg K)	λ (W /mk)
Aluminum	2719	871	202.4
Lithium-ion	2904	894	1.035

Table II. Thermo-physical properties of nanoparticles used (28, 29)

Nanoparticules	ρ (kg/m^3)	C_p (J/ kg K)	λ (W /mk)
Al_2O_3	3970	765	40
Cu	8954	385	401
C	3500	509	2300

4. Governing equations

The energy conservation equations for the cell (battery) and liquid coolant (water) are presented below (30).

$$\rho_b \, C_b \frac{\partial T}{\partial t} = \nabla \cdot (\lambda_b \nabla T) + \dot{Q} \tag{1}$$

$$\rho_w \, C_w \frac{\partial T_w}{\partial t} = \nabla \cdot (\lambda_b \nabla T_w) - \nabla \cdot (\rho_w C_w \vec{v} \, T_w) \tag{2}$$

The equations for the conservation of mass and the momentum of liquid cooling are as follows (31):

$$\frac{d\rho_w}{dt} + \nabla \cdot (\rho_w \vec{v}) = 0 \tag{3}$$

$$\frac{d}{dt}(\rho_w \vec{v}) + \nabla \cdot (\rho_w \vec{v}\vec{v}) = -\nabla p \tag{4}$$

For nanofluid flow simulation, we opted for the mixture two-phase model. The equations governing the flow are presented below (32).

$$\nabla \cdot (\rho_m \, \vec{V}_m) = 0 \tag{5}$$

$$\nabla \cdot \left(\sum_{k=1}^{n} (\rho_k \, C_{pk} \, \phi_k \, V_k \, T) \right) = \nabla \cdot (k_m \nabla T) \tag{6}$$

$$\rho_m \, \vec{V}_m \, \nabla \vec{V}_m = -\nabla p_m + (\mu_m \nabla \vec{V}_m) + \rho_m + \nabla \cdot \left(\sum_{k=1}^{n} (\phi_k \, \rho_k \, \vec{V}_{dr,k} \, \vec{V}_{dr,k}) \right) \tag{7}$$

where the k-th phase's drift velocity is calculated as follows :

$$\vec{V}_{dr,k} = \vec{V}_k - \vec{V}_m \tag{8}$$

The mixture properties are defined below.

$$\text{Velocity:} \quad \vec{V}_m = \frac{\sum_{k=1}^{n} \rho_k \, \phi_k \, \vec{V}_k}{\rho_m} \tag{9}$$

$$\text{Density:} \quad \rho_m = \sum_{k=1}^{n} \rho_k \, \phi_k \tag{10}$$

$$\text{Viscosity:} \quad \mu_m = \sum_{k=1}^{n} \phi_k \, \mu_k \tag{11}$$

5. Mesh independence study

To assess the influence of grid size on the calculations, a grid sensitivity study was conducted, varying the total number of grid distributions in the radial and axial directions. Various combinations of grids were analyzed to ensure that the numerical results were independent of the mesh size used. Table III shows the evolution of the average Nusselt number as a function of the number of cells for a range of Reynolds numbers between 710 and 1775. It was found that increasing the number of meshes does not change the solution but does require more computation time. In this case, we used a mesh with 447 095 cells, since this value is the best in terms of both accuracy and processing timesThese results underscore the fundamental principles of fluid dynamics and heat transfer in battery thermal management. Maintaining optimal fluid velocities is crucial for achieving a uniform temperature distribution and enhancing the overall cooling performance. This physical understanding highlights the necessity of balancing flow dynamics with thermal requirements to optimize battery operation and longevity.. In fact, better accuracy can be obtained by using grid sizes with more nodes, but increasing the density of the cells would in turn increase the computational burden.

Table III. Mesh independence study

	Cells number			
	390210	**447095**	**580043**	
Re		**Nu**		$\varepsilon_{\max}$
710	37.04	37.20	37.17	0.004
1065	47.19	47.95	48.02	0.017
1420	53.33	53.82	54.11	0.014
1775	77.12	77.45	77.78	0.008

6. Results and interpretations

6.1. Effect of velocity inlet on cell temperature distribution

This study focused on exploring how the fluid inlet velocity influences the cooling efficiency of the battery module. Four distinct inlet velocities (0.1, 0.2, 0.3, and 0.4 m/s) were examined under controlled inlet temperature and module conditions. Fig. 2 presents the temperature contours across the module after a rapid charging cycle at varying inlet velocities. Notably, when the inlet velocity is below 0.2 m/s, the temperature distribution within the module exhibits significant non-uniformity.

Figs. 3 and 4 present the module's peak temperature and maximum temperature differential ($\Delta T_{\max}$) as a function of different inlet velocities. Initially, both metrics decrease sharply and stabilize around velocities exceeding 0.3 m/s. This implies that an inlet velocity of 0.3 m/s can adequately facilitate efficient cooling within this water cooling system.

These results underscore the fundamental principles of fluid dynamics and heat transfer in battery thermal management. Maintaining optimal fluid velocities is crucial for achieving a uniform temperature distribution and enhancing the overall cooling performance. This physical understanding highlights the necessity of balancing flow dynamics with thermal requirements to optimize battery operation and longevity.

6.2. Effect of nanofluids on temperature distribution

This study investigated the impact of using nanofluids as coolants. Three types of nanoparticles were employed: copper, alumina, and fullerene. We used a mixture model to simulate the two-phase flow of the nanofluids, with water as the primary phase and nanoparticles dispersed in the base liquid as the secondary phase.

Fig. 5 illustrates the evolution of the temperature difference within the module when nanoparticles are dispersed in water. The results demonstrate that nanofluids can effectively reduce module temperatures thanks to their significantly enhanced heat transfer, which is facilitated by their high thermal conductivity of nanoparticles, *i.e.*, the measure of a material's ability to conduct heat, which plays a crucial role in enhancing the heat dissipation capacity. Notably, the fullerene/water coolant exhibits superior performance, attributed to fullerene's exceptional thermophysical properties, including high thermal conductivity and heat capacity.

Figs. 6 to 9 depict the temperature contours across the module for four different coolants under identical conditions (an inlet temperature of 298 K, an inlet velocity of 0.3 m/s, and a nanoparticle volume fraction of 0.01). These findings underscore the physical mechanisms underlying nanofluid cooling, emphasizing the importance of nanoparticle selection and concentration in optimizing thermal management strategies for battery systems.

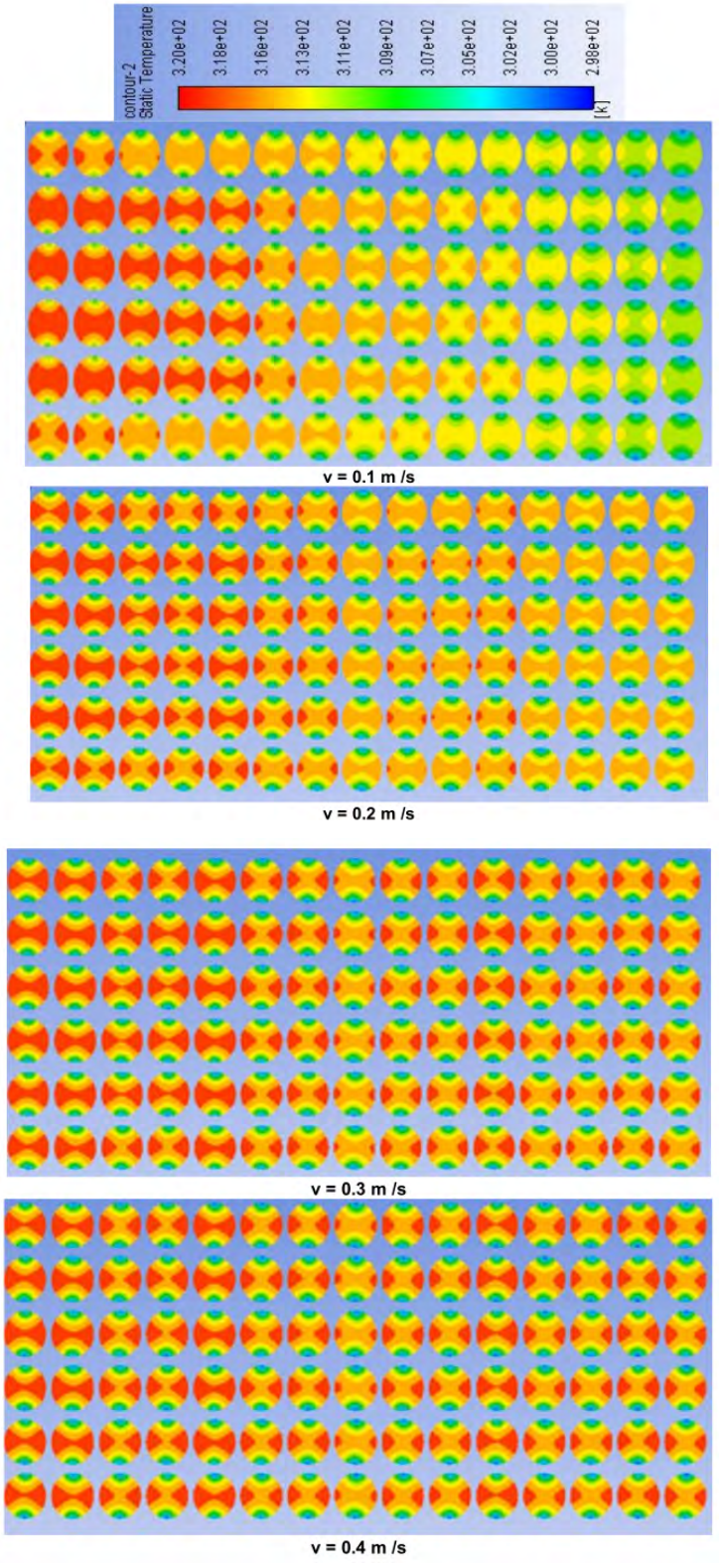

Figure 2. Module temperature contours for different inlet velocities

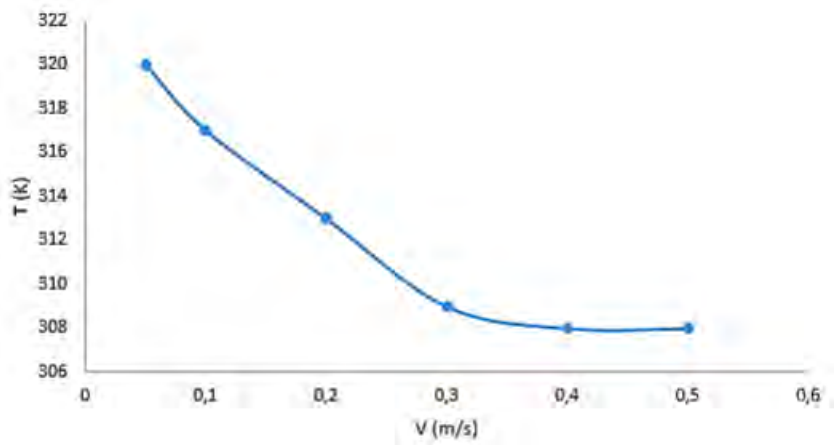

Figure 3. T_{max} of the module as a function of the inlet velocity

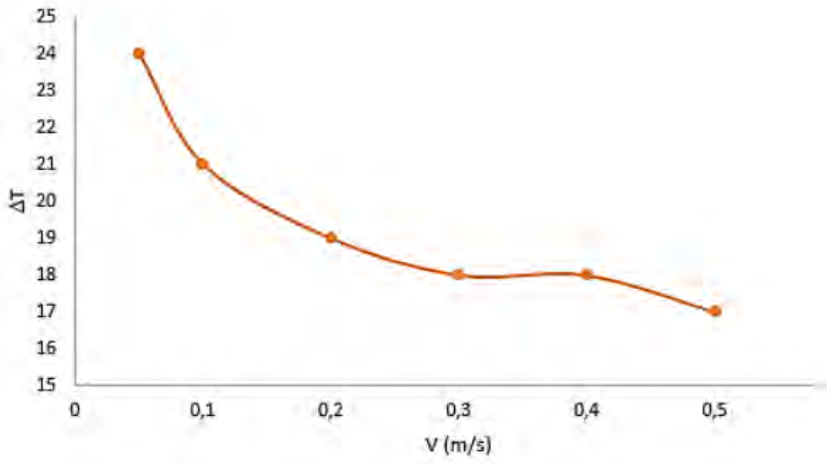

Figure 4. ΔT_{max} of the module as a function of the inlet velocity

6.3. Effect of nanofluids on heat transfer

Fig. 10 demonstrates that the Nusselt number increases proportionally with the Reynolds number and is significantly influenced by the physical properties of the fluid utilized. Notably, the use of nanofluids shows a marked enhancement in this value.

Fig. 11 highlights that the highest Nusselt number was achieved with water/fullerene as the cooling fluid. This notable improvement can be attributed to the exceptional thermal conductivity of fullerene nanoparticles. Thermal conductivity plays a pivotal role in heat transfer efficiency, as it enables a faster dissipation of heat from the battery module. Fullerene's high thermal conductivity enhances convective heat transfer within the cooling system, leading to a more effective cooling performance.

These observations underscore the importance of nanoparticle selection and its impact on enhancing the thermal transport properties of nanofluid-based cooling systems. By optimizing fluid composition

and flow dynamics, engineers can effectively improve heat dissipation and enhance the overall thermal management of battery systems.

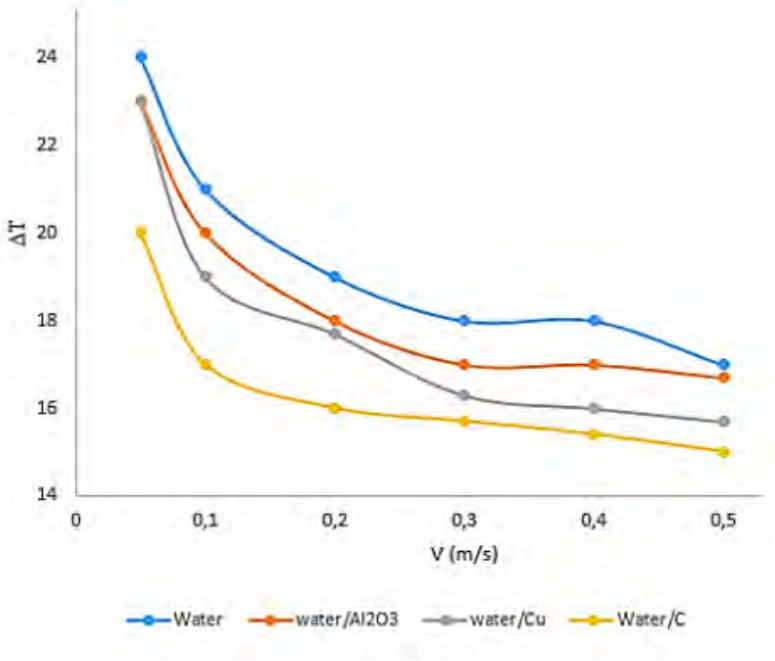

Figure 5. Effect of nanofluids on the ΔT_{max} of the module as a function of the inlet velocity

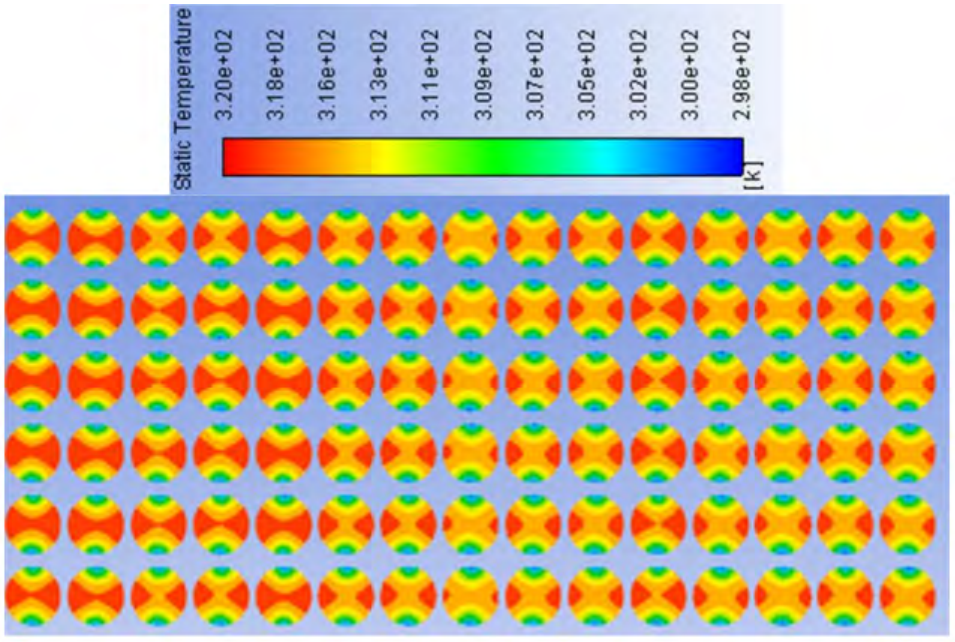

Figure 6. Module temperature contours (cooling fluid: water)

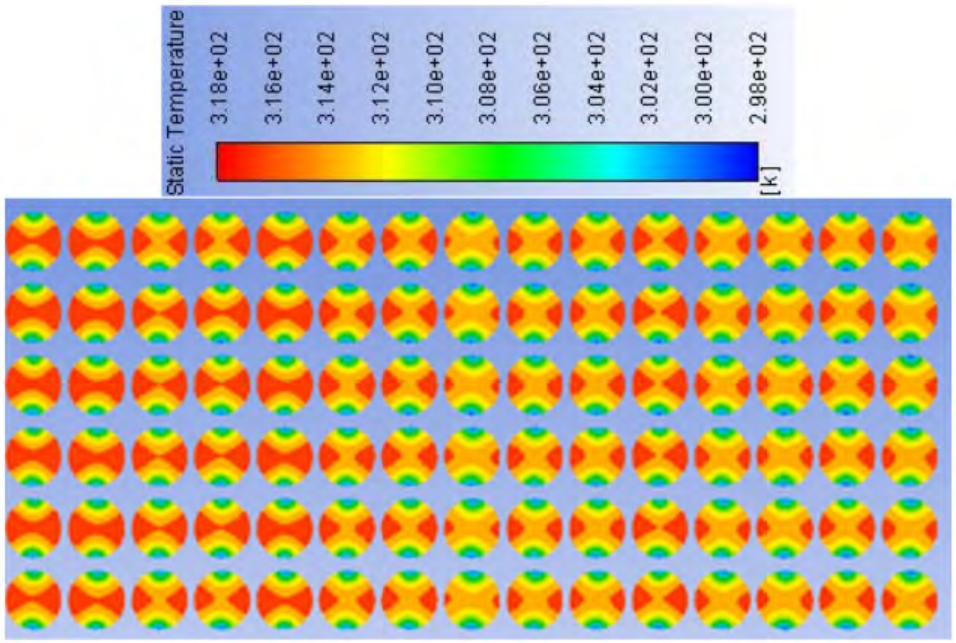

Figure 7. Module temperature contours (cooling fluid: water/Al_2O_3)

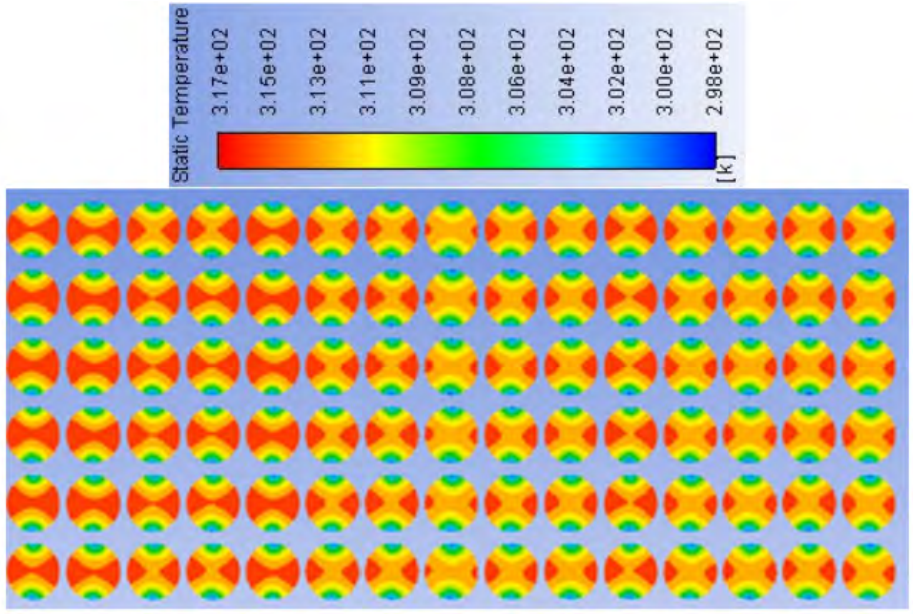

Figure 8. Module temperature contours (cooling fluid: water/Cu)

6.4. Effect of nanoparticle volume fraction on temperature distribution

To investigate the impact of the fullerene nanoparticle volume fraction on the module's temperature distribution, the volume concentration was varied from 0.01 to 0.04. The results are depicted in Fig. 12, where it is evident that the temperature difference decreases with an increasing volume fraction. This reduction indicates that nanofluids effectively contribute to battery cooling.

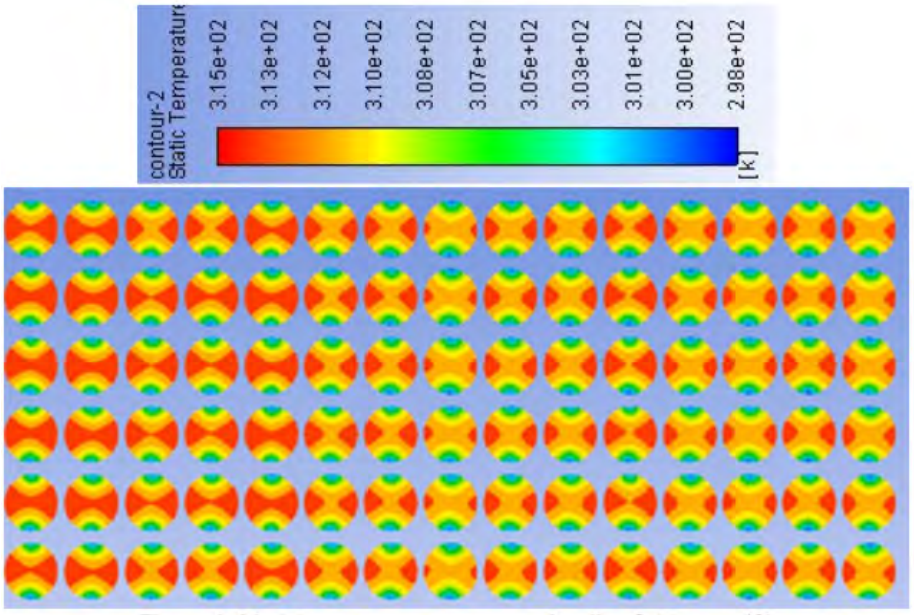

Figure 9. Module temperature contours (cooling fluid: water/C)

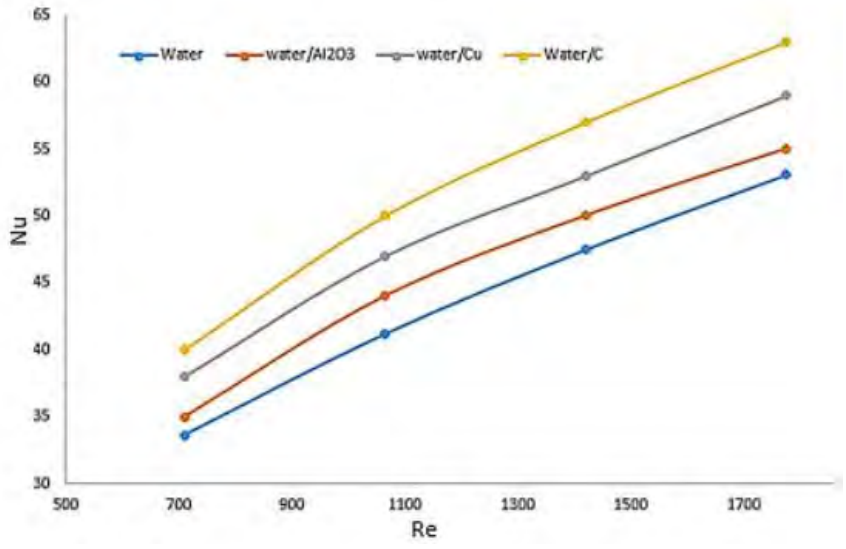

Figure 10. Effect on nanofluids on the Nusselt number as a function of the Reynolds number

It has been widely recognized in the industry that the optimal operating temperature range for Li-Ion Batteries is between 20 and 40 °C, with the temperature difference (ΔT) ideally controlled below 6 °C. Effective thermal management, facilitated by nanofluid cooling systems, plays a critical role in maintaining these temperature parameters within safe and efficient limits.

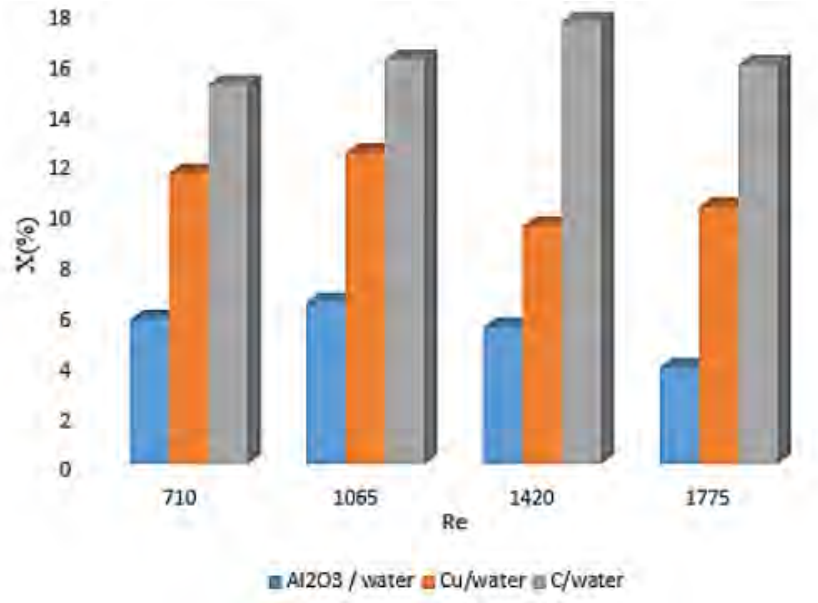

Figure 11. Rate of heat transfer improvement in the presence of nanofluids (ϕ=0.01)

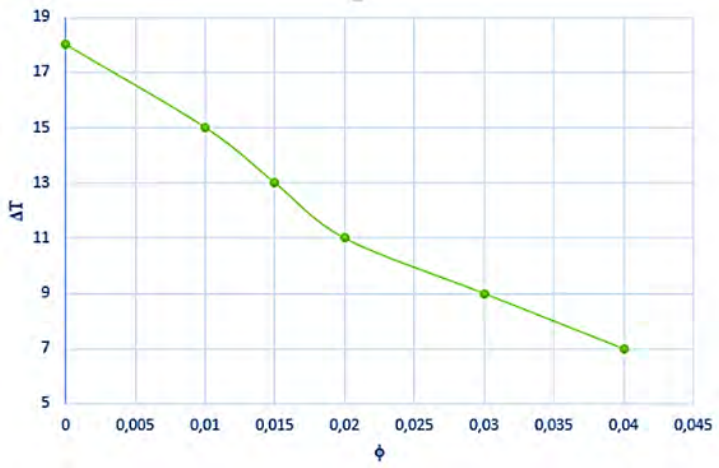

Figure 12. Variation in temperature difference as a function of the fullerene nanoparticle volume fraction (Te=298k, V=0.3 m/s)

7. Conclusion

In this work, a two-dimensional numerical study was conducted, with the aim of investigating the cooling of a Li-ion battery using nanofluids. We employed a stationary laminar regime and utilized the mixture multiphase model to simulate a two-phase flow. The key findings are summarized below.

- The temperature distribution within the battery module exhibits non-uniformity at inlet velocities below 0.2 m/s.
- Temperature differences stabilize noticeably for inlet velocities exceeding 0.3 m/s.

- The incorporation of nanofluids leads to significantly reduced module temperatures.
- Fullerene nanoparticles demonstrate superior cooling performance compared to other nanoparticle types.
- Achieving a nanoparticle volume fraction exceeding 2 % results in a nearly uniform temperature distribution within the module, as well as in reduced cell temperatures.

These results underscore the effectiveness of nanofluids in enhancing battery cooling efficiency, with fullerene nanoparticles proving particularly advantageous. Optimizing the nanoparticle concentration and flow dynamics can effectively improve thermal management strategies for Li-ion battery systems.

8. Author contributions

Amina Benabderrahmane: was mainly responsible for the development of the methodology, the implementation of the numerical model, and the collection and organization of the results. She also prepared the first draft of the manuscript.
Samir Laouedj: contributed to the conceptualization of the study and the validation of the results obtained. He supervised the research work, provided critical revisions to the manuscript, and ensured the scientific consistency of the paper.

9. Funding

This research received no external funding.

10. Data availability

The data will be made available upon request.

11. Conflicts of interest

The authors declare no conflict of interest.

12. Use of artificial intelligence

During this work, the authors did not employ any technologies associated with artificial intelligence.

References

[1] W. Li *et al.*, "A holistic electrothermal profiles online sensing method with sparse sensor system in large-format battery pack," *IEEE Trans. Ind. Elect.*, vol. 72, no. 10, pp. 10257-10266, 2025. https://doi.org/10.1109/TIE.2025.3555004 ↑4

[2] S. Vashisht, D. Rakshit, S. Panchal, M. Fowler, and R. Fraser, "Experimental estimation of heat generating parameters for battery module using inverse prediction method," *Int. Comm. Heat Mass Trans.*, vol. 162, art. 108539, 2025. https://doi.org/10.1016/j.icheatmasstransfer.2024.108539 ↑4

[3] E. Yousefi *et al.*, "Electrochemical-thermal modeling of phase change material battery thermal management systems: investigating mesh types for accurate simulations," *Int. J. Heat Mass Tran.*, vol. 247, art. 127107, 2025. https://doi.org/10.1016/j.ijheatmasstransfer.2025.127107 ↑4

[4] A. H. Vakilzadeh, A. B. Sarvestani, K. Javaherdeh, R. Kamali, and S. Panchal, "To what extent does local oscillation influence the thermal performance of finned PCM-based energy storage systems: A numerical study," *Int. J. Heat Fluid Flow*, vol. 114, art. 109798, 2025. https://doi.org/10.1016/j.ijheatfluidflow.2025.109798 ↑4

[5] Q. Yao, P. Kollmeyer, J. Chen, S. Panchal, O. Gross, amd A. Emadi, "Study of high-power and high-energy lithium-ion batteries: From parameter analysis to physical modeling and experimental validation" SAE Technical Paper, 2025. [Online]. Available: https://www.sae.org/publications/technical-papers/content/2025-01-8372/ ↑4

[6] H. Alhumade, E. Almatrafi, M. Rawa, A. S. El-Shafay, C. Qi, and Y. Khetib, "Numerical study of simultaneous use of non-Newtonian hybrid nano-coolant and thermoelectric system in cooling of lithium-ion battery and changes in the flow geometry," *J. Power Sources*, vol. 540, art. 231626, 2022. https://doi.org/10.1016/j.jpowsour.2022.231626 ↑4

[7] Y. Yang *et al.*, "Thermal-electrical characteristics of lithium-ion battery module in series connection with a hybrid cooling," *Int. J. Heat Mass Tran.*, vol. 184, art. 122309, 2022. https://doi.org/10.1016/j.ijheatmasstransfer.2021.122309 ↑5

[8] G. Liao, W. Wang, F. Zhang, E. Jiaqiang, J. Chen, and E. Leng, "Thermal performance of lithium-ion battery thermal management system based on nanofluid," *Appl. Therm. Eng.*, vol. 216, art. 118997, 2022. https://doi.org/10.1016/j.applthermaleng.2022.118997 ↑5

[9] M. Faizan, S. Pati, and P. Randive, "Implications of novel cold plate design with hybrid cooling on thermal management of fast discharging lithium-ion battery," *J. Energy Storage*, vol. 53, art. 105051, 2022. https://doi.org/10.1016/j.est.2022.105051 ↑5

[10] A. Sarchami *et al.*, "A novel nanofluid cooling system for modular lithium-ion battery thermal management based on wavy/stair channels," *Int. J. Therm. Sci.*, vol. 182, art. 107823, 2022. https://doi.org/10.1016/j.ijthermalsci.2022.107823 ↑5

[11] K. Joshi, D. Dandotiya, C. S. Ramesh, and S. Panchal, "Numerical analysis of battery thermal management system using passive cooling technique," SAE Technical Paper, 2023. [Online]. Available: https://doi.org/10.4271/2023-01-0990 ↑5

[12] S. Panchal, V. Pierre, M. Cancian, O. Gross, F. Estefanous, and T. Badawy, "Development and validation of cycle and calendar aging model for 144Ah NMC/graphite battery at multi temperatures, DODs, and C-rates," SAE Technical Paper, 2023. [Online]. Available: https://doi.org/10.4271/2023-01-0503 ↑5

[13] H. A. Hasan, S. Jenan, M. A. Azher, S. S. Hakim, and K. Sopian, "Improve the performance of solar thermal collectors by varying the concentration and nanoparticles diameter of silicon dioxide, Open Engineering, vol. 12, no. 1, pp. 743–751, 2022. https://doi.org/10.1515/eng-2022-0339 ↑5

[14] K. A. Ameen, M. J. A. Hasan, Al-Dulaimi, A. M. Abed, and F. Haidar, "Improving the performance of air conditioning unit by using a hybrid technique," *MethodsX*, vol. 9, art. 101620, 2022. https://doi.org/10.1016/j.mex.2022.101620 ↑5

[15] W. Li *et al.*, "An internal heating strategy for lithium-ion batteries without lithium plating based on self-adaptive alternating current pulse," *IEEE Trans. Vehic. Tech.*, vol. 72, no. 5, pp. 5809–5823, 2022. https://doi.org/10.1109/TVT.2022.3229187 ↑5

[16] H. A. Hasan, S. S. Jenan, J. M. Mahdi, H. Togun, M. A. Azher, R. K. Ibrahim, and W. Yaïci, "Experimental evaluation of the thermoelectrical performance of photovoltaic-thermal systems with a water-cooled heat sink," *Sustainability*, vol. 14, no. 16, art. 10231, 2022. https://doi.org/10.3390/su141610231 ↑5

[17] R. Braga *et al.*, "Transient electrochemical model development and validation of a 144 Ah cell performance under different drive cycles conditions," SAE Technical Paper, 2023. [Online]. Available: https://doi.org/10.4271/2023-01-0513 ↑5

[18] N. S. Rukman *et al.*, "Bi-fluid cooling effect on electrical characteristics of flexible photovoltaic panel," *J. Mech. Electr. Power, and Veh. Tech.*, vol. 12, no. 1, pp. 51–56, 2021. https://doi.org/10.14203/J.MEV.2021.V12.51-56 ↑5

[19] C. Vivek, A. S Dhoble, S. Panchal, D. Fowler, and D. Fraser, "Experimental and numerical investigation on thermal characteristics of 2×3 designed battery module," 2023. [Online]. Available: https://dx.doi.org/10.2139/ssrn.4568465 ↑5

[20] H. N. Khaboshan, F. Jaliliantabar, A. Abdullah, and S. Panchal, "Improving the cooling performance of cylindrical lithium-ion battery using three passive methods in a battery thermal management system," *Appl. Therm. Eng.*, vol. 227, art. 120320, 2023. https://doi.org/10.1016/j.applthermaleng.2023.120320 ↑5

[21] K. A. Ameen., M. J. Al-Dulaimi, H. A. Abrahem, and H. A. Hasan, "Experimental study to increase the strength of the adhesive bond by increasing the surface area arrangement," *IOP Conf. Ser. Mater. Sci. Eng.*, vol. 765, pp. 1–10, 2020. https://doi.org/10.1088/1757-899X/765/1/012054 ↑5

[22] A. M. Aboghrara, B. T. H. T. Baharudin, M. A. Alghoul, N. M. Adam, A. A. Hairuddin, H. A. Hasan, "Performance analysis of solar air heater with jet impingement on corrugated absorber plate," *Case Stud. Therm. Eng.*, vol. 10, pp. 111–120, 2017. https://doi.org/10.1016/j.csite.2017.04.002 ↑5

[23] H. Abdulrasool, A. Ali, L. Abdulredh, and M. A. Azher, "Numerical investigation of nanofluids comprising different metal oxide nanoparticles for cooling concentration photovoltaic thermal CPVT," *Cleaner Eng. Tech.*, vol. 10, art. 100543, 2022. https://doi.org/10.1016/j.clet.2022.100543 ↑5

[24] H. Togun *et al.*, "Numerical simulation on heat transfer augmentation by using innovative hybrid ribs in a forward-facing contracting channel," *Symmetry*, vol. 15, no. 3, art. 690, 2023. https://doi.org/10.3390/sym15030690 ↑5

[25] A-dulaimi, J. Mustafa, H. H. Areej, H. A. Hasan, and F. A. Hamad, "Energy and exergy investigation of a solar air heater for different absorber plate configurations," *Int. J. Automot. Mech. Eng.*, vol. 20, no. 1, pp. 10258–10273, 2023. https://journal.ump.edu.my/ijame/article/view/7317/2742 ↑5

[26] A. Hasan, H. T. Husam, M. A. Azher, I. M. Hayder, and N. Biswas, "A novel air-cooled Li-ion battery (LIB) array thermal management system – a numerical analysis," *Int. J. Therm. Sci.*, vol. 190, art. 108327, 2023. https://doi.org/10.1016/j.ijthermalsci.2023.108327 ↑5

[27] M. Bahiraei, F. Nazri, and G. A. Saif, « Electrochemical-thermal model of pouch-type lithium-ion batteries," *Electrochimica Acta*, vol. 247, pp. 569-587, 2017. http://dx.doi.org/10.1016/j.electacta.2017.06.164 ↑6, 7

[28] M. S. A. Kashkooli, F. M. Ghalambaz, and A. J. Chamkha, "Free convection of hybrid Al2O3-Cu water nanofluid in a differentially heated porous cavity," *Adv. Powder Tech.*, vol. 28, no. 9, pp. 2295-2305, 2017. https://doi.org/10.1016/J.APT.2017.06.011 ↑7

[29] Y. Pan *et al.*, "Advances in photocatalysis based on fullerene C60 and its derivatives: Properties, mechanism, synthesis, and applications," *App. Catal. B Environ*, vol. 265, art. 118579, 2020. https://doi.org/10.1016/j.apcatb.2019.118579 ↑7

[30] Z. Rao, Z. Qian, Y. Kuang, and Y. Li, "Thermal performance of liquid cooling based thermal management system for cylindrical lithium-ion battery module with variable contact surface," *Appl. Therm. Eng.*, vol. 123, pp. 1514–1522, 2017. https://doi.org/10.1016/j.applthermaleng.2017.06.059 ↑7

[31] Y. Huo, Z. Rao, X. Liu, and J. Zhao, "Investigation of power battery thermal management by using mini-channel cold plate," *Energy Convers. Manage.*, vol. 89, pp. 387–395, 2015. https://doi.org/10.1016/j.enconman.2014.10.015 ↑7

[32] A. Benabderrahmane, A. Benazza, S. Laouedj, and J. P. Solano, "Numerical analysis of compound heat transfer enhancement by single and two-phase models in parabolic trough solar receiver," *Mechanika*, vol. 23, pp. 55-61, 2017. https://doi.org/10.5755/j01.mech.23.1.14053 ↑7

UNIVERSIDAD DISTRITAL
FRANCISCO JOSÉ DE CALDAS

Ingeniería

https://revistas.udistrital.edu.co/index.php/reving/issue/view/1295

DOI: https://doi.org/10.14483/23448393.23272

Research

Experimental Performance of a Two-Stage Cross-Coupled MOS-Based Circuit in the Solar and Piezoelectric Energy Harvesting

Análisis experimental del rendimiento de un circuito basado en MOS de par cruzado de dos etapas en la captación de energía solar y piezoeléctrica

Joydeep Banerjee[1]

[1]Assistant professor, Department of Electronics & Communication Engineering, MCKV Institute of Engineering, Howrah, India.

Abstract

Context: Energy harvesting has positioned itself an emerging area of research due to recent developments in low-power electronics, the Internet of Things, and artificial intelligence. Various diode-based circuits and alternatives have been proposed in the literature, but the application of CMOS cross-coupled circuits, specifically in piezoelectric energy-harvesting systems, has not been properly explored.
Method: An experimental study was conducted in order to assess the performance of a two-stage cross-couple MOS-based voltage multiplier in piezoelectric and solar energy harvesting. A piezoelectric disc was used to evaluate the output. The piezoelectric output was obtained by applying a small pressure to the input, and a 6 V panel was employed in the solar energy setup.
Results: The proposed circuit provides a 1.91-fold voltage gain in the piezoelectric energy harvester.
Conclusions: The two-stage MOS-based cross-coupled voltage multiplier circuit performs better than the diode-based alternative in the piezoelectric energy harvester. These experimental results show encouraging prospects for green energy, low-power electronics, and Internet of Things applications, among others.

Keywords: piezoelectric energy, cross-coupled MOS, voltage multiplier, solar boost converter, solar energy harvesting.

Article history

Received:
Feb 20th, 2025

Modified:
Jul 28th, 2025

Accepted:
Sep 1st, 2025

Ing, vol. 30, no. 3, 2025, e23272

*Correspondence: idjoydeepbu81@gmail.com

Resumen

Contexto: La recolección de energía se ha posicionado como un área de investigación emergente debido a los desarrollos recientes en electrónica de baja potencia, el Internet de las Cosas y la inteligencia artificial. La literatura ha propuesto diversos circuitos basados en diodos y otras alternativas, pero la aplicación de circuitos CMOS de tipo *cross-coupled*, específicamente en sistemas piezoeléctricos de recolección de energía, no ha sido explorada adecuadamente.
Método: Se llevó a cabo un estudio experimental para evaluar el desempeño de un multiplicador de voltaje de dos etapas basado en transistores MOS tipo *cross-coupled* en la recolección de energía piezoeléctrica y solar. Se utilizó un disco piezoeléctrico para evaluar la salida. La señal piezoeléctrica se obtuvo aplicando una pequeña presión en la entrada, y en la configuración solar se empleó un panel de 6 V.
Resultados: El circuito propuesto proporciona una ganancia de voltaje de 1.91 veces en el recolector de energía piezoeléctrica.
Conclusiones: El circuito multiplicador de voltaje de dos etapas, basado en transistores MOS tipo *cross-coupled*, presenta un mejor desempeño que la alternativa basada en diodos en el recolector de energía piezoeléctrica. Estos resultados experimentales brindan perspectivas alentadoras para aplicaciones de energía verde, electrónica de baja potencia y el Internet de las Cosas, entre otras.

Palabras clave: energía piezoeléctrica, MOS *cross-coupled*, multiplicador de voltaje, convertidor elevador solar, recolección de energía solar

Table of contents

Page

1. Introduction 2
2. Cross-coupled MOS-based voltage multipliers and their advantages 3
3. Experimental setup and performance analysis 4
4. Comparison 7
5. Conclusions 9
6. Funding 10
7. Data availability 10
8. Conflicts of interest 10
9. Use of artificial intelligence 10

1. Introduction

Energy harvesting has positioned itself an emerging area of research due to recent developments in low-power electronics, the Internet of Things (IoT), and artificial intelligence (AI). Various diode-based circuits and alternatives have been proposed in the literature, aiming for the development of different technologies (1–3).

For instance, (4) presented a review on powering different wireless sensors from ambient energy sources. Multiband RF energy-harvesting circuits (5) have also been proposed. (6) discussed the recent advancements in different energy-harvesting technologies, and (7) proposed the use of CMOS circuits for efficient RF-to-DC energy conversion. (8) used an NMOS RF-to-DC rectifier, achieving a

57.6 % power efficiency. However, it is difficult to implement diode-based circuits in typical CMOS processes (9,10). MOS-based energy harvesting circuits are rather scarce in the specialized literature, and they yield lower output voltage and power compared to conventional diode-based energy-harvesting circuits (11,12). This is due to the large drain-to-source voltage drop (13).

MOS-based circuits (Dickson, Villard, *etc.*) offer better a performance. Among them, the Dickson charge pump is very popular in energy harvesting. For example, (9) proposed a high-gain MOS-based traditional Dickson charge pump circuit, and (10) introduced a step-up converter using a MOSFET-based Dickson charge pump. The latest development is a cross-couple MOS-based circuit (14, 15), which significantly improves AC-to-DC conversion efficiency while exhibiting a low ripple at the output when compared to MOS-based Dickson charge pumps. Furthermore, (16) proposed a modified cross-coupled energy-harvesting circuit that provided 46 % efficiency using 180 nm CMOS technology. On the other hand, (17) proposed a cross-coupled active rectifier-booster for broadband wireless energy harvesting, and (18) proposed a self-bias cross-coupled MOS rectifier for RF energy harvesting. (19) compared the performance of diode-based and cross-coupled MOS-based circuits. However, to the best of the author's knowledge, the application of CMOS cross-coupled circuits, specifically in piezoelectric energy-harvesting circuits, has not been properly explored in the literature. This work proposes a cross-coupled voltage multiplier circuit for solar (20–23) and piezoelectric energy (24–26) harvesting applications.

This study evaluated the experimental performance of a two-stage MOS-based cross-coupled voltage multiplier circuit for piezoelectric and solar energy-harvesting systems. 3205 n-channel and 9250 p-channel MOSFETs, as well as 100 nF capacitors, were used for designing the aforementioned circuit. The basic block diagram of this proposal is shown in Fig. **1**. In addition, it should be noted that a self-driven solar-powered boost converter (27,28) was considered.

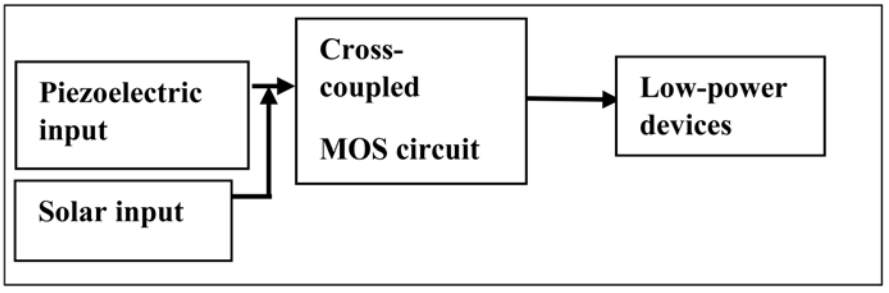

Figure 1. Block diagram of the cross-coupled MOS-based piezoelectric energy-harvesting circuit

2. Cross-coupled MOS-based voltage multipliers and their advantages

The two-stage cross-coupled MOS-based voltage multiplier circuit (29) is shown in Fig. **2**. The circuit consists of two n-channel MOS and two p-channel MOS at every stage. It has a low threshold voltage

drop and is suitable for energy-harvesting applications. The output voltage for the n-stage using Eq. (1).

$$D_{DC} = N \cdot V_m \tag{1}$$

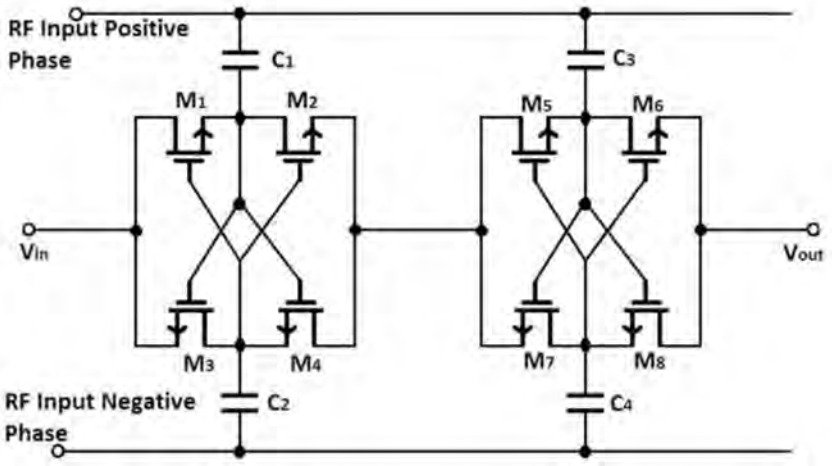

Figure 2. Two-stage cross-coupled MOS-based energy-harvesting circuit

3. Experimental setup and performance analysis

A simple experimental setup was designed to analyze the performance of the proposed circuit. A 1 MHz function generator was used for applying the input voltage, as well as a dual trace CRO for observing the input and output waveform. The output voltage was measured by means of a voltmeter.

For the experimental study, a 1 V peak AC signal was applied at the input of the two-stage cross-coupled voltage multiplier circuit, which provided a 747 mV DC voltage at the output (Fig. 3).

Next, the performance of the multiplier circuit was studied in the context of a piezoelectric energy harvester, as shown in Fig. 4. Using one finger, a small pressure was applied on the disc-type piezoelectric materials. This yielded a 6.88 V rectified DC output voltage for a 3.6 V AC input.

The output current of the Piezo-electric harvester was also measured. The maximum DC output current of the proposed multiplier circuit was 8 uA for a 1 KOhm load at the output (Fig. 5).

Then, we assessed the output performance of a three-stage Schottky diode-based voltage multiplier circuit in the piezoelectric energy harvester. This circuit is a combination of the Greinacher and Villard voltage multiplier circuits. At the input, a 2.5 V AC input signal was applied via piezoelectric pressure, as shown in Fig. 6. The analyzed circuit provided a 3.62 V rectified DC output voltage. This experimental study revealed that cross-coupled voltage multiplier circuits yield a comparatively higher output voltage than their diode-based counterparts in piezoelectric energy-harvesting circuits.

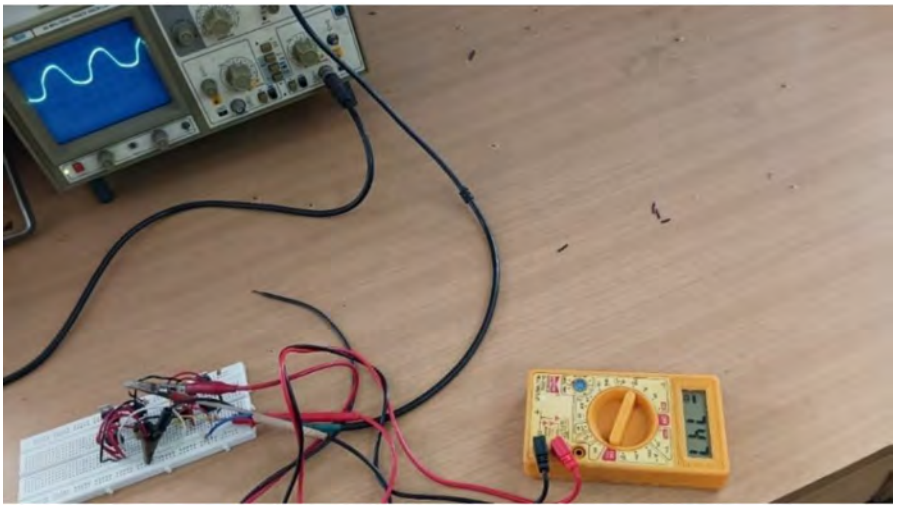

Figure 3. Rectified DC output voltage of the proposed circuit

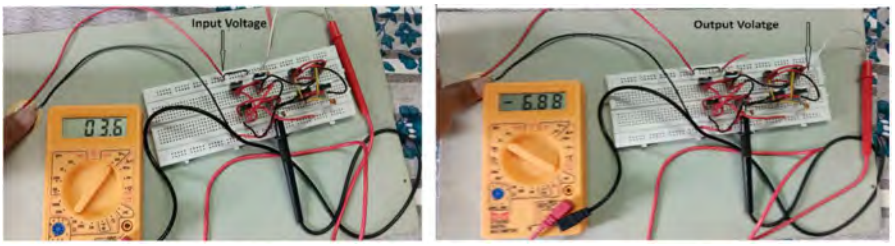

Figure 4. AC input and rectified DC output of the two-stage cross-coupled piezoelectric harvester

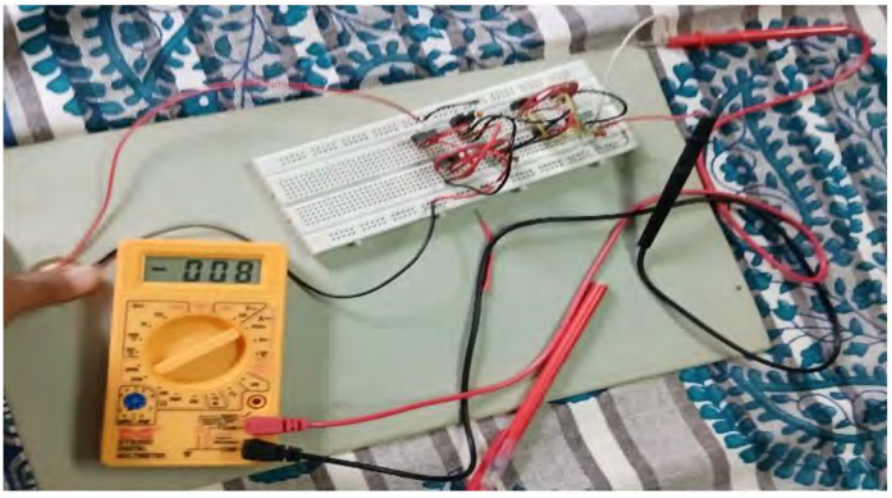

Figure 5. Output current of the proposed piezoelectric energy harvester

The different experimental output parameters of the piezoelectric energy harvester were determined for varying load resistance values. This is summarized in Table I.

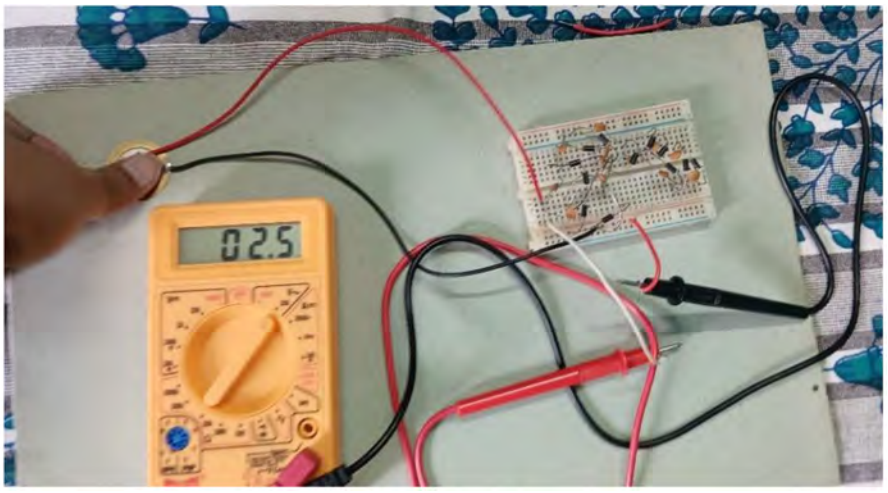

Figure 6. Input voltage from of the piezoelectric energy harvester with the diode-based circuit

Table I. Output parameters of the piezoelectric energy harvester for different load resistances

Maximum input voltage (V)	Load resistance (KΩ)	Output voltage (mV)	Output current (μA)	Output power (μW)
5.86	0.220	2.27	25	0.056
	1	8	20	0.16
	10	127	17	2.15
	100	1130	13	14.69
	1000	7380	10	73.8
	Open	8620	-	-

Afterwards, the performance of the cross-coupled voltage multiplier circuit was analyzed on a solar energy source. To this effect, a 6 V solar panel was used, with the aim of enhancing its output voltage. The DC output of the solar panel was converted into a pulse signal by means of a pulse generator, using a simple 7414 IC. The output voltage was 1.40, as well as 1.35 V for the open circuit, for a 1 MΩ resistance (Fig. 7).

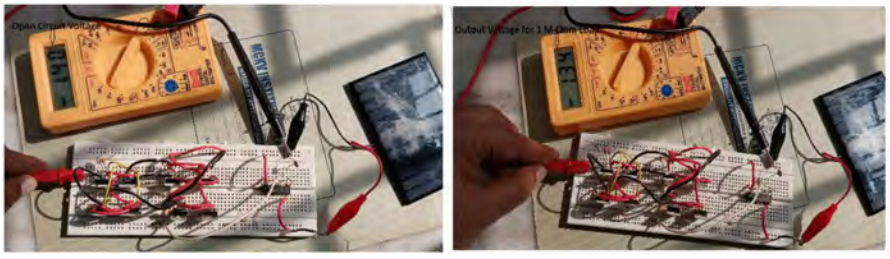

Figure 7. Voltages obtained for a 1 MΩ load resistance

The experimental results show that the cross-coupled voltage multiplier circuit provides a better output for the piezoelectric energy harvester when compared to the solar panel.

4. Comparison

Using ORCAD 10.5, the simulated performance of the proposed cross-coupled voltage multiplier circuit was determined, as shown in Fig. 8. The results were compared against the findings from our experiments. The simulated *vs.* experimental output performance of the circuit in the piezoelectric energy harvester is shown in Fig. 9. Note that the experimental values almost follow the simulated ones. The same AC input voltage of 3.6 V was applied in both studies. As previously mentioned, 3205 n-channel and 9250 p-channel MOSFETs, as well as 100 nF capacitors, were used for designing the proposed circuit. Both MOS have a low resistance, and the 9250 p-channel exhibits a fast switching speed. On the other hand, the simulation employed a 3205 N MOSFET and 100 nF capacitors. The 3205 N MOSFET had a resistance of 8 mΩ. These MOSFETs can be operated at a 100 V drain-to-source voltage. By means of simulation, a transient analysis of the proposed circuit was carried out.

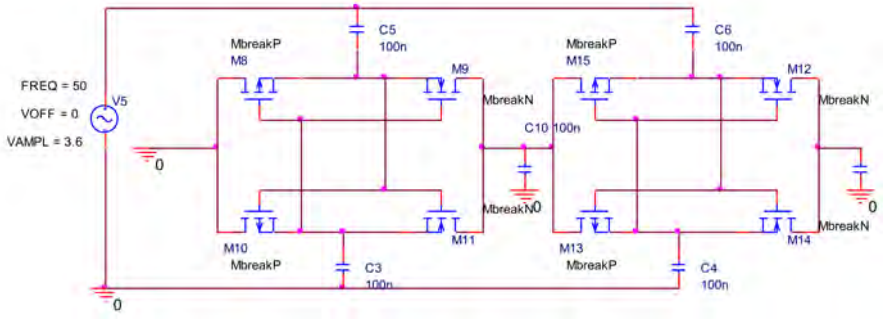

Figure 8. Two-stage cross-coupled MOS-based voltage multiplier circuit

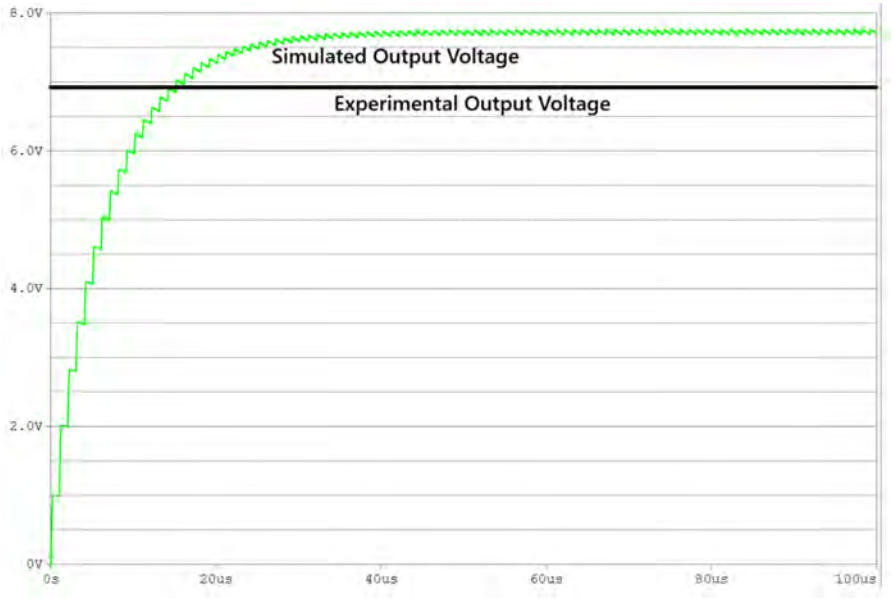

Figure 9. Comparison between experimental and simulated results

The output power and the efficiency of the proposed circuit were also determined: it provides 2.2 mW of rectified output power for a 100 Ω load under a 1 V AC input (Fig. 10). The input power was calculated using Eq. (2).

$$P_{\text{in}} = \frac{V^2_{\text{peak-peak}}}{2 \cdot \sqrt{2} \cdot R_L} \tag{2}$$

3.53 mW were obtained for a 1 V AC input and a 100 Ω load resistance.

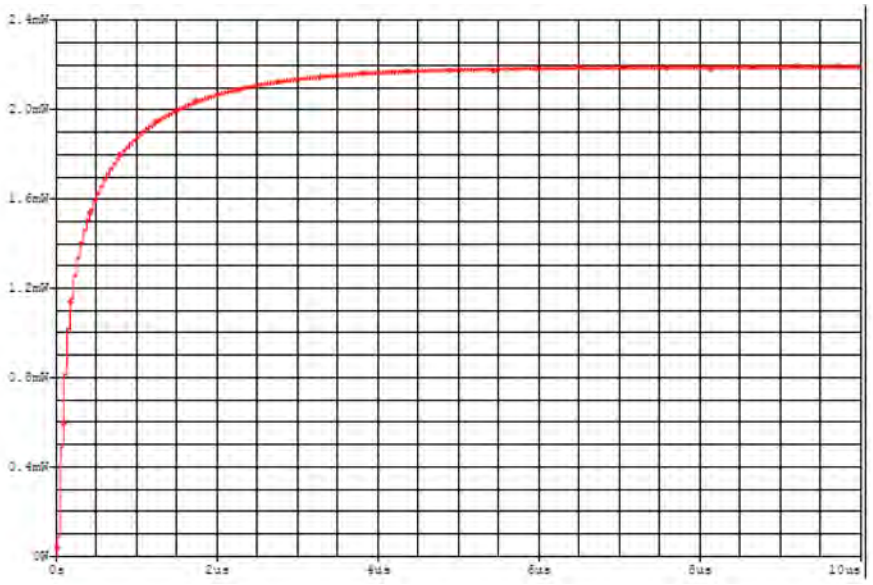

Figure 10. Simulated power for a 100 Ω load resistance

The proposed circuit exhibited a 62.32 % efficiency, as calculated using Eq. (3).

$$\%\text{Efficiency} = \frac{P_{\text{out}}}{P_{\text{in}}} \times 100\,\% \tag{3}$$

This experimental study revealed that our cross-coupled voltage multiplier is suitable for enhancing the output level of the analyzed piezoelectric energy harvester and solar-powered boost converter (Fig. 11). Table II compares the output performance of different energy-harvesting sources.

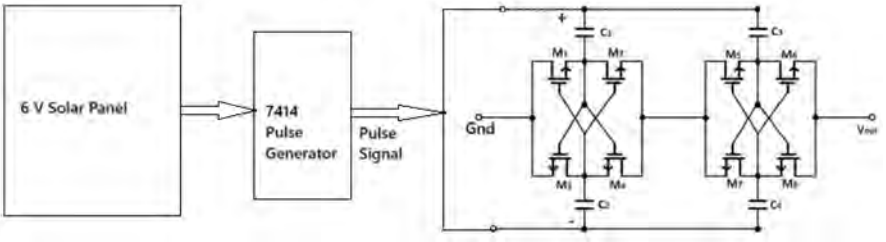

Figure 11. Solar-powered energy harvester

Table II. Comparison of experimental and simulated results for the proposed energy harvester

Energy harvesting circuit	Method	V_{in} (V)	V_{out} (V)
Cross-coupled MOS-based voltage multiplier circuit	Experimental values	3.6	6.86
	Simulated values	3.6	7.2

The design parameters of the proposed circuits are summarized in Table III.

Table III. Design parameters of the MOS-based cross-coupled circuit

Circuit	Components	Load resistance values
Two-stage cross-coupled voltage multiplier	IRF 3205, 9540N MOSFET, 100 nF capacitors,	220 Ω, 1 KΩ, 10 KΩ, 1 MΩ

A comparison of the author's proposed circuit against other energy-harvesting systems in the published literature is given in Table IV. This proposal shows significant improvements.

Table IV. Performance comparison *vs.* previously published energy-harvesting circuits

Energy harvesting circuit	Maximum output voltage (V)	Design Approach, complexity, size, cost	Applications
Proposed MOS-based piezoelectric energy harvesting circuit	6.88	Simple circuit, easy to manufacture, small size, low cost	IoT devices, low-power electronics
Prototype of a piezo energy harvester (30)	1.8	Easy to manufacture, small size	Power conditioning
Piezoelectric voltage multiplier circuit (31)	4.3 V	Simple circuit, easy to design, small size, low cost	Mobiles with keypad and sound vibrations
Piezoelectric nanogenerators and vibrational energy harvesters (32)	1.5	Complex design	Analysis for energy harvesting devices

5. Conclusions

This work evaluated the experimental performance of a two-stage cross-coupled MOS-based voltage for piezoelectric and solar energy harvesting. The results show that the designed circuit performs better in piezoelectric energy harvesting, as it enhances the input voltage by 1.91 times.

A diode-based circuit was also evaluated in the piezoelectric energy harvester, providing a 1.44-fold increase in the output voltage compared to the input. The experimental study showed that the two-stage MOS-based cross-coupled voltage multiplier circuit performs better than the diode-based alternative, with encouraging prospects for green energy, low-power electronics, and IoT, among others.

6. Funding

This research received no external funding.

7. Data availability

The data will be made available upon request.

8. Conflicts of interest

The authors declare no conflict of interest.

9. Use of artificial intelligence

During this work, the authors did not employ any technologies associated with artificial intelligence.

References

[1] M. Alibakhshikenari, V. B. Singh, C. H. See, R. A. A. Alhameed, F. Falcone, and E. Limiti, "Energy harvesting circuit with high RF-to-DC conversion efficiency," in *Proc. IEEE Int. Symp. Antennas Propag. North Amer. Radio Sci. Meet.*, Montreal, QC, Canada, 2020, pp. 1299–1300. https://doi.org/10.1109/IEEECONF35879.2020.9329604 ↑2

[2] N. Singh, "Low profile multiband rectenna for efficient energy harvesting at microwave frequencies," *Int. J. Elect.*, vol. 106, no. 12, pp. 2057–2071, 2019. https://doi.org/10.1080/00207217.2019.1636302 ↑2

[3] U. Alvarado, A. Juanicorena, I. Adin, B. Sedano, I. Gutiérrez, and J. D. No, "Energy harvesting technologies for low-power electronics," *Trans. Emerg. Telecomm. Tech.*, vol. 23, no. 8, pp. 728–741, 2012. https://doi.org/10.1002/ett.2529 ↑2

[4] M. D. Ker, S. L. Chen, and C. H. Tsai, "A new charge pump circuit dealing with gate-oxide reliability issue in low-voltage processes," in *Proc. IEEE Int. Symp. Circ. Syst. (ISCAS)*, Vancouver, BC, Canada, 2004, pp. 321–324. ↑2

[5] B. Jyostna and S. Murthy, "Low power CMOS start-up charge pump with power gating technique," *Int. J. Sci. Eng. Res.*, vol. 52, no. 4, pp. 1114–1118, 2016. ↑2

[6] W. Samakkhee, K. Phaebua, and T. Lertwiriyaprapa, "5.8 GHz rectifier circuit for electromagnetic energy harvesting system," in *Proc. Int. Symp. Ant. Propag. (ISAP2017)*, Phuket, Thailand, 2017, pp. 133–136. https://doi.org/10.1109/ISANP.2017.8229029 ↑2

[7] F. Sari and Y. Uzun, "A comparative study: Voltage multipliers for RF energy harvesting system," *Comm. Fac. Sci. Univ. Ankara*, vol. 61, no. 1, pp. 2–23, 2019. https://doi.org/10.33769/aupse.469183 ↑2

[8] H. Goncalves, J. Fernandes, and M. Martins, "A study on MOSFET rectifiers maximum output voltage for RF power harvesting circuits," in *Proc. IEEE Int. Symp. Circ. Syst. (ISCAS)*, Lisbon, Portugal, 2013, pp. 2964–2967. https://doi.org/10.1109/ISCAS.2013.6572501 ↑2

[9] Q. Li, J. Wang, D. Niu, and Y. Inoue, "A two-stage CMOS integrated highly efficient rectifier for vibration energy harvesting applications," *J. Int. Council Elect. Eng.*, vol. 4, no. 4, pp. 336–340, 2014. https://doi.org/10.1080/22348972.2014.11011893 ↑3

[10] G. Chong *et al.*, "CMOS cross-coupled differential-drive rectifier in subthreshold operation for ambient RF energy harvesting – Model and analysis," *IEEE Trans. Circ. Syst II Exp. Briefs*, vol. 66, no. 12, pp. 1942–1946, 2019. https://doi.org/10.1109/TCSII.2019.2895659 ↑3

[11] S. S. Chouhan and K. Halonen, "A modified cross coupled rectifier based charge pump for energy harvesting using RF to DC conversion," in *Proc. Eur. Conf. Circ. Theor. Des. (ECCTD)*, Dresden, Germany, 2013, pp. 1–4. https://doi.org/10.1109/ECCTD.2013.6662231 ↑3

[12] S. Fan *et al.*, "A cross-coupled active rectifier–booster regulator integrated circuit for broadband wireless energy harvesting system," in *MTT-S Int. Wireless Symp. (IWS)*, Shanghai, China, 2020, pp. 1–3. https://doi.org/10.1109/IWS49314.2020.9359959 ↑3

[13] M. E. C. Andam, C. M. P. Canja, and M. A. Capilayan, "A design of self-biased cross coupled rectifier with integrated dual threshold voltage for RF energy harvesting application," in *Proc. 8th Int. Conf. Amb. Syst. Net. Tech.*, Madeira, Portugal, 2017, pp. 384–391. ↑3

[14] J. Banejee, "Comparison of cross couple MOS based and Schottky diode based RF energy harvesting circuits using Wilkinson power combiner," *Frequenz*, vol. 77, pp. 133–146, 2023. https://doi.org/10.1515/freq-2022-0018 ↑3

[15] M. W. Aljibory, H. T. Hashim, and W. N. Abbas, "A review of solar energy harvesting utilising a photovoltaic–thermoelectric integrated hybrid system," *Mater. Sci. Eng.*, vol. 1067, art. 012115, 2021. https://doi.org/10.1088/1757-899X/1067/1/012115 ↑3

[16] L. Xiao, Y. S. Wu, and L. S. Yang, "Parametric study on thermoelectric conversion performance of a concentrated solar-driven thermionic-thermoelectric hybrid generator," *Int. J. Energy Res.*, vol. 42, pp. 656–672, 2018. https://doi.org/10.1002/er.3849 ↑3

[17] D. Hao *et al.*, "Solar energy harvesting technologies for PV self-powered applications: A comprehensive review," *Renew. Energy*, vol. 188, pp. 678–697, 2022. https://doi.org/10.1016/j.renene.2022.02.066 ↑3

[18] D. K. Sah, N. Mazumdar, P. Pal, and T. Amgoth, "A comprehensive study of solar energy harvesting system in wireless sensor networks," in *Proc. Int. Conf. Elect. Electron. Comp. Eng. (UPCON)*, Prayagraj, India, 2022, pp. 1–6. https://doi.org/10.1109/UPCON56432.2022.9986433 ↑3

[19] N. Samal and O. J. Shiney, "Energy harvesting using piezoelectric transducers: A review," *J. Sci. Res.*, vol. 65, no. 3, pp. 3842–3847, 2021. https://doi.org/10.37398/JSR.2021.650320 ↑3

[20] M. H. Amiri *et al.*, "Piezoelectric energy harvesters: A critical assessment and a standardized reporting of power-producing vibrational harvesters," *Nano Energy*, vol. 106, pp. 1–35, 2023. https://doi.org/10.1016/j.nanoen.2022.108073 ↑3

[21] J. Ghazanfarian, M. Mohammadi, and K. Uchino, "Piezoelectric energy harvesting: A systematic review of reviews," *Actuators*, vol. 10, no. 12, pp. 1–40, 2021. https://doi.org/10.3390/act10120312 ↑3

[22] S. Dam and P. Mandal, "An integrated DC–DC boost converter having low-output ripple suitable for analog applications," *IEEE Trans. Power Electron.*, vol. 33, no. 6, pp. 5108–5117, 2018. https://doi.org/10.1109/TPEL.2017.2735491 ↑3

[23] M. Maalandish, S. H. Hosseini, S. Ghasemzadeh, and E. Bab, "A novel multiphase high step-up DC/DC boost converter with lower losses on semiconductors," *IEEE J. Emer. Sel. Topics Power Electron.*, vol. 7, no. 1, pp. 541–554, 2019. https://doi.org/10.1109/JESTPE.2018.2830510 ↑3

[24] L. Rodríguez, E. Raygada, C. Silva, and J. Saldaña, "Design of a CMOS cross-coupled voltage doubler," in *Proc. IEEE ANDESCON*, Arequipa, Peru, 2016, pp. 1–4. https://doi.org/10.1109/ANDESCON.2016.7836258 ↑3

[25] D. Kumar, P. Chaturvedi, and N. Jejurikar, "Piezoelectric energy harvester design and power conditioning," in *Proc. Conf. Elect. Electron. Comp. Sci.*, 2014, pp. 1–6. https://doi.org/10.1109/SCEECS.2014.6804491 ↑3

[26] G. Revathi and R. Ingitham, "Piezoelectric energy harvesting system in mobiles with keypad and sound vibrations," *Int. J. Eng. Res. Tech. (IJERT)*, vol. 1, no. 4, pp. 1–4, 2012. ↑3

[27] M. H. Amiri *et al.*, "Piezoelectric energy harvesters: A critical assessment and a standardized reporting of power-producing vibrational harvesters," *Nano Energy*, vol. 106, pp. 1–12, 2023. https://doi.org/10.1016/j.nanoen.2022.108073 ↑3

[28] M. Maalandish, S. Hossein Hosseini, S. Ghasemzadeh, and E. Babaei, "A novel multiphase high step-up DC/DC boost converter with lower losses on semiconductors," *IEEE J. Emerg. Sel. Topics Power Electron.*, vol. 7, no. 1, pp. 541–554, 2019. https://doi.org/10.1109/JESTPE.2018.2830510 ↑3

[29] L. Rodriguez, E. Raygada, C. Silva, and J. Saldaña, "Design of a CMOS cross-coupled voltage doubler," in *Proc. IEEE ANDESCON*, Arequipa, Peru, 2016, pp. 1–4. https://doi.org/10.1109/ANDESCON.2016.7836258 ↑3

[30] D. Kumar, P. Chaturvedi , and N. Jejurikar, "Piezoelectric energy harvester design and power conditioning," in *Proc. IEEE Students' Conf. Elect., Electron. Comput. Sci. (SCEECS)*, 2014, pp. 1–6. https://doi.org/10.1109/SCEECS.2014.6804491 ↑9

[31] G. Revathi, and R. Ingitham, "Piezoelectric energy harvesting system in mobiles with keypad and sound vibrations," *Int. J. Eng. Res. Technol. (IJERT)*, vol. 1, no. 4, pp. 1–4, 2012 ↑9

[32] M. H. Amiri *et al.*, "Piezoelectric energy harvesters: A critical assessment and a standardized reporting of power-producing vibrational harvesters," *Nano Energy*, vol. 106, pp. 1–12, 2023. https://doi.org/10.1016/j.nanoen.2022.108073 ↑9

UNIVERSIDAD DISTRITAL
FRANCISCO JOSÉ DE CALDAS

Ingeniería

https://revistas.udistrital.edu.co/index.php/reving/issue/view/1295

DOI: https://doi.org/10.14483/23448393.22877

Research

Integration of Systemic and Participatory Approaches in Decision-Making for the Achievement of SDG 7 in Rural Areas

Integración de enfoques sistémicos y participativos en la toma de decisiones para el logro del ODS 7 en zonas rurales

Diana García-Miranda[1], Francisco Santamaría-Piedrahita[2], César Trujillo-Rodríguez[3], and Marcel Castro-Sitiriche[4]

[1, 2, 3]Universidad Distrital Francisco José de Caldas (Bogotá, Colombia), Colombia
[4]Universidad de Puerto Rico (Mayagüez, Puerto Rico), Universidad del Cauca, Colombia

Abstract

Context: This article examines access to electrification in rural areas within the framework of Sustainable Development Goal 7 (SDG7), which seeks to ensure access to modern, affordable, and sustainable energy for all. It identifies common barriers to energy access in rural communities and highlights the limitations of conventional approaches, emphasizing the need for integrative and participatory decision-making processes in rural electrification projects.

Method: This study proposes an integrative decision-making model based on design thinking, the systemic approach, participatory action research (PAR), and the principles of behavioral economics. This model prioritizes community participation and the cultural and contextual appropriateness of electrification solutions, supported by participatory tools such as empathy maps and digital surveys to identify both explicit and latent energy needs and preferences.

Results: The results show that integrating participatory and behavioral approaches strengthens community governance, improves the acceptance of electrification systems, and optimizes the use of technical and financial resources. Active community engagement increases trust in energy solutions, while behavioral design strategies promote more efficient energy use without compromising user comfort. Additionally, participatory tools reveal non-obvious energy demands and social barriers often overlooked by purely technical assessments.

Conclusions: The findings demonstrate that a successful rural electrification depends not only on technological solutions, but also on inclusive, context-aware decision-making processes. The proposed integrative model contributes to sustainable human development by enhancing the acceptance and long-term sustainability of electrification projects in rural areas.

Keywords: rural electrification, sustainable development, SDG, decision making, community participation

Article history

Received:
November 13th, 2024

Modified:
July 28th, 2025

Accepted:
August 5th, 2025

Ing, vol. 30, no. 3, 2025, e22887

*Correspondence: cltrujillo@udistrital.edu.co

Resumen

Contexto: Este artículo examina el acceso a la electrificación en zonas rurales en el marco del Objetivo de Desarrollo Sostenible 7 (ODS7), que busca garantizar el acceso a energía moderna, asequible y sostenible para todos. Se identifican las barreras comunes en el acceso energético en comunidades rurales y se destacan las limitaciones de los enfoques convencionales, resaltando la necesidad de procesos de toma de decisiones integradores y participativos en los proyectos de electrificación rural.

Método: Este estudio propone un modelo integrador de toma de decisiones basado en el *design thinking*, el enfoque sistémico, la investigación-acción participativa (IAP) y los principios de la economía del comportamiento. Este modelo prioriza la participación comunitaria y la adecuación cultural y contextual de las soluciones de electrificación, apoyándose en herramientas participativas como los mapas de empatía y las encuestas digitales para identificar necesidades y preferencias energéticas tanto explícitas como latentes.

Results: Los resultados muestran que la integración de enfoques participativos y conductuales fortalece la gobernanza comunitaria, mejora la aceptación de los sistemas de electrificación y optimiza el uso de los recursos técnicos y financieros. La participación activa de las comunidades incrementa la confianza en las soluciones energéticas, mientras que las estrategias de diseño conductual promueven un uso más eficiente de la energía sin comprometer la comodidad del usuario. Asimismo, las herramientas participativas permiten identificar demandas energéticas no evidentes y barreras sociales que suelen ser ignoradas por evaluaciones exclusivamente técnicas.

Conclusiones: Los hallazgos evidencian que el éxito de la electrificación rural no depende únicamente de soluciones tecnológicas, sino también de procesos de toma de decisiones inclusivos y sensibles al contexto. El modelo integrador propuesto contribuye al desarrollo humano sostenible al mejorar la aceptación y la sostenibilidad a largo plazo de los proyectos de electrificación en zonas rurales.

***Palabras clave*:** electrificación rural, desarrollo sostenible, ODS, toma de decisiones, participación comunitaria

Table of contents

Page

1. Introduction 2

2. Sustainable development, the 2030 Agenda, and SDG7 5

3. Principles to be considered in rural electrification projects 6

3.1 Good living, or Sumak Kawsay 6

3.2 Responsible well-being 7

3.3 Consumption habits and satisfaction 8

4. Decision-making in rural electrification projects 9

4.1 Design thinking 10

4.2 Systemic approach 11

4.3 Participatory action research 11

4.4 Behavioral economics 12

5. Methodological proposal for decision-making in rural electrification projects 13

6. Preliminary findings 17

7. Conclusions 24

8. Author contributions 24

1. Introduction

In 2015, the United Nations issued the 2030 Agenda for Sustainable Development and formulated the Sustainable Development Goals (SDGs). This agenda comprises 17 goals to transform the world, creating a route that allows for global sustainable development by 2030, under the vision of 'leaving no one behind' (1). One of these goals, SDG7, focuses on universal access to modern, reliable, sustainable, and affordable energy (2). Herein lies the fundamental challenge of policy formulation and the energy trilemma (3)–(7).

However, an assessment of the global monitoring framework shows that indicators in rural areas are lower than the proposed targets (4), (8), (9). Global access to electricity in rural areas has increased significantly in recent decades, but this number is still too low for achieving the 2030 target (10). 14% of the world's population, about 800 million people, live in areas with no access to modern energy systems. About 84% of these people live in rural areas, and more than 95% of people without electricity live in countries in Africa, sub-Saharan Africa, and developing Asia. In addition, many of those who have access to electricity receive a poor-quality service and are therefore unable to reap the socioeconomic benefits and well-being levels that electricity service can provide (10), (11).

Users in rural areas are heterogeneous, and, in some cases, may act contrary to the community's expectations and concerns regarding their electrification system. In order to improve their well-being, electrification projects should consider innovation processes for energy solutions that involve collective participation and respect for the environment, which are two characteristic elements of the Sumak Kawsay vision (or 'Good living') (12), (13). Furthermore, the role of technology in development, local empowerment (key to well-being) (14), responsible welfare (where the personal, social, and environmental converge under a new prism) (15), and people's realities must be taken into account in order to meet their needs (16).

This study is motivated by the critical need to transition from traditional technocratic approaches to holistic and contextual frameworks in the field of rural electrification. Conventional models often fragment planning and implementation processes, failing to account for the complexities and interdependencies inherent in rural contexts, particularly in developing regions such as Latin America. This integrative work proposes a collaborative methodology that combines several approaches into a cohesive operational framework, aiming to facilitate a more adaptive rural energy planning strategy. In the literature, (17) highlight the need for comprehensive rural electrification policies that address energy supply while incorporating social, economic, and environmental considerations. They argue that fragmented strategies result in inadequate implementation and overlook vital local needs. Thus, integrating diverse perspectives through a holistic framework is paramount.

The work of (18) illustrates the impact of photovoltaic (PV) systems on isolated communities, demonstrating that a contextual understanding of energy solutions leads to more successful rural electrification practices. Their findings emphasize the importance of tailoring energy solutions to the unique socioeconomic contexts of communities and support the argument for a framework that can be adapted across various settings. This idea resonates with the studies conducted by (19), who advocate for the use of geographic information systems (GIS) as a method to locally assess rural electrification alternatives. This approach allows decision-makers to consider community-specific factors, such as geographic constraints and infrastructure availability, when planning energy interventions. By accounting for these local factors, a more integrated and sustainable energy approach can be established.

Furthermore, the need for context-aware methodologies is emphasized by the community-based solar mini-grid management frameworks discussed by (20), who highlight the importance of effective management and community engagement, which are crucial for the sustainability of rural electrification projects. This example highlights the importance of stakeholder involvement and the necessity of community-centric strategies in energy planning.

A key point in discussions about holistic planning is the need to consider the socio-emotional impact of electrification on communities. (21) argue that sustainable electrification can transform the social and economic well-being of regions, such as Mixteca in Oaxaca, Mexico, by promoting inclusive development through multidimensional analyses incorporating both quantitative and qualitative data. This type of analysis is essential for identifying the genuine needs of communities and developing targeted and effective interventions. Furthermore, the inclusion of participatory methodologies in planning is crucial. (22) propose the use of participatory rural appraisal (PRA), which allows community members to identify and prioritize their problems through a collaborative approach. This approach empowers citizens and ensures that the solutions adopted align with true local priorities, thereby improving the sustainability of electrification projects.

The study by (23) emphasizes the importance of considering rural electrification within a wider context, where investments in renewable energy should be coupled with improvements in access to technology and infrastructure development. This interconnected approach suggests that electrification policies should be holistic and coordinated with other development initiatives in order to maximize their economic and social benefits.

The active participation of women in planning is another crucial element in achieving sustainable rural development and electrification. Studies such as (24) highlight how gender barriers limit women's inclusion, although there have been improvements in their participation in community assemblies. Increasing female representation in planning decisions is not only a matter of equity; it also promotes a more comprehensive and diverse vision, which can lead to more sustainable solutions.

In addition, it is essential to create specific planning instruments that consider local realities. The work of (25) in the Chorotega region of Costa Rica emphasizes the importance of designing territorial rural development plans (TRDPs) that cater to the unique characteristics and needs of each territory, thereby facilitating a tailored approach that enables a more targeted development, focused on people's well-being.

Synthesizing these insights, the proposed framework encompasses methods that combine participatory practices, contextual analysis, and integrative planning strategies, ensuring that the voices of rural populations inform the energy solutions they adopt. This multi-faceted approach aims to bridge the existing gap in rural electrification strategies, providing a replicable model that is adaptable to various cultural and geographical contexts, thus promoting long-term sustainability and resilience in energy access.

This article proposes the integration of systemic and participatory approaches into decision-making in order to facilitate access to electrification in rural areas. It is organized as follows. Section 2 discusses how the effective implementation of SDG7 in these areas can improve social, economic, and environmental conditions. Section 3 presents the key principles for rural electrification projects, *i.e.*, cultural respect, community participation, and the integration of social and environmental factors to ensure sustainable implementation. Sections 4 and 5 introduce the proposed decision-making methodology for rural electrification, integrating systemic analysis, PAR, design thinking, and behavioral economics to address technical and socio-contextual complexities within a coherent operational framework. Section 6 describes the preliminary validation of the proposed model through participatory exercises and simulated scenarios, highlighting the social, technical, and behavioral findings that demonstrate its applicability and explanatory value. Finally, the conclusions of this work are presented in Section 7.

2. Sustainable development, the 2030 Agenda, and SDG7

The literature on the subject of *sustainable development* (SD) is both abundant and discordant (26). The most commonly cited definition is that proposed by the United Nations Commission on Environment and Development, also known as the *Bruntland Commission*, in 1987 (10): "sustainable development is development that meets the needs of the present without compromising the ability of future generations to meet their own needs."

The concept of *SD* has acquired a deeper meaning with the adoption of the 2030 Agenda. Beyond the traditional focus on social inclusion, economic growth, and environmental protection, two essential components have been added: collective participation and peace (2), (27). Moreover, the notion of *integrated and holistic thinking* is visibly entering the global policy discourse (7).

The 2030 Agenda gives rise to the 17 SDGs, providing concrete form to the challenge of moving from an approach based on economic growth and income to a comprehensive approach that includes the multiple dimensions that influence people's progress (28), (29). These goals represent humanity's consensus on the type of development that people want to reach, establishing a minimum of opportunities and well-being levels to which every human being is entitled and defining humanity's obligations to the planet and its future generations (30). SDG7 plays an essential role in achieving all other SDGs; 125 of the 169 proposed targets are related to energy use (5).

Thus, the SDGs are not just items on a list; they represent a holistic approach to creating long-term solutions to structural gaps (2) and addressing key systemic barriers to sustainable development, such as inequality, unsustainable production and consumption patterns, inadequate infrastructure, and the lack of adequate jobs (5), (27), (31).

3. Principles to be considered in rural electrification projects

There are diverse opinions on the different development models and the setbacks they have caused—in some cases, failures associated with technical assistance—, perceptible in the loss of identity and cultural values and the reduction of spaces for participation and democratic exercise (32), (33). SD should take place within the framework of the search for sustainable societies, with freedom, participation, justice, and opportunities for human development, especially for the less privileged sectors of society (34).

An integral vision of SD should test new models of interaction for the development and management of resources (*e.g.*, electricity), combining technical expertise and the collaboration of academia while enriching and expanding social, cultural, and physical aspects, relying on the cultural richness of people, local citizen organization and participation, and decision-makers. Some of these assumptions are listed below.

3.1 Good living, or Sumak Kawsay

This is a paradigm of well-being, alternative to the Western paradigm, derived from the modern cosmovision known as *development*, which offers the possibility of building a society based on the harmonious coexistence of human beings and their diversity, in harmony with nature and based on the recognition of the diversity of cultural values that exist in each country and around the world (12), (13), (35).

It is worth mentioning that the concept and vision of *good living* is found in different indigenous peoples of Latin America (Table I), but it is not limited to them. Similar approaches can be found in other multicultural contexts with a critique of the classical development model (12), (35).

Table I. Good living of indigenous peoples of Latin America (36)–(40)

Name	Indigenous group	Country	General translation
Sumak Kawsay	Quechua	Ecuador	Living well, good living
Shiir Wara	Achuar	Ecuador	Well-being, good living
Penker Pujustin	Shuar	Ecuador	Well-being, good living
Suma Qamaña	Aymara	Bolivia	Living well, good living
Teko Kavi, Ñandereko	Guaraní	Paraguay	Harmonious life
Lekil Kuxlejal	(Maya) Tsotsil and Tseltal	México	Dignified and just life
Yeknemillis	Nahua	México	Good life
Küme Mongen	Mapuche	Chile	Harmonious life
Utz K'aslemal	(Maya) K´Iche and Kaqchikel	Guatemala	Good life
Allin Kawsay	Quechua	Peru	Life in balance
Kametsa Asaiki	Asháninka	Peru	Autonomous life
Bunkwanarrua	Misak	Colombia	Harmony with the territory and the community
Ley de Origen	Koguis, wiwas, arhuacos y kankuamos	Colombia	Vital balance
Ñañu	Pemón	Venezuela	Good life

One of the key aspects of Sumak Kawsay is the role of participation. The community is the place where reciprocity, complementarity, solidarity, spirituality, and self-righteousness are developed (12). Sumak Kawsay is taken as an example of the kind of concept that should be used as a goal for local terms to define community-based efforts. This vision draws on the thinking of Amartya Sen, who advocates for a development that focuses on human freedoms rather than economic growth (41). Sumak Kawsay goes straight to the heart of what humanity wants and what should be the primary goal of governments: a good quality of life.

3.2 Responsible well-being

The human development approach proposed by the United Nations emerges as an alternative to economic approaches that are overly concerned with the growth of the gross national product and the national income. It considers that the well-being of a society depends on the use of income and not on the level of income itself, that the expansion of production and wealth should be only a means, while the end of development should be human well-being (42).

The concept of *responsible well-being* is related to Sumak Kawsay, which should be a guide for analyzing the energy needs of households and communities (43) (44) proposed responsible well-being as a way to combine concepts of welfare and personal responsibility. This approach gives a prominent role to personal well-being and does not require an altruistic citizen behavior.

(43) delved deeper into the issue by examining responsible well-being in terms of energy consumption, employing Max-Neef's energy threshold hypothesis in terms of economic growth and quality of life, where any consumption beyond a threshold is not responsible and does not improve individual well-being.

Three regions are identified in the curve in Fig. 1. Region 1 shows low levels of consumption, bounded by a minimum necessary consumption point. This level of consumption is a necessary but not sufficient condition for achieving welfare in the context of the 21st century. There is a strong increase in well-being in the poverty region related to the increase in consumption, an increase between 1 and 2 is 100%, but an increase from 0 to 1 is ∞ (45). Region 2, or the *responsible well-being region*, contains levels of energy consumption that allow achieving individual welfare, but it does not extend to an excessive consumption that is likely to limit the ability of others to access a good quality of life, ultimately reducing individual well-being (43). Finally, in region 3, which is characterized by the transgression of Manfred Max-Neef's threshold hypothesis, formulated from the perspective of ecological economics (45), further increases would not improve quality of life; they might even reduce it.

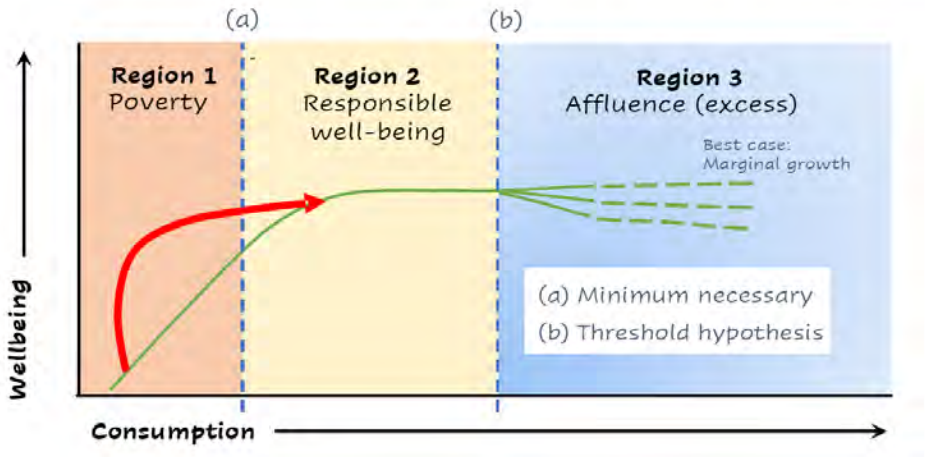

Figure 1. Responsible well-being and threshold limit (43)

Furthermore, actions, choices, and decisions are beyond individual actions. Personal well-being is linked to the well-being of others and to the ecosystem that supports it, so, in practice, the concept of *responsible well-being* contributes effectively to a comprehensive human development project (43).

3.3 Consumption habits and satisfaction

A connection has long been established between technology and everyday life, not only in relation to devices, but also including the human behaviors towards them, especially with electrical energy and household appliances (46). Needs and habits are strong enough for the adoption of the new useful technologies or products that users incorporate into their way of life (34), wherein comfort and satisfaction are intrinsically linked to the use of electrical energy (47).

Daily activities related to household energy are influenced by the way in which these activities are performed. Satisfaction is based on occupants' perceptions and how their expectations can be met (47). The concept of *sustainability*, based on the satisfaction of human development needs, invites a broadening of our perspective beyond merely meeting needs, aiming at increasing capabilities and focusing on people's empowerment, their freedoms, and their ability to be agents of change (48).

4. Decision-making in rural electrification projects

The ability of technology to meet rural energy needs has already been demonstrated, especially for those based on renewable energy sources, such as solar PV systems, small wind power generators, micro- and mini-hydropower plants, and biomass and diesel generators (49), (50). However, the strategies used to implement these solutions determine their viability and impact on the quality of life and the promotion of socioeconomic development in rural communities. In this sense, we propose organizing these strategies into three main levels of generation and distribution systems, ranging from individual systems to microgrids connected to the grid or to other microgrids, which can provide different benefits or services depending on what is required. This is shown in Fig. 2.

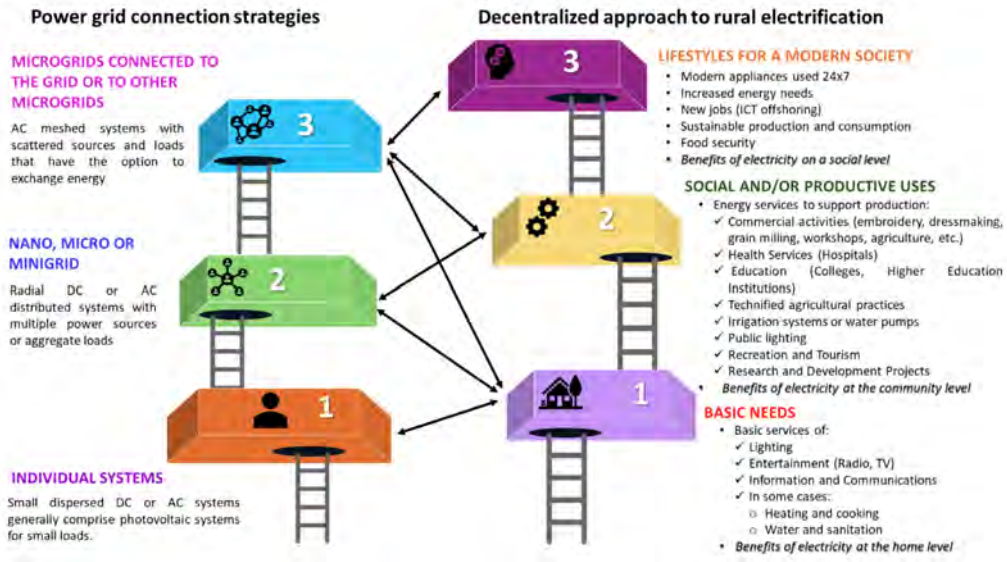

Figure 2. Proposal for the organization of generation and distribution strategies in rural areas

Individual systems (level 1). This is the most basic level, generally consisting of small DC or AC systems (*e.g.*, PVs) serving small and dispersed loads typical of isolated rural dwellings. The main advantage of these systems is their simplicity and low initial cost, which makes them an immediate solution for areas with very low population density. However, their limited capacity means that they cover only the lowest level of energy access, limiting their impact on community productivity and economic development.

Nano-, micro-, or mini-grids (level 2). These provide distributed, radial systems that can operate on DC or AC power, aggregating multiple energy sources and loads. These grids offer a more robust power supply than individual systems and allow for both social and productive uses. At the community level, these solutions enable significant improvements in social and economic well-being, provide sufficient energy for critical infrastructure, and promote sustainable development in rural areas.

Microgrids connected to the grid or to other microgrids (level 3). At the most advanced level, connected microgrids offer AC meshed systems that enable energy exchange with other microgrids or with the main power grid. These grids are designed to operate flexibly, adapting to both distributed energy resources and distributed loads. Not only does this type of grid meet the energy needs of the community; it also supports modern lifestyles by allowing the use of technology applications 24 hours a day, promoting food security and sustainable production.

However, introducing technologies without considering cultural contexts and preferences often leads to low technology adoption or the inefficient operation of electricity services (51), (52). Predominantly technocratic approaches are more like technological wishlists than representations of the real needs and capabilities of a community, or of the well-being that comes from using electrical or electronic devices in households, especially for the poorest.

In the discourse around the SDGs, electrification facilitates the satisfaction of basic needs and improves people's standard of living (as proposed by human capital theories), which is, therefore, where the emphasis should be placed.

In this context, we propose a strategy for decision-making in rural electrification projects that combines design thinking, the systemic approach, PAR, and the principles of behavioral economics.

4.1 Design thinking

Design thinking is a creative and collaborative methodology that places users at the center of the design process and promotes innovation through a nonlinear, iterative, and collaborative approach (53)–(56). In the context of rural electrification projects, it is possible to identify the following qualities of design thinking (53)–(56):

- *Focus on human needs*. By placing people at the center of the design process, electrification solutions can be better tailored to the real needs of the community.
- *Innovation and creativity*. In the phases pertaining to design and solutions (many of them innovative and creative), the interaction between different key stakeholders is fundamental.
- *Rapid prototyping*. One of the strengths of this methodology is the creation of pilots and prototypes, as well as the rapid testing of solutions within the community. Testing energy systems—or emulating them in a reduced environment—allows learning from mistakes, adapting to local conditions, and improving the solution before full implementation.
- *Continuous iteration*. Through the continuous cycle of feedback and improvement, solutions can be adapted based on direct community interaction. This ensures that the final system is efficient, functional, and accepted by end users.

4.2 Systemic approach

This is a methodology that considers the interaction between different elements and actors within a system in order to address complex problems (57)–(59). In rural electrification projects, a systemic approach is fundamental to understanding the interrelationships between technical, social, economic, political, and environmental factors. This approach has the following qualities for rural electrification projects (57)–(59):

- *Mapping of linkages:* identifying how technical decisions affect social (equity of access), economic (cost of implementation), and environmental (use of natural resources) dimensions.
- *Informed decision-making:* using multi-criteria analysis or simulation tools to assess how different electrification alternatives affect a system, ensuring a holistic approach to structured decision-making as well as the involvement of all stakeholders.
- *Managing complexity*: facilitating a more flexible and adaptive decision-making process that is able to respond to changes in the local context or in the community's needs, given that electrification projects in remote rural areas often face many dynamic and changing factors, such as those associated with energy policy, economic, or climatic conditions.

4.3 Participatory action research

PAR is a collaborative research methodology that involves community members throughout the process (60)–(64). It focuses on solving concrete problems that affect the community while generating practical and meaningful knowledge and ensuring that the proposed solutions are tailored to local needs and capacities. It consists of four main phases: planning, action, monitoring, and reflection. In the context of rural electrification projects, PAR includes the following (60)–(64):

- *Community empowerment:* active involvement of the community in all stages of the project, from needs assessment to implementation and monitoring.
- *Shared diagnosis and local adaptability:* enabling the design of solutions adapted to the community's specific context (climatic, economic, cultural), as the community itself participates in the diagnosis and planning process.
- *Capacity building:* involving community members in the implementation and operation of the electricity system, thereby ensuring that they acquire technical skills for the maintenance and management of the infrastructure.
- *Trust building:* active participation in decision-making, fostering a greater sense of ownership and commitment among the members of the community.
- *Sustainable solutions:* addressing not only energy needs, but also cultural, social, and environmental issues by integrating local knowledge and community perspectives.

4.4 Behavioral economics

This approach regards humans as irrational and emotional beings influenced by cognitive biases, mental shortcuts (heuristics), emotional factors, and experience when making decisions (60)–(64). Behavioral economics combines principles from economics and psychology to explain why people, in practice, do not always make rational or optimal decisions.

In rural electrification projects, the use of nudges is essential for encouraging the adoption of sustainable energy technologies. Some strategic nudges adapted to the studied context include the following:

- *Making it visible and common.* Examples of neighboring communities that already use renewable systems successfully can create a 'herd effect', motivating other households to follow the same trend.
- *Using standard options.* Offering standardized alternatives makes decision-making easier.
- *Emphasizing immediate benefits.* Visible improvements should be highlighted, such as reduced costs or the ability to extend study time with night lighting.
- *Deferring losses*. Allowing for deferred payments or instalment financing reduces the sense of initial financial loss.
- *Making it automatic and hassle-free.* Automatic payment plans with instalments adapted to families' ability to pay could be established.
- *Establishing new habits.* Training project staff to guide communities in sustainable energy practices encourages the creation of new habits.

- *Tied or bundled enrolment*. Integrating energy technology into the adoption of social or community programs facilitates access to systems.
- *Reducing cognitive overload.* Adoption processes could be simplified by providing clear and structured information.
- *Encouraging self-monitoring.* Energy savings targets could be set using meters that allow for real-time consumption monitoring.
- *Encouraging positive behavior.* Publicly recognizing communities that adopt sustainable practices creates a motivating effect.

5. Methodological proposal for decision-making in rural electrification projects

Integrating the four approaches described in the previous section makes it possible to address issues related to the adoption, sustainability, and appropriation of energy technologies in rural communities while maximizing the active participation of local actors in the planning and implementation process, overcoming the limitations of traditional approaches that often fail to capture the complexity of human behavior and isolated rural communities.

Considering the above, the proposed methodology addresses the main complexities associated with community participation in electrification projects while considering technical, economic, social, political, environmental, and regulatory aspects, whose influence may vary depending on the type of user, the region, or the time horizon considered.

The systemic approach allows incorporating some variables with intrinsic characteristics and therefore cannot be evaluated in a fragmented manner. An example of this interconnection is the behavior of user demand, which simultaneously influences and is influenced by economic, technological, social, and environmental factors. Behavioral economics allow for improved acceptance and adoption of new technologies, facilitating the transition to sustainable energy systems through strategies that reduce resistance to change. Meanwhile, PAR encourages active community participation, involving its members in all phases of the project and enabling culturally relevant and accepted solutions. This participation is also essential for ensuring long-term technical, social, and economic sustainability, as it allows the community to manage and operate the systems autonomously, strengthening its independence and commitment to the project.

Fig. 3 summarizes the phases of the comprehensive participatory rural electrification process proposed by the authors.

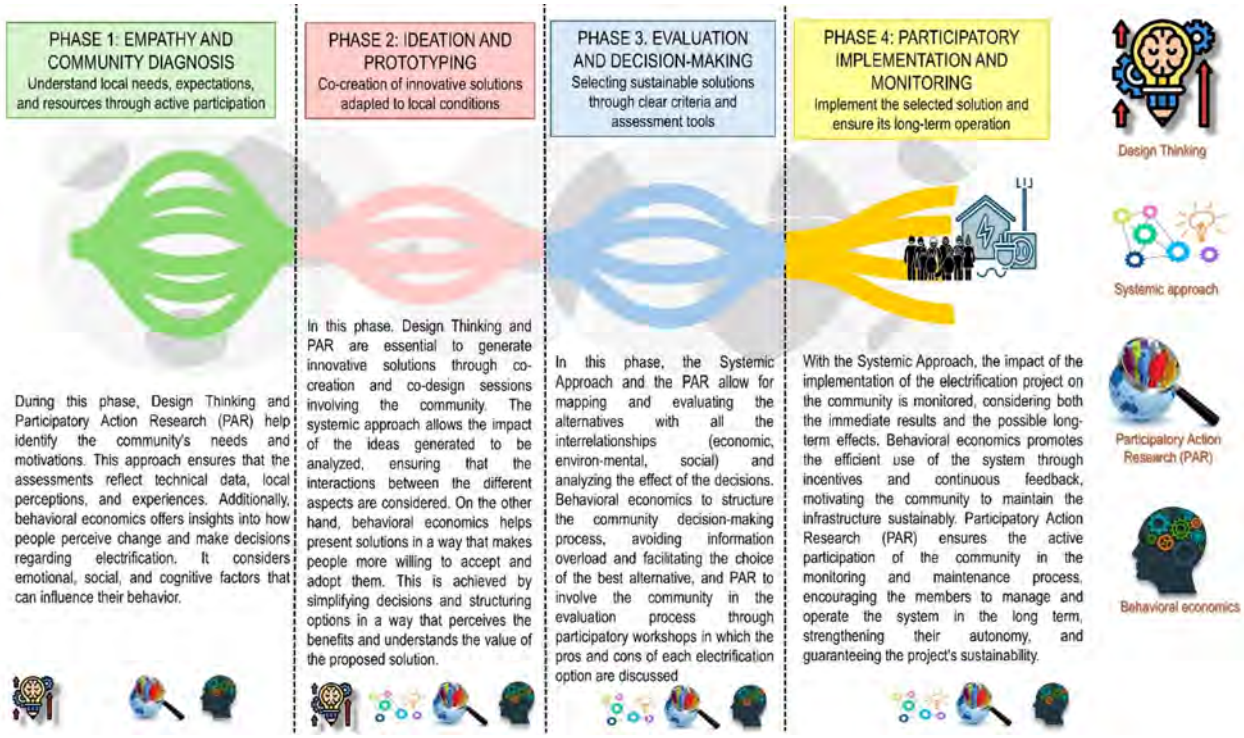

Figure 3. Phases of the comprehensive participatory rural electrification process framework

Some of the suggested tools for the implementation of this methodology are presented below.

- **Empathy map.** This is a tool for design thinking processes and participatory projects that helps to understand the needs, thoughts, and behaviors of the members of a community. This representation allows visualizing different dimensions of the human experience, facilitating the creation of more people-centered solutions.
- **A day in the life of...** This technique is based on experiencing the conditions of a user first-hand. It is useful in rural electrification projects, as it facilitates the identification of barriers and opportunities from the perspective of those who will benefit from the project.
- **Tell me about the last time you...** This technique invites the participant to narrate a significant personal experience related to electrification or access to energy.
- **Construction of archetypes in a community.** Here, archetypes are identified which help to understand social dynamics, as well as the way in which different actors influence the development and implementation of rural electrification initiatives.
- **Present and future scenario map.** This map is divided into two-time axes (present and future) and into several categories. Common patterns or problems are identified, grouping similar ideas. Participants are asked to imagine different possible futures derived from the implementation of diverse energy solutions.

- **Multicriteria decision matrix.** This technique allows comparing various electrification alternatives while considering technical, economic, environmental, and social criteria, facilitating an objective and balanced decision.
- **PESTLE.** *Political, economic, social, technological, legal*, and *environmental analysis* is a key tool for identifying the external factors that can influence a rural electrification project.
- **Decision tree diagram.** This tool allows visualizing the options and their consequences over time, considering risks, benefits and future decisions.
- **Effort-impact matrix.** This technique evaluates alternatives while considering the effort required to implement them and the impact they will have on the community.
- **Participatory social audit**. This approach allows the community to evaluate the transparency and efficiency of a project's implementation, generating trust and strengthening participatory management.

It is not necessary to incorporate all the tools simultaneously when working with the community. However, to the extent that more tools can be included, the sustainability of the rural electrification process in a specific community will increase. An example of the PESTLE analysis for a rural community is shown in Fig. 4.

Finally, as an input within the methodology, a survey using the Survey123 app is proposed as a tool for obtaining data, which enables direct interaction with an undetermined group of users, in order to identify the household appliances that they consider for their well-being at home, their consumption habits, their ranking of preferences, and the perception of user satisfaction regarding the use of appliances.

Figure 4. PESTLE Analysis. Adapted from (65)–(68).

Fig. 5 presents the QR code to access the survey form.

Figure 5. QR code to Survey123

The survey questions are divided into sections according to the topic to be addressed:

- **Characteristics of the inhabitants and the house**. Statistics are obtained on reference parameters regarding energy consumption, including the number of rooms in the house, the area, the number of people living in the house, and the family income (frequency and quantity).
- **Characteristics of the electricity service.** Statistics are obtained on service provision, including the type of connection, the average energy consumption, and service reliability (*i.e.*, the number of days that power was available, the hours of interruption, and the frequency of interruption).
- **Electrical devices.** The new needs within society have led users to require a greater number of electrical devices to support their daily activities. This section explores essential appliances, the factors influencing decisions when acquiring devices for the household, the perceived sufficiency of equipment to meet daily needs, the frequency of use of different devices, and the types of technologies adopted, among other relevant aspects related to energy use and well-being.
- **Desirability.** An evaluation model is proposed to compare users' current conditions with their level of satisfaction when postponing an activity to a different time period, thereby capturing preferences, priorities, and perceived trade-offs in daily energy use.

The above-presented elements are key in situation diagnosis during the planning and design of rural electrification systems, providing multiple strategies with real options based on how people use technology in their daily lives, with the purpose of enhancing well-being.

To understand users and consider these aspects in designing technological solutions, active and direct participation is a valuable approach. Thus, information (including spatial data) can be collected and analyzed using web or mobile devices, grouping questions according to the answers. The survey has the possibility of sending data anonymously, which simplifies and speeds up the contribution while generating fewer concerns about data privacy.

6. Preliminary findings

A preliminary validation of the proposed approach was conducted by applying participatory tools in exploratory workshops and simulation exercises with academic stakeholders. 16 students from the Electrical Engineering program of Universidad Distrital Francisco José de Caldas participated in the activity. The students were selected based on their personal experience in rural areas, or if they had relatives who lived in such areas.

During the exercise, the students assumed different roles, *e.g.*, community leaders, surveyors, technical experts, and community members (end users). They participated as potential beneficiaries of the proposed electrification systems.

Due to the low female participation in STEM disciplines, this trend was intentionally maintained in the exercise, in order to simulate the gender imbalance that is often present in real-world rural electrification contexts.

Three representative scenarios were developed to reflect the typical conditions of rural Colombian communities:

- Minimal energy access
- Restricted access with a gradually expanding grid
- A system with technical issues and low community trust in the electricity provider

Each scenario was accompanied by the three descriptive narratives (Table II), which were used as discussion triggers.

The characteristics of the simulated surveys applied to the 'users' are presented in Tables III to V. These participatory experiences validated the applicability of the model in real-world contexts and revealed significant findings from both methodological and social perspectives.

Table II. Descriptive narratives of each scenario

Scenery 1	Scenery 2	Scenery 3
Don Álvaro, village leader" Every day, I get up at 5:30 a.m., before the sun rises over the mountains. We are six of us in my family: my wife, my children, and I. We have an old TV that only works when there's a signal, two cell phones that we all use together, and some rechargeable lamps just for the night. The electricity comes and goes. Some days, we cook with firewood. The rural network is unstable, and when it rains, it's out of the question: the electricity goes out for hours. Today, I walked to school to drop the children off. There, a teacher was trying to connect a tablet to the Internet with her data plan. It's not enough for everyone, but something is achieved. In the afternoon, I went to the neighboring village for a meeting with officials who promised improvements, but we already know that it will take years. Life here continues with the basics. Progress is slow, but we continue fighting so that our children have what we didn't have: real access to information.	*Mrs. Miriam, president of the JAC* Today started early with the sound of the refrigerator, which we were finally able to buy with the help of a small subsidy. We have six devices at home: two cell phones, a television, a small refrigerator, a light bulb, and a fan. The electrical grid has improved, and for the past few months, it has been operating longer. Now, almost everyone has at least one device connected. Internet access is provided through a small operator, and even when it goes down, it's useful for sending messages and checking community WhatsApp groups. During the day, I helped two neighbors make video calls with their children in the city. In the afternoon, I accompanied the electric company technician on his tour, showing him where there are poles in poor condition. Although connectivity is limited, the change is already noticeable. Many people have started taking online courses or selling products on social media. We are learning to trust, little by little. It's still lacking, but we are no longer so isolated.	*Don Ernesto, community leader* The morning began with an unexpected visit of technicians from a company that wants to install solar panels. They say that it's a clean and cheap solution, but people here don't trust them. A few years ago, other people promised us the same thing, and the equipment broke down shortly after, and no one responded to fix the problem. I have seven devices at home, including a small refrigerator we bought with great effort. The electricity grid works, though with ups and downs, and some people already have solar energy systems donated by an NGO. But half of the community still prefers the conventional grid. Today, I organized a meeting at the community center to listen to the company. They spoke kindly, but when we asked them about warranties and maintenance, they hesitated. People left with more questions than answers. At night, under the light of a barely illuminating solar lamp, I think about the future. We want to move forward, but with dignity and respect. We are not ignorant; we just want to be heard and respected.
Sandra, mother of three sons I get up before the rooster and heat water on the wood stove. At home, we only have a portable television that we use when there's a signal, and an old cell phone that I share with my husband. We charge it at my sister-in-law's house, who lives closer to the utility pole. The children do homework using notebooks and the books the school sent us months ago. The teacher sometimes sends them WhatsApp audio recordings, but we only hear them when we climb the hill where there's a signal. Today, I did laundry early, cooked rice with sardines, and then went to the village to get candles. In the afternoon, the children played outside because we don't have Internet or enough light to read. We dream of having a good refrigerator one day, but first, we need a good power grid.	*Julián, day laborer* My name is Julián, and I work as a day laborer on nearby farms. We are five people in my family, and we have several things we couldn't have imagined before: a small refrigerator, three cell phones, a fan, a television, and even a blender that my wife uses to make juices that she sells at school. Thanks to the improved electricity grid, there's almost always electricity now. At night, we watch the news, although sometimes the signal drops out. When I have data, I use my cell phone to watch agricultural videos on YouTube. Today, I went to work on a banana farm, and, when I got back, I checked my daughter's homework she did online. We still don't understand everything, but she's teaching me. It's clear that life is changing, slowly, but surely.	*Lucía, grandmother and caregiver* I'm Lucía, 68 years old, and I take care of my two grandchildren. The house has electricity, a small refrigerator, a television, cellphones... all thanks to the electrical grid installed years ago. Recently, some men wearing hard hats came to say they'd install solar panels. I don't like it. A neighbor installed them, and three months later, they didn't work. Today, I turned on the television early and watched the news while my grandchildren got ready for school. Sometimes, I help them with homework they're doing on their cellphones. The neighbor tells me that the panels will make us pay less, but I prefer to pay a little more and be safe. It's not that we don't want progress; it's that we want things to work well.

Miguelito, 9-year-old boy

My name is Miguelito, and I'm in third grade. I live with my mom, my grandmother, and my two sisters. We have a cellphone at home. Sometimes my mom lets me watch animal videos when we go to town and there's a signal.

Today, I woke up to the roosters. My mom cooked the *arepas* over firewood because the electricity was out again. I walked to school with my sisters. The teacher told us the homework was on the phone, but we don't have Internet at home, so I had to write it in my notebook.

In the afternoon, I went to the river to collect water. Then, I did my homework by the light of the sunset because the lamp wouldn't turn on properly. Sometimes, I dream of having a computer like the ones that are used in the city.

Carolina, young entrepreneur

I'm Carolina, 22 years old, and I sell *arepas* and yogurts on my sidewalk. Earlier, everything used to be communicated by word of mouth, but, since the Internet arrived (although slowly), I learned to use WhatsApp and Facebook to offer my products.

Today, I got up at 4:30 to prepare the orders. I cooled the yogurts in my solar-powered cooler that an NGO installed. It's not very powerful, but it works. I took photos of my products and posted them. Then, I went to deliver them on my motorcycle.

In the afternoon, I watched a video on how to improve my sales. I also helped a neighbor enroll her daughter at SENA (National Learning Service) using her cellphone. Sometimes, the electricity goes out, and, when the router is broken, no one comes quickly, but every day I feel like I can do more.

Don Tomás, a lifelong farmer

I'm Don Tomás, 72 years old. I live with my wife on a small farm. I've grown corn and cassava all my life. Recently, a company has installed solar panels on some houses, but I didn't want them. I don't believe in them.

Today, I worked in the pasture and helped my wife with the garden. We have conventional electricity, which sometimes goes out, but it's enough. We watch TV at night and only use our cellphones to call our children. The company came again to offer us the panels, and I said no. Here, everyone knows what they have. It's not that I'm against it, but I want to see it work well for others first. I've been promised many things in life that don't come true.

Table III. Scenario 1: very limited access

Household	People	Devices (TV/ Cell/Light)	Energy Source	Works Well	Internet	Internet Use Frequency	Main Limitations
1	5	TV, cellphones	Solar panel	Sometimes	No	Rarely	Poor signal, power outages
2	4	Cellphones, lighting	Rural grid	Regular	No	Never	No coverage, high cost
3	6	TV, Cellphone, Lighting	Rural grid	Yes	Yes	Once a week	Limited data
4	3	Cellphone, TV, lighting	Diesel generator	Sometimes	No	Never	Expensive fuel, limited use time
5	7	Cellphones, lighting	Rural grid	Yes	Yes	Daily	Slow, unstable signal
6	2	TV, lighting	Solar panel	Sometimes	No	Never	Only works during the day
7	5	TV, cellphone, lighting	Rural grid	Yes	Yes	2-3 times/week	Low speed
8	4	Cellphone, lighting	Rural grid	Sometimes	No	Never	Inadequate devices
9	6	Cellphones	Solar panel	Yes	Yes	Daily	High mobile data costs
10	3	TV, lighting	Solar panel	Sometimes	No	Never	Weather-dependent energy
11	5	TV, cellphone, lighting	Rural grid	Regular	Yes	Weekends	Time constraints, weak signal

12	4	Cellphones, lighting	Rural grid	Yes	Yes	Daily	Time restrictions (*e.g.*, school)
13	2	TV, cellphone	Solar panel	Sometimes	No	Never	No network, local use only
14	6	Cellphones	Rural grid	Yes	Yes	Daily	Shared device usage
15	3	TV, cellphone, lighting	Rural grid	Regular	No	Never	Obsolete equipment

Table IV. Scenario 2: limited access with expanding grid

Household	People	Devices	Energy Source	Works Well	Internet	Internet Use Frequency	Main Limitations
1	5	TV, cellphones, Lights, Fridge	Rural grid	Yes	Yes	Daily	Limited data
2	4	Cellphones, lights, radio, fridge	Rural grid	Yes	Yes	Several times a week	Low speed
3	6	TV, cellphones, lights, speaker	Rural grid	Regular	Yes	Daily	Occasional power outages
4	3	TV, lights, cellphones, Fan, fridge	Hybrid (solar + grid)	Sometimes	No	Rarely	Unstable power, poor coverage
5	7	TVs, cellphones, lights, fridge	Rural grid	Yes	Yes	Daily	Cost of mobile data
6	2	TV, cellphones, lights, mini-fridge	Solar panel	Regular	No	Never	Daytime-only use, no Internet
7	5	TV, cellphones, lights, radio, fridge	Rural grid	Yes	Yes	Weekends	Lack of shared devices
8	4	TV, lights, cellphones, basic fridge	Rural grid	Sometimes	Yes	Rarely	Expensive data, unstable connection
9	6	Cellphones, lights, speaker, fridge	Rural grid	Yes	Yes	Daily	Slow network, overcrowded use
10	3	TV, cellphones, lights, fridge	Rural grid	Regular	Yes	Weekly	Limited time or work availability
11	5	TV, cellphones, lights, radio, fridge	Rural grid	Yes	Yes	Daily	Data with limited speed
12	4	Cellphones, lights, TV, fridge	Rural grid	Yes	Yes	Daily	Old equipment, slow network
13	2	Cellphones, lights, portable fridge	Solar panel	Regular	No	Never	No coverage, limited energy

14	6	TV, cellphones, lights, fridge	Rural grid	Yes	Yes	Daily	Low capacity for streaming or online learning
15	3	TV, lights, cellphones, fridge	Rural grid	Regular	Yes	Weekly	Monthly cost, prioritized for other expenses

Table V. Scenario 3: institutional support with community distrust

Household	People	Devices	Energy Source	Works Well	Internet	Internet Use Frequency	Opinion on Renewables	Main Limitations
1	5	TV, cellphones, lights, fridge	Rural grid	Yes	Yes	Daily	Prefer existing grid, distrust	Fear of failure, lack of maintenance
2	4	Cellphones, lights, radio	Donated solar panel	Sometimes	No	Never	Accepted with doubts	Lack of system understanding
3	6	TV, lights, fridge, cellphones	Hybrid (grid + solar)	Regular	Yes	Weekly	Indifferent, mixed usage	Lack of technical guidance
4	3	TV, cellphones, lights	Rural grid	Yes	No	Never	Rejected due to past issues	Resistance to change
5	7	TV, cellphones, fridge, lights	Rural grid	Yes	Yes	Daily	Waiting to see results	Company distrust
6	2	TV, lights, cellphones	Institutional solar	Sometimes	No	Never	Accepted out of necessity	Partial functionality
7	5	TV, cell phones, lights	Rural grid	Yes	Yes	Weekends	Do not see the need to switch	Poor communication with company
8	4	TV, lights, fridge	Hybrid (grid + solar)	Regular	Yes	Rarely	Satisfied but still skeptical	Fear of misuse or lack of understanding
9	6	Cellphones, lights, fridge	Rural grid	Yes	Yes	Daily	Curious, want more information	Lack of community workshops
10	3	TV, cellphones, lights	SHS	Regular	Yes	Weekly	Use it for lower cost, there are still doubts	Lack of technical support
11	5	TV, cellphones, fridge, lights	Rural grid	Yes	Yes	Daily	Reject based on negative rumors	Unclear information

12	4	TV, cell-phones, lights	Rural grid	Yes	Yes	Daily	Refuse to engage	Lack of institutional trust
13	2	TV, lights, portable fridge	Solar panel	Sometimes	No	Never	Use it but would not recommend	Low performance
14	6	TV, lights, fridge, cellphone	Rural grid	Yes	Yes	Daily	Uninterested in change	Prefer what they already know
15	3	TV, cell-phone, lights, fridge	Hybrid	Regular	Yes	Weekly	Still evaluating the experience	Limited direct communication with community

During the workshops, hypothetical rural electrification scenarios were presented, considering different levels of access and community organization. Due to limited energy availability, individual solar systems were initially prioritized. However, after applying participatory tools, a collective need for community lighting systems emerged, aiming to enable shared nighttime activities.

In scenarios with limited but expanding access, even though some households had basic refrigerators, there was still a strong interest in having equipment for productive uses. This required a reevaluation and resizing of the initially proposed infrastructure.

Finally, in contexts with active institutional support, the community showed a significant interest in clean technologies, such as PV systems. However, they also expressed distrust in the long-term sustainability and maintenance of these systems, especially regarding ongoing technical support and transparent service delivery.

The following key findings were identified based on these exercises and the integration of the aforementioned approaches (design thinking, the systemic approach, PAR, and behavioral economics):

- It was identified that electrical equipment fulfills its intended function, and that certain devices are also perceived as indicators of well-being.
- An underrepresentation of collective needs was found in conventional diagnoses. The tools used revealed non-explicit energy demands, such as perimeter lighting for security or the possibility of simultaneously charging mobile devices in community areas.
- Narrative and visual techniques helped to identify non-technical social barriers, such as institutional mistrust, a lack of knowledge about technology maintenance, and limited participation of women and youth in energy-related decision-making. These barriers, rendered invisible by purely technical approaches, can compromise the long-term sustainability of the implemented systems.

- It is important to incorporate indicators of satisfaction and well-being into project evaluations, recognizing subjective dimensions such as autonomy, trust in technology, and community control as essential factors for technological adoption.
- The application of the principles of behavioral economics, such as symbolic incentives, public visibility, and behavioral anchors, increased participants' willingness to adopt sustainable technologies and change their consumption habits.

These findings confirm that the proposed methodological model enables the integration of technical criteria with social, cultural, and emotional dimensions, ensuring that none of these dimensions override the others. Furthermore, the model facilitates the identification of emerging behaviors in contexts of incipient electrification, and it anticipates demand growth scenarios that traditional models do not consider. Furthermore, the use of digital tools (*e.g.*, Survey123), adapted with a participatory approach, enables not only the characterization of consumption patterns, but also the collection of perceptions on family satisfaction, aspirations, and priorities, which are critical elements for guiding well-being-based decisions.

This methodological approach provides a flexible and scalable platform for improving decision-making processes in rural electrification from an integrative perspective. Overcoming the limitations of technocratic approaches, the model promotes context-sensitive, socially appropriate, and sustainable long-term decisions.

7. Conclusions

Success in rural electrification depends not only on technological implementation, but also on decision-making processes that actively incorporate the perspectives and priorities of the beneficiary communities. The proposed methodology emphasizes the importance of participatory and behavioral approaches that address the interrelationships between technical, social, economic, and environmental factors in order to ensure that energy solutions are sustainable and accepted by users. The adoption of a participatory and integrative (holistic) decision-making model ensures that rural communities not only have access to energy but are also involved in the management and long-term sustainability of projects, facilitating a positive impact on their well-being and development.

In this regard, government entities, system operators, academic institutions, and international cooperation agencies are encouraged to consider the following strategic guidelines:

- Incorporate participatory and user-centered design tools from the initial stages of project identification and formulation.
- Fund mechanisms that encompass energy infrastructure, capacity building, community strengthening, and social assessment processes.

- Apply multidimensional impact indicators that include satisfaction levels, technological adoption, and community self-management capacity.
- Promote social and technological innovation from the territories by recognizing and supporting local initiatives that promote equitable and sustainable access to energy.

This set of actions is consistent with the transition towards fair, resilient, and culturally relevant energy models, as proposed in the literature on energy justice and sustainable development (15). Thus, the main contribution of this research is not limited to formulating a theoretical model; it translates into a methodological proposal that seeks to strengthen community energy governance, ensure the sustainability of implemented solutions, and effectively contribute to achieving SDG7 in isolated rural regions.

8. Author contributions

Diana Garcia-Miranda: conceptualization, methodology, investigation, and writing (original draft). **Francisco Santamaria:** formal analysis, writing (review and editing). **César Trujillo Rodríguez:** formal analysis, writing (review and editing). **Marcel Castro-Sitiriche:** methodology and supervision.

9. Funding

This research received no external funding.

10. Data availability

The data will be made available upon request.

11. Conflicts of interest

The authors declare no conflict of interest.

10. Use of artificial intelligence

During this work, the authors did not employ any technologies associated with artificial intelligence.

References

[1] United Nations, "Consensus reached on new sustainable development agenda to be adopted by world leaders in september - united nations sustainable development," 2015. [Online]. Available: https://www.un.org/sustainabledevelopment/blog/2015/08/transforming-our-world-document-adoption/

[2] CEPAL, "La Agenda 2030 y los Objetivos de Desarrollo Sostenible: una oportunidad para América Latina y el Caribe. Objetivos, metas e indicadores mundiales," 2019. https://www.cepal.org/es/publicaciones/40155-la-agenda-2030-objetivos-desarrollo-sostenible-oportunidad-america-latina-caribe

[3] I. Alloisio, A. Zucca, and S. Carrara, "SDG 7 as the enabling factor for sustainable development: The role of technology innovation in the electricity sector," 2015. [Online]. Available: https://icsd.wpengine.com/wp-content/uploads/2017/01/AlloisioUpdate.pdf

[4] IRENA, "Tracking SDG7: The energy progress report," 2018. [Online]. Available: https://www.irena.org/publications/2018/May/Tracking-SDG7-The-Energy-Progress-Report/

[5] S. Oparaocha and H. O. Ibrekk, "Accelerating SDG7 achievement policy briefs in support of the first SDG7 review at the UN high-level political forum 2018," United Nations, 2018. [Online]. Available: https://sustainabledevelopment.un.org/content/documents/25571804578ESDG7_Policy_Briefs_REV_3.pdf%0Ahttps://sustainabledevelopment.un.org/content/documents/18041SDG7_Policy_Brief.pdf

[6] F. Fuso Nerini *et al.*, "Mapping synergies and trade-offs between energy and the Sustainable Development Goals," *Nat. Energy*, vol. 3, no. 1, pp. 10–15, 2018. https://doi.org/10.1038/s41560-017-0036-5

[7] D. McCollum, L. G. Echeverri, S. Pachauri, J. Rogelj, and P. Kabat, "Connecting the Sustainable Development Goals by their energy," 2017. [Online]. Available: https://pure.iiasa.ac.at/id/eprint/14567/1/WP-17-006.pdf

[8] Sustainabel Development Solutions Network, "SDG Index and Dashboards 2018," *2018. [Online]. Available:* https://www.unsdsn.org/resources/sdg-index-and-dashboards-2018/?gad_=1&gad_3253704546&gbraid=0AAAABdu6wyzM5zX0Or6ekp9Idhbm14BV&gclid=Cj0KCQiAxonKBhC1ARIsAIHq_ltBCM2UGEtrYeD4Px9cqMvYmPGobF2jeQw64Euevb7BJvcW1DngpnMaAkStEALw_wcB

[9] M. Planelles and Cristina Delgado, "El 13% de la población mundial aún no tiene acceso a la electricidad," El País, 2018. [Online]. Available: https://elpais.com/economia/2018/05/02/actualidad/1525257286_099135.html

[10] IEA, "Access to electricity – SDG7: Data and projections – Analysis," 2024. [Online}. Available: https://www.iea.org/reports/sdg7-data-and-projections/access-to-electricity

[11] G. Andersen, "Guide to appropiate electrification for rural areas of developing countries," 1997. [Online]. Available: https://www.appropedia.org/Appropriate_technology_graduate_thesis_literature_review

[12] C. M. Fileccia, N. Caravaggio, and E. Conte, "Buen Vivir : Sumak Kawsay and reality," 2013. [Online]. Available: https://www.researchgate.net/publication/337155232_Buen_Vivir_betwee_Sumak_Kawsay_and_reality

[13] S. M. Ajila, "Sumak Kawsay: ¿estrategia política o filosofía de vida?" 2017. [Online]. Available: https://dspace.ups.edu.ec/handle/123456789/14860

[14] M. J. Castro-Sitiriche, E. Park, and E. Colombo, "Native power and local empowerment," *Ansole News*, no. 3, pP. 9-11. https://ansole.org/download/ANSOLE_News_3.pdf

[15] M. J. Castro-Sitiriche, and M. Ndoye, "On the links between sustainable wellbeing and electric energy consumption," *African J. Sci. Tech. Innov. Dev.*, vol. 5, no. 4, pp. 327–335, 2013. https://doi.org/10.1080/20421338.2013.809279

[16] ENERGIA, "Poor people's energy outlook 2016," 2016. [Online]. Available: https://energia.org/document/poor-peoples-energy-outlook-2016/

[17] F. O. Omole, O. K. Olajiga, and T. M. Olatunde, "Challenges and successes in rural electrification: A review of global policies and case studies," *Eng. Sci. Tech. J.*, vol. 5, no. 3, pp. 1031–1046, Mar. 2024. https://doi.org/10.51594/ESTJ.V5I3.956

[18] J. Lata-García, L. Flores-Bastidas, P. P. Rosero, and F. Jurado, "Social, environmental and techno-economic impact of rural electrification isolated with photovoltaic systems," *Rev. Gestão Soc. Ambient.*, vol. 18, no. 2, art. e5368, 2024. https://doi.org/10.24857/RGSA.V18N2-124

[19] J. Domínguez, C. Bellini, L. Arribas, J. Amador, M. T. Pérez, and A. M. M. Ávila, "IntiGIS-local: A geospatial approach to assessing rural electrification alternatives for sustainable socio-economic development in isolated communities – A case study of Guasasa, Cuba," Preprints.org, Jun. 2024. [Online]. Available: https://doi.org/10.20944/PREPRINTS202406.0532.V1

[20] A. N. Barsei, E. Pamungkasih, J. Sabtohadi, B. T. Asmoro, Y. Anindyasari, and A. Saputra, "Community-based centralized solar mini-grid management for rural electrification: Evidence from remote villages," *E3S Web Conf.*, vol. 506, art. 03001, Mar. 2024. https://doi.org/10.1051/E3SCONF/202450603001

[21] F. C. Fonseca, H. F. Azcona, C. G. Prado, R. R. Pérez, and J. M. C. Aceves, "Impacto socioemocional de la electrificación sostenible en la Región Mixteca, Oaxaca: Un análisis multidimensional basado en datos cuantitativos y cualitativos," *LATAM Rev. Latinoamericana Cien. Soc. Human.*, vol. 6, no. 2, pp. 3113–3137, Apr. 2025. https://doi.org/10.56712/LATAM.V6I2.3817

[22] D. G. Díaz, R. A. R. Roby, and E. M. Herrera, "Empoderamiento comunitario y desarrollo sostenible en territorios rurales," *REA Rev. Cien. Espec. Educ. Ambient.*, vol. 4, no. 1, pp. 162–181, May 2025. https://doi.org/10.48204/REA.V4N1.7336

[23] T. Yangailo, "El impacto de las energías renovables y el acceso a la tecnología en el desempeño económico de Zambia," *Tiempo Econ.*, vol. 12, no. 1, pp. 1–36, Jan. 2025. https://doi.org/10.21789/24222704.2149

[24] Á. A. Cisneros, C. R. T. Oré, R. A. Cisneros, C. A. Palomino, and F. L. Nina, "Mujeres en la planificación territorial rural en los Andes de Ayacucho [Perú]," *Prometeica Rev. Filos. Cien.*, vol. 32, pp. 1–11, Mar. 2025. https://doi.org/10.34024/PROMETEICA.2025.32.18653

[25] M. V. Venegas, M. S. Arroyo-Zeledón, A. Á. Artavia, A. Aguilar-Ellis, F. Sáenz-Ségura, and C. G. Benavides, "Contexto regional y planificación del desarrollo en la región Chorotega, Costa Rica," *Vinculación Univ. Soc.*, vol. 1, no. 2, pp. 15–38, Feb. 2025. https://doi.org/10.48204/3072-9629.6955

[26] G. Gallopin, "Sostenibilidad y desarrollo Sostenible: un enfoque sistémico," 2003. [Online]. Available: https://cmapspublic.ihmc.us/rid=1L16P93FL-F37B29-1JZ/lcl1864p.pdf

[27] Naciones Unidas, "Objetivo 7: garantizar el acceso a una energía asequible, segura, sostenible y moderna." [Online]. Available: https://www.un.org/sustainabledevelopment/es/energy/

[28] International Energy Agency, "Access to electricity." [Online]. Available: https://www.iea.org/sdg/electricity/

[29] M. Nilsson, D. Griggs, M. Visbeck, and C. Ringler, "A draft framework for understanding SDG interactions," *Chem. Int.*, vol. 38, no. 6, pp. 29–29, 2016. https://doi.org/10.1515/ci-2016-0632

[30] R. Davies, "The sustainable development goals as a network of targets. Monitoring and Evaluation NEWS," *Dep. Econ. Soc. Aff.*, vol. 1, no. 141, pp. 1–17, 2015. http://www.un.org/esa/desa/papers/2015/wp141_2015.pdf

[31] I. Alloisio and A. Zucca, "SDG 7 as the enabling factor for sustainable development: the role of technology innovation in the electricity sector," 2015, [Online]. Available: http://ic-sd.org/wp-content/uploads/sites/4/2017/01/AlloisioUpdate.pdf

[32] B. K. Journal and B. K. Sovacool, "Success and failure in the political economy of solar electrification: Lessons from World Bank Solar Home System [SHS] projects in Sri Lanka and Indonesia," *Energy Policy*, vol. 123, pp. 482–493, 2018. https://doi.org/10.1016/j.enpol.2018.09.024

[33] D. Nieusma and D. Riley, "Engineering Studies Designs on development: engineering, globalization, and social justice Designs on development: engineering, globalization, and social justice," *Eng. Stud.*, vol. 1, no. 1, pp. 29-59, 2010. https://doi.org/10.1080/19378621003604748

[34] S. Hostettler, E. Hazboun, and A. Gadgil, Eds., *Sustainable access to energy in the Global South: Essential technologies and implementation approaches*. London, UK: Springer, 2015. https://doi.org/10.1007/978-3-319-20209-9

[35] E. Gudynas and A. Acosta, "A renovación de la cr tica al desarrollo y el buen vivir como alternativa," *Utop. Prax. Latinoamericana*, vol. 16, no. 53, pp. 71–83, 2011.

[36] F. G. T. Zerpa and O. E. G. Ñáñez, "Naturaleza, cuerpo y tarén en la sociedad originaria pemón," *Rev. Derecho Reforma Agrar.*, vol. 0, no. 38, pp. 137–160, 2012. http://erevistas.saber.ula.ve/index.php/revistaagraria/article/view/6553

[37] "4 principios que el pueblo arhuaco le transmite a los colombianos para cuidar la naturaleza," Colombia Visible. [Onine]. Available: https://colombiavisible.com/4-principios-que-el-pueblo-arhuaco-le-transmite-a-los-colombianos-para-cuidar-la-naturaleza/

[38] British Council Colombia, "Acerca de los Misak." [Online]. Available: https://www.britishcouncil.co/artes/cultura-desafios-globales/proyectos-pasados/sembrando-nuestros-saberes/misak/acerca

[39] S. Barletti and J. Pablo, "La comunidad en los tiempos de la Comunidad: bienestar en las Comunidades Nativas asháninkas," *Bull. Inst. Français Étud. Andines*, vol. 45, no. 1, pp. 157–172, Apr. 2016. https://doi.org/10.4000/BIFEA.7904

[40] "Allin Kawsay [El Buen Vivir]." [Online]. Available: https://allinkawsay.org.pe/

[41] S. HOLLY, "Economic theory, freedom and human rights: The work of Amartya Sen," *Econ. Outlook*, vol. 10, no. 1, pp. 28–35, 2001.

[42] "UNDP | United Nations Development Programme." [Online]. Available: https://www.undp.org/

[43] L. J.-R. Castro-Sitiriche, and J. Marcel, "'Responsible wellbeing and energy threshold,'" *ETHOS Gub. Rev. Cent. Desarr. Pensam. Ét, Of. Ét. Gub.*, vol. VII, pp. 64–126, 2014. https://ecourses.uprm.edu/mod/page/view.php?id=60710

[44] R. Chambers, "Editorial: Responsible well-being – A personal agenda for development," *World Dev.*, vol. 25, no. 11, pp. 1743–1754, 1997. https://doi.org/10.1016/S0305-750X[97]10001-8

[45] M.Max-Neef,"Fromtheoutsidelookingin:Experiencesinbarefooteconomics,"1992.[Online].Available: https://www.daghammarskjold.se/wp-content/uploads/2014/08/From_the_outside_looking_in.pdf

[46] X. Wu, "Men purchase, women use: Coping with domestic electrical appliances in rural China," *East Asian Sci. Tech. Soc. Int. J.*, vol. 2, no. 2, pp. 211–234, 2008. https://doi.org/10.1215/s12280-008-9048-3

[47] S. Ortiz, M. Ndoye, and M. Castro-Sitiriche, "Satisfaction-based energy allocation with energy constraint applying cooperative game theory," *Energies*, vol. 14, no. 5, art. 1485, 2021. https://doi.org/10.3390/en14051485

[48] PNUD, "La próxima frontera: desarrollo humano y el Antropoceno," 2020. [Online]. Available: https://mexico.un.org/sites/default/files/2021-12/Desarrollo%2520humano%2520y%2520el%2520Antropoceno %281%29.pdf

[49] D. Akinyele, R. Rayudu, and R. Blanchard, "Sustainable microgrids for energy-poor communities: A spotlight on the planning dimensions," *IEEE Smart Grid Mag.*, vol. 7, pp. 1–8, 2016. https://smartgrid.ieee.org/bulletins/july-2016/sustainable-microgrids-for-energy-poor-communities-a-spotlight-on-the-planning-dimensions

[50] B. Domenech, M. Ranaboldo, L. Ferrer-Martí, R. Pastor, and D. Flynn, "Local and regional microgrid models to optimise the design of isolated electrification projects," *Renew. Energy*, vol. 119, pp. 795–808, 2018. https://doi.org/10.1016/j.renene.2017.10.060

[51] Y. Malakar, "Studying household decision-making context and cooking fuel transition in rural India," *Energy Sustain. Dev.*, vol. 43, pp. 68–74, 2018. https://doi.org/10.1016/j.esd.2017.12.006

[52] V. Rai, D. C. Reeves, and R. Margolis, "Overcoming barriers and uncertainties in the adoption of residential solar PV," *Renew. Energy*, vol. 89, no. November, pp. 498–505, 2016. https://doi.org/10.1016/j.renene.2015.11.080

[53] M. Stickdorn, M. Hormess, A. Lawrence, and J. [Economist] Schneider, "This is service design doing: Applying service design thinking in the real world: A practitioner's handbook," 2017, [Online]. Available: https://vufind.lboro.ac.uk/Record/522558

[54] A. Combelles, C. Ebert, and P. Lucena, "Design thinking," *IEEE Softw.*, vol. 37, no. 2, pp. 21–24, Mar. 2020. https://doi.org/10.1109/MS.2019.2959328

[55] L. Waidelich, A. Richter, B. Kolmel, and R. Bulander, "Design thinking process model review," in *2018 IEEE Int. Conf. Eng. Tech. Innov.*, Aug. 2018. https://doi.org/10.1109/ICE.2018.8436281

[56] R. Wolniak, "Systemy wspomagania w inżynierii produkcji inżynieria systemów technicznych," *Syst. Wspomagania W Inżynierii Prod.*, vol. 6, no. 6, pp. 247–255, 2017. https://www.scirp.org/reference/referencespapers?referenceid=3581222

[57] E. Blomkamp, "Systemic design practice for participatory policymaking," *Policy Des. Pract.*, vol. 5, no. 1, pp. 12–31, 2022. https://doi.org/10.1080/25741292.2021.1887576

[58] M. Guillen-Royo, "Applying the fundamental human needs approach to sustainable consumption corridors: participatory workshops involving information and communication technologies," *Sust. Sci. Pract. Pol.*, vol. 16, no. 1, pp. 114–127, Dec. 2020. https://doi.org/10.1080/15487733.2020.1787311

[59] OPSI, "Follow the rabbit: A field guide to systemic design." [Online]. Available: https://oecd-opsi.org/toolkits/follow-the-rabbit-a-field-guide-to-systemic-design/

[60] J. Radtke, L. Holstenkamp, J. Barnes, and O. Renn, "Concepts, Formats, and Methods of Participation: Theory and Practice," in *Handbuch Energiewende und Partizipation*, L. Holstenkamp and J. Radtke, Eds. Wiesbaden, Germany: Springer Fachmedien, 2018. pp. 21–42. https://doi.org/10.1007/978-3-658-09416-4_2

[61] P. Schweizer-Ries, Socio-environmental research on energy sustainable communities: Participation experiences of two decades, in *Renewable Energy and the Public,* P. Devine-Wright, Ed. London, UK: Routledge, 2011, cg. 13. https://www.taylorfrancis.com/chapters/edit/10.4324/9781849776707-19/socio-environmental-research-energy-sustainable-communities-participation-experiences-two-decades-petra-schweizer-ries

[62] A. Revez, N. Dunphy, C. Harris, G. Mullally, B. Lennon, and C. Gaffney, "Beyond forecasting: Using a modified Delphi method to build upon participatory action research in developing principles for a just and inclusive energy transition," *Int. J. Qual. Methods*, vol. 19, pp. 1–12, 2020. https://doi.org/10.1177/1609406920903218

[63] H. Bradbury, "Action Research – Participative self in transformative action. A precis," Participatory Methods, 2022. [Online]. Available: https://www.participatorymethods.org/resource/action-research-participative-self-in-transformative-action-a-precis/

[64] P. Schweizer-Ries, "Energy sustainable communities: Environmental psychological investigations," *Energy Policy*, vol. 36, no. 11, pp. 4126–4135, 2008. https://doi.org/10.1016/j.enpol.2008.06.021

[65] W. Kenton, "What Is PEST Analysis? Its applications and uses in business," Investopedia, 2025. [Online]. Available: https://www.investopedia.com/terms/p/pest-analysis.asp

[66] B. Igliński, A. Iglińska, M. Cichosz, W. Kujawski, and R. Buczkowski, "Renewable energy production in the Łódzkie Voivodeship. the PEST analysis of the RES in the voivodeship and in Poland," *Renew. Sustain. Energy Rev.*, vol. 58, pp. 737–750, 2016. https://doi.org/10.1016/j.rser.2015.12.341

[67] F. Hussain, "Impact of PESTLE Factors on Power Generation Projects of Bangladesh," 2013. [Online]. Available: https://dspace.bracu.ac.bd/xmlui/handle/10361/3737

[68] C. Zalengera, R. E. Blanchard, P. C. Eames, A. M. Juma, M. L. Chitawo, and K. T. Gondwe, "Overview of the Malawi energy situation and A PESTLE analysis for sustainable development of renewable energy," *Renew. Sustain. Energy Rev.*, vol. 38, pp. 335–347, 2014. https://doi.org/10.1016/j.rser.2014.05.050

Authors and biographies

Diana García-Miranda

Received her BS and MSc degrees in Electrical Engineering from Universidad Nacional de Colombia in 1999 and 2006. and her PhD degree in Engineering from Universidad Distrital Francisco José de Caldas in 2024. Its doctoral research focused on decision-making methodologies for rural electrification projects in isolated areas using a systemic and sustainable development approach. In 2006, she joined the Faculty of Electrical Engineering at Universidad Distrital Francisco José de Caldas, where she currently works as a full professor and is member of the Research Group on Electrical Systems and Energy Efficiency (GISE3). Her research interests include rural electrification and sustainable development.

Francisco Santamaría

Received his BS and MSc degrees in Electrical Engineering, as well as a PhD in Engineering from Universidad Nacional de Colombia in 2002, 2007, and 2013, respectively. In 2010, he joined the Faculty of Electrical Engineering at Universidad Distrital Francisco José de Caldas, where he currently works as a full professor and is member of the Research Group on Electrical Systems and Energy Efficiency (GISE3). His research interests include lightning protection, electromagnetic compatibility, electric mobility, and energy management.

César Trujillo-Rodríguez

Received his BS degree in Electronics Engineering from Universidad Distrital Francisco José de Caldas (Bogotá, Colombia), in 2003, an MSc degree in Electrical Engineering from Universidad Nacional de Colombia in 2006, and a PhD in Electronics Engineering from Universidad Politécnica de Valencia (Spain) in 2012. He is a full professor at the Department of Electrical Engineering of Universidad Distrital Francisco José de Caldas, where he currently teaches courses on analog circuits and power electronics. His main research interests include the modeling and control of power converters applied to distributed generation and microgrids.

Marcel Castro-Sitiriche

Received his BSc degree in Electrical Engineering from the University of Puerto Rico, Mayagüez Campus (UPRM), in 2000, as well as a PhD in Electrical Engineering from Howard University (Washington DC, USA) in 2007. He has been a professor of Electrical Engineering at UPRM since 2008. From 2014 to 2015, he spent a year at the Nelson Mandela African Institution of Science and Technology (Arusha, Tanzania) as a Fulbright Scholar. His research interests include energy justice, appropriate technology, rural microgrids, solar home systems, rural electrification, power electronics, and responsible wellbeing. His latest efforts have been focused on the concept of *bottom-up grids* for remote rural areas and power decentralization for resilience and energy justice.

UNIVERSIDAD DISTRITAL
FRANCISCO JOSÉ DE CALDAS

Ingeniería

https://revistas.udistrital.edu.co/index.php/reving/issue/view/1295

DOI: https://doi.org/10.14483/23448393.22204

Research

Modeling a Fixed-Bed System with Coal Volatiles Post-Combustion for Ceramic Kiln Firing

Modelamiento de un sistema de lecho fijo con poscombustión de volátiles del carbón para hornos de cocción de cerámicos

Marco A. Ardila-Barragán[1], María del Pilar Triviño-Restrepo[1], Luis F. Lozano-Gómez[1], Naren N. Ardila-Otálora[1]*, Brigith D. Cruz-Molina[1], Fabián R. Jiménez-López[1], Alfonso López-Díaz[1], and Jaime A. Riaño-Villamizar[2]

[1]Universidad Pedagógica y Tecnológica de Colombia (Tunja, Colombia).
[2]Inversiones Ladrillos Maguncia SAS (Sotaquirá-Boyacá, Colombia).

Abstract

Context: It is estimated that, in Colombia, more than 1300 brick industries consume around 5800 Tcal/year, which are supplied by coal, biomass, wood, and gas combustion. The most commonly used kilns are down-draught, wherein coal combustion is produced on fixed-grate beds, emitting greenhouse gases and other pollutants. As a contribution to solving this problem, this work presents the model of a fixed-bed system with coal volatiles post-combustion.

Method: Temperature, time, coal consumption, and combustion products were monitored in a down-draught kiln, in order to determine their mass, energy, and thermal efficiency balances. Coal characterization was performed under ASTM standards, ashes were determined via XRD, XRF, and TGA, and emissions were obtained using a gas analyzer. The thermodynamic model used to design the 3D reactor was based on coal-burning analysis.

Results: The process lasted 3166 min, consuming 2150 kg of coal. The combustion gases exhibited a varying composition of CO_2, CO, O_2, and hydrocarbons. The temperature on the grate reached 900 °C, and we recorded 1000 °C in the dome and 600 °C at the chimney base. The temperature difference between the dome and the chimney base explains the heat transferred for ceramic baking. The calorific value of the char was 19.52 % higher than that of the coal used. The composition of the ash showed silicon oxide, mullite, and goethite. The 3D model consists of a grate with preheater ducts for the secondary air post-combustion of the volatiles.

Conclusions: The outcome of this research was the 3D model of a fixed-bed grate for coal combustion and volatiles post-combustion. With its implementation, we expect to improve air quality and reduce the effects of the process on human health, as well as its operating costs.

Keywords: secondary air, ceramic firing, coal combustion, down-draught kiln, fixed-bed grill, post-combustion

Article history

Received: May 22nd, 2024

Modified: Sep 14th, 2025

Accepted: Oct 20th, 2025

Ing, vol. 30, no. 3, 2025, e22204

*Correspondence: naren.ardila@uptc.edu.co

Resumen

Contexto: Se estima que, en Colombia, más de 1300 industrias ladrilleras consumen alrededor de 5800 Tcal/año, provenientes de la combustión de carbón, biomasa, leña y gas. Los hornos más comunes son los de tiro descendente, en los cuales la combustión del carbón se realiza sobre parrillas fijas, emitiendo gases de efecto invernadero y otros contaminantes. Como contribución a la solución de este problema, este trabajo presenta el modelo de un sistema de lecho fijo con poscombustión de volátiles del carbón.
Método: Se monitorearon la temperatura, el tiempo, el consumo de carbón y los productos de combustión en un horno de tiro descendente, a fin de determinar los balances de masa, energía y eficiencia térmica. La caracterización del carbón se realizó bajo las normas ASTM, las cenizas se analizaron mediante XRD, XRF y TGA, y las emisiones se determinaron utilizando un analizador de gases. El modelo termodinámico empleado para el diseño del reactor 3D se basó en el análisis de la combustión del carbón.
Resultados: El proceso tuvo una duración de 3166 minutos, con un consumo de 2150 kg de carbón. Los gases de combustión presentaron una composición variable de CO_2, CO, O_2 e hidrocarburos. La temperatura en la parrilla alcanzó los 900 °C, y se registraron 1000 °C en la cúpula y 600 °C en la base de la chimenea. La diferencia de temperatura entre la cúpula y la base de la chimenea explica el calor transferido para la cocción de la cerámica. El poder calorífico del char fue 19.52 % superior al del carbón utilizado. La composición de las cenizas mostró la presencia de óxido de silicio, mullita y goethita. El modelo 3D consiste en una parrilla con conductos precalentadores para el aire secundario destinado a la poscombustión de los volátiles.
Conclusiones: El resultado de esta investigación fue el modelo 3D de una parrilla de lecho fijo para la combustión de carbón y la poscombustión de volátiles. Con su implementación, se espera mejorar la calidad del aire y reducir los efectos del proceso sobre la salud humana, así como sus costos operativos.

Palabras clave: aire secundario, cocción de cerámicos, combustión de carbón, hornos colmena, parrilla de lecho fijo, poscombustión

Table of contents

Page

1. Introduction 3

2. Material and methods 3
- 2.1. Phase I: field data collection 4
- 2.2. Phase II: mass balance, energy balance, and thermal efficiency calculations 4
- 2.3. Phase III: thermodynamic and 3D modeling 6
  - 2.3.1. 3D modeling 6

3. Results 7
- 3.1. Technical and technological description of the firing process 7
- 3.2. Characterizing the coal and solid combustion products 7
- 3.3. Characterization of the solid combustion products 9
- 3.4. Thermal profile of the beehive kiln 9
- 3.5. Evolution of emissions and gas . . 10
- 3.6. Thermodynamic modeling 12

4. Discussion 14

5. Conclusions 16

6. Author contributions 16

7. Acknowledgments 17

8. Funding 17

9. Data availability 17

10. Conflicts of interest 17

11. Use of artificial intelligence 17

1. Introduction

In 2016, China contributed significantly to global brick production, accounting for 54of the total output, followed by India (11 %), Pakistan (8 %), Bangladesh (4 %), and the rest of the world (23 %) (1). For the 2020-2025 period, the compound annual growth rate was expected to exceed 3 % (2). In 2015, Colombia reported a production of more than 10 Mt of fired clay, with an annual energy consumption ranging from 5 to 7 Tcal. This energy supply was obtained mainly from coal (62-71 %), wood (20-25 %), coal-biomass mixtures (7 %), and gas (0.00172-3 %). The production process is carried out at diverse scales, in artisanal, semi-merchandized artisanal, small, medium, and large-scale enterprises (3).

The most commonly used artisanal kilns in Colombia and other Latin American countries are of the beehive and trench types (4), where coal combustion takes place in fireboxes (3) equipped with a fixed-bed grate. These systems emit greenhouse gases and other pollutants (CO_2, CO, SO_2, CXHY, NOX, $PM_{2,5}$, and PM_{10}). Such contaminants pose health risks to the local population and the surrounding environment, and their environmental impacts have led to the implementation of increasingly stringent regulations aimed at reducing the deterioration of ecosystems (5–8).

Coal combustion in a fixed bed at atmospheric pressure is carried out without control over the amount of air supplied, an issue that is further complicated by the lack of homogeneity in the fuel particle size. Another peculiarity is that the heating of the load occurs at a low rate, promoting the release of uncombusted volatiles, leading to their direct emission into the environment in the form of soot (9).

To improve the productivity of the brickmaking sector, various technologies have been proposed, which are aimed at improving the energy efficiency of the aforementioned kilns, decreasing coal consumption, and reducing pollutant emission levels (10). These improvements can be achieved through the implementation of technological upgrades, such as the mechanization and automation of the process. In this vein, our research focused on the development of the 3D model of a solid carbonaceous material combustion system with volatiles post-combustion (SCMCS-VPC), designed for artisanal kilns with fixed-bed grates used for ceramic firing.

2. Material and methods

This research consisted of an experimental study for the development of the SCMCS-VPC, with the purpose of minimizing the emission of volatiles generated during the ceramic firing process (10) in inverted-flame beehive-type kilns (11) equipped with a fixed-bed grate which utilize coal combustion (Fig. **1**). The fieldwork was conducted at the Maguncia brick industry, located in the jurisdiction of Sotaquirá, and at ceramic handicraft factories in the municipality of Ráquira, both in the department of Boyacá. The project was executed in three phases.

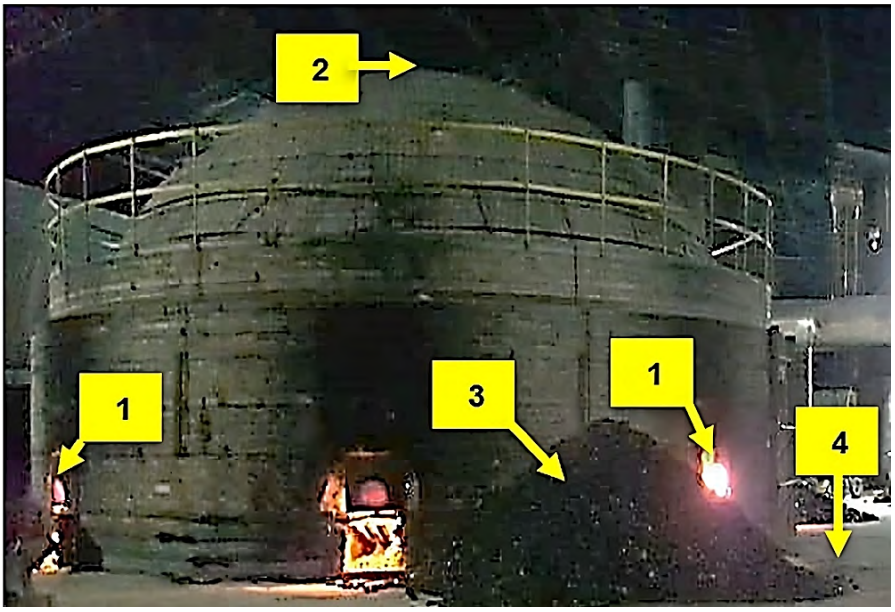

Figure 1. Sampling points for charge and temperature monitoring in an inverted-flame beehive kiln. 1: Burners 1 and 2; 2: dome thermocouple; 3: coal feed pile; 4: chimney-based thermocouple

2.1. Phase I: field data collection

This phase involved characterizing the coal through the ASTM's standard procedures; the analysis of solid combustion products using DRX, FRX, and TGA techniques; and the monitoring of the combustion process via temperature recording with type-K thermocouples and a data logger, which was complemented by photography and video documentation. The fuel supply was weighed on a digital scale with a precision of 0.1 kg, and the composition of the gaseous emissions was determined using an E Instruments E8500 Plus analyzer. Based on this information, the operating parameters were established in order to calculate the mass and energy balance.

2.2. Phase II: mass balance, energy balance, and thermal efficiency calculations

The combustion process for ceramic firing in an inverted flame beehive kiln is analytically described in Eq. (1), which represents the mass and energy balances.

$$C_{TSm} + \text{air} + E_{Ign} = E_{Gen} + G_{chm} + Cnz_{acm} + C_{inq} \tag{1}$$

where:

- C_{TSm} = total coal supplied to the firing process
- E_{Ign} = ignition energy
- E_{Gen} = thermal energy generated by combustion
- G_{chm} = chimney gases
- Cnz_{acm} = ashes accumulated during firing

- C_{inq} = unburned coal

C_{TSm} corresponds to the sum of the partial loads fed into each burner. The total burned coal (C_{Tqm}) is calculated using Eq. (2).

$$C_{Tqm} = C_{TSm} - H_{Hum} - Cnz_{acm} - V_{CxHy} - C_{inq} \tag{2}$$

where:

- H_{Hum} = moisture in the total coal supplied
- V_{CxHy} = volatile compounds

The composition of G_{chm}, which was determined by means of the combustion analyzer, is expressed in Eq. (3).

$$G_{chm} = CO_2 + V_{CxHy} + CO + O_2 + N_2 \tag{3}$$

The accumulated ashes (Cnz_{acm}), defined in Eq. (4), consist of the ashes from the total burned coal (Cnz_{CTqm}) and C_{inq}.

$$Cnz_{acm} = Cnz_{CTqm} + C_{inq} \tag{4}$$

The percentage of unburned coal in the ashes ($\%C_{inq}$) is calculated via Eq. (5).

$$\%C_{inq} = \frac{C_{inq}}{Cnz_{acm}} \times 100 \tag{5}$$

The energy balance is calculated using Eqs. (6) to (9).

$$E_T = E_{Tent} - E_{Tsld} \tag{6}$$

$$E_{Tent} = E_{C_{TSm}} + E_{Ign} \tag{7}$$

$$E_{Tsld} = E_{C_{Tqm}} + E_{C_{inq}} \tag{8}$$

$$E_T = (E_{C_{TSm}} + E_{Ign}) - \left(E_{C_{Tqm}} + E_{C_{inq}}\right) \tag{9}$$

where:

- E_T = total energy
- E_{Tin} = total energy input
- E_{Tout} = total energy output
- $E_{C_{TSm}}$ = total energy from the supplied coal
- E_{Ign} = ignition energy
- $E_{C_{Tqm}}$ = energy from the total burned coal
- $E_{C_{inq}}$ = energy from the total unburned coal

Energy is determined as a function of heat (Q) and mass, as shown in Eq. (10).

$$Q = m_{C_{Tqm}} * VC \tag{10}$$

where:

- $m_{C_{Tqm}}$ = total mass of burned coal
- VC = calorific value

The thermal efficiency (η) of the combustion process for ceramic firing in the beehive kiln corresponds to the ratio between $E_{C_{Tqm}}$ and $E_{C_{TSm}}$. This is calculated by means of Eq. (11).

$$\eta = \frac{E_{C_{Tqm}}}{E_{C_{TSm}}} = \frac{Q_{C_{Tqm}}}{Q_{C_{TSm}}} \tag{11}$$

where:

- $Q_{C_{Tqm}}$ = heat from total coal burned
- $Q_{C_{TSm}}$ = heat from total coal supplied

The heat from the total burned coal ($Q_{C_{Tqm}}$) is obtained from Eq. (10), while the heat supplied ($Q_{C_{TSm}}$) is calculated via Eq. (12).

$$Q = m_{C_{TSm}} * VC \tag{12}$$

where:

- $m_{C_{TSm}}$ = Mass of the total coal supply

2.3. Phase III: thermodynamic and 3D modeling

Thermodynamic modeling was performed based on the analysis of the burned coal (12) from burners equipped with a fixed-bed grate, where the air enters through the lower section of the kiln and passes through the fuel (Fig. 2). This process operates with the kiln door open, and air is regulated empirically by adjusting the chimney draft. Consequently, it is not possible to control combustion under stoichiometric parameters. Hence, black smoke emissions are generated from chimneys, indicating an incomplete combustion and energy losses due to unburned volatile hydrocarbons (9, 13), which may lead to severe pollution issues. For the reactor design (Fig. 3), we employed the French method for product designed (14).

The baseline was set as follows: air temperature: 25 °C; average autoignition temperature of the low-rank coal: 250 °C (15); ignition temperature of the volatiles: 400 °C.

2.3.1. 3D modeling

Based on the thermodynamic modeling and the fuel consumption curves, we calculated the stoichiometry of the combustion of 5 kg of coal with 30 % excess air (16). From the results obtained, the grate area, the air flow, and the dimensions and distribution of the ducts were determined, along with the required primary and secondary air supplies. Finally, the 3D model was created, using SolidWorks to design the components, assemble the complete system, and generate manufacturing drawings.

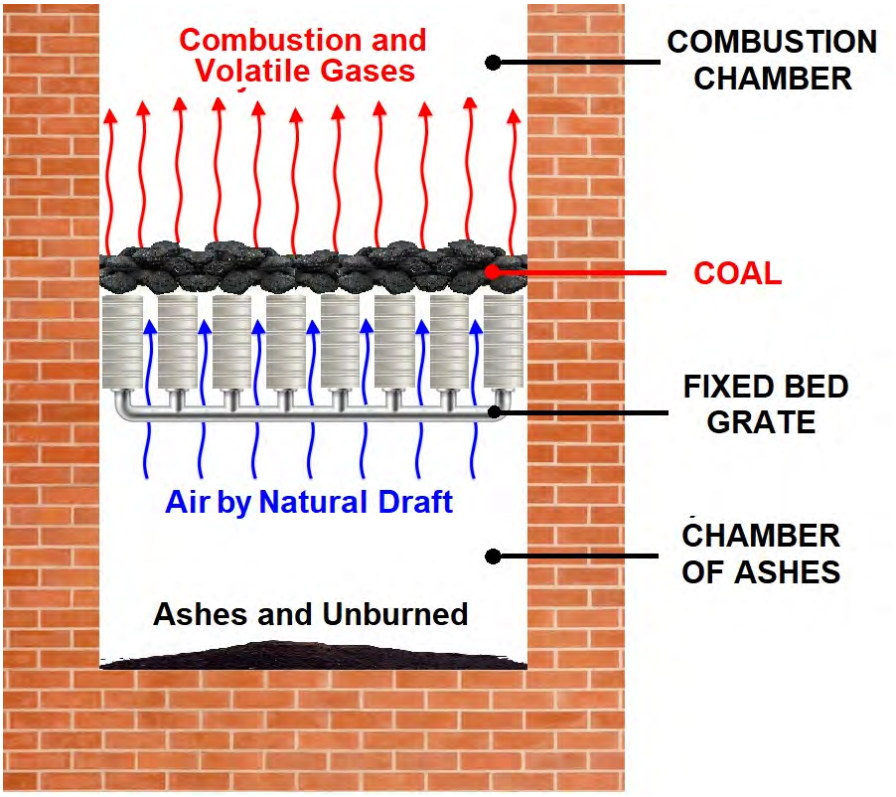

Figure 2. Schematic representation of the coal combustion process in a fixed-bed grate burner

3. Results

3.1. Technical and technological description of the firing process

The firing of the ceramic load in the beehive kiln was achieved through the heat generated during the combustion of coal in fireboxes equipped with a fixed-bed grate. The total coal supply, as a function of time, is shown in Fig. 4.

The total duration of the firing process was 52.76 h (3166 min), with a coal consumption of 2.15 t, supplied in 23 kg batches, with incremental increases averaging 1 kg at 35 min intervals. This procedure was maintained until the maximum gas temperatures were reached: 1050 °C in the dome, and 637 °C at the base of the chimney. It can be inferred that the heat difference between these two points corresponds to the energy consumed during the ceramic firing process, as well as to heat and convection losses through the kiln walls.

3.2. Characterizing the coal and solid combustion products

Sampling of the coal and solid combustion products (ashes and unburned material) was conducted in two fireboxes. The results of this characterization are presented in Table I.

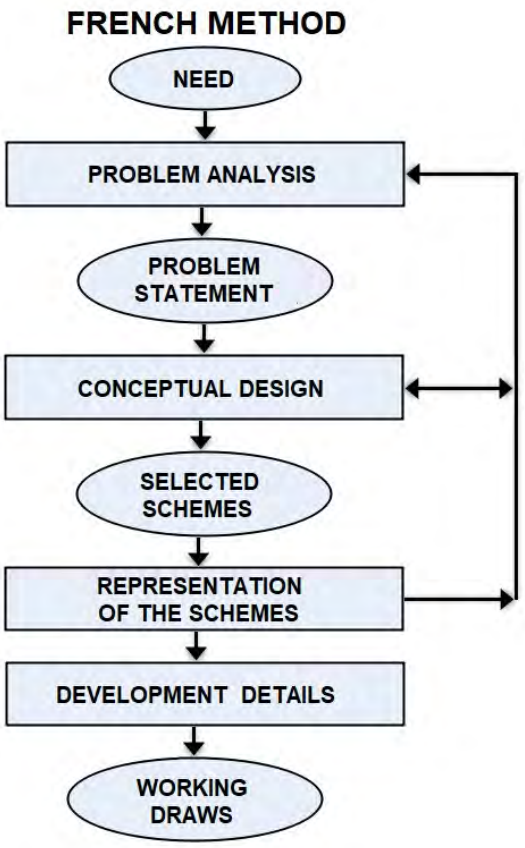

Figure 3. Flow diagram of the French method for product design

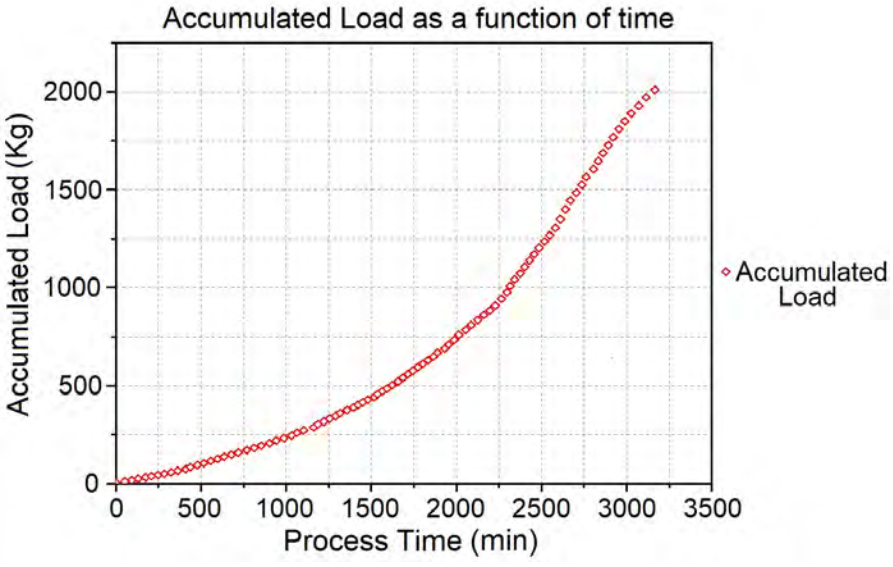

Figure 4. Coal consumption during the firing process

Table I. Characterization of coal and solid combustion products

SAMPLE	% H_2O	%Cz	%MV	%CF	%S	CV (Kcal/Kg)	IHL	%C_{inq}
COAL	2.57	7.05	43.25	47.14	0.96	5850.00	1.00	-
PSC H1	0.49	91.90	2.36	5.25	0.15	7226.00	0.00	8.90
PSC H2	0.36	91.48	2.12	6.04	0.13	7312,00	0.00	1020

Note: sample H_2O: moisture – ASTM D3173; Cz: ashes – ASTM D3174; MV: volatile matter – ASTM D3175; CF: fixed carbon – ASTM D3172; S: sulfur – ASTM D4239; CV calorific value – ASTM D2015; IHL: free swelling index – ASTM D750; C_{inq} unburned coal; PSC: solid combustion products; H1: firebox 1; H2: firebox 2

This table shows that the differences between the percentages of moisture, ashes, volatile matter, and fixed carbon in the solid combustion byproducts are less than 1 %. From these data, it can be deduced that the combustion efficiency of the analyzed fireboxes is similar. Furthermore, the average calorific value of the unburned material increased by 19.52 % compared to the original coal. This behavior explains the formation of char (17). Lastly, 14.59 % of the sulfur contained in the coal was retained in the solid combustion products; we inferred that the remaining percentage was released through gaseous emissions.

3.3. Characterization of the solid combustion products

The elemental composition (expressed in the form of percentages) was determined via X-ray fluorescence (XRF) analysis (Fig. 5), and the phase distribution was obtained through X-ray diffraction (XRD) (Fig. 6). We found 52.8 % Si, 25.4 % Al, and 6.08 % Fe as major elements, as well as Na, Mg, P, Cl, K, Ca, Ti, Sr, and Pd in lower proportions. The phases identified via XRD were 41.0 % silicon oxide, 42.2 % mullite, and 15.7 % goethite.

The thermal behavior was determined through a differential scanning calorimetry thermogravimetric analysis (DSC-TGA). The thermogram in Fig. 7 presents the mass loss curves as a function of temperature and the energy variation resulting from the phase and compositional changes in the solid combustion residues.

3.4. Thermal profile of the beehive kiln

The temperature monitoring data, obtained as a function of time, are presented in Fig. 8. These correspond to measurements taken at the dome (CUP), chimney base (CHM), and fireboxes 1 (HNL1) and 2 (HNL2).

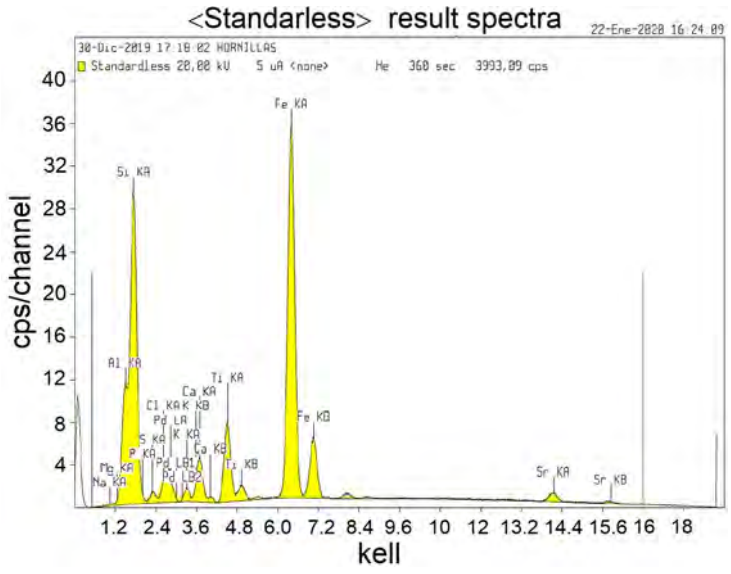

Figure 5. FRX spectrum

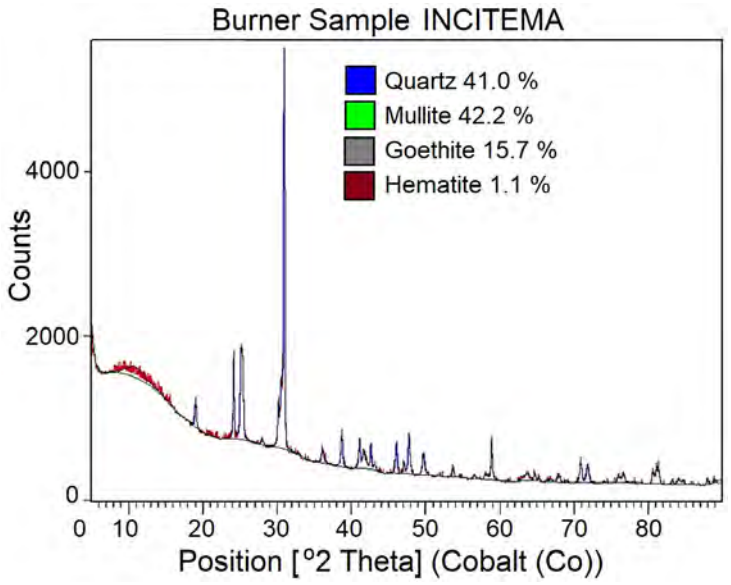

Figure 6. XRD diffractogram

3.5. Evolution of emissions and gas

We documented the emissions via photographs for one loading cycle over an average period of 45 min, in order to determine the characteristics of the chimney emissions. This is shown in Fig. 9.

The results of the gas analysis for six loading cycles—at 45min intervals—are represented by dotted boxes, which enclose the maximum hydrocarbon emission peaks (Fig. 10) associated with the loading periods. In Fig. 11, the dotted lines emphasize the ascending regions of the CO and CO_2 curves, which

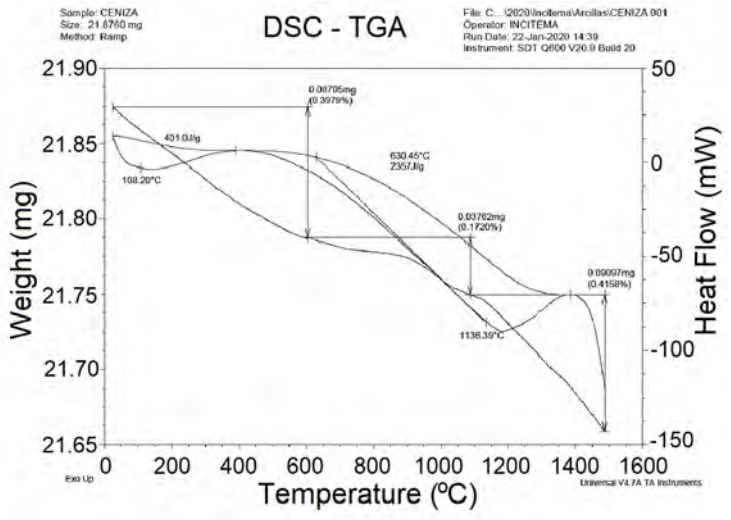

Figure 7. TGA thermogram

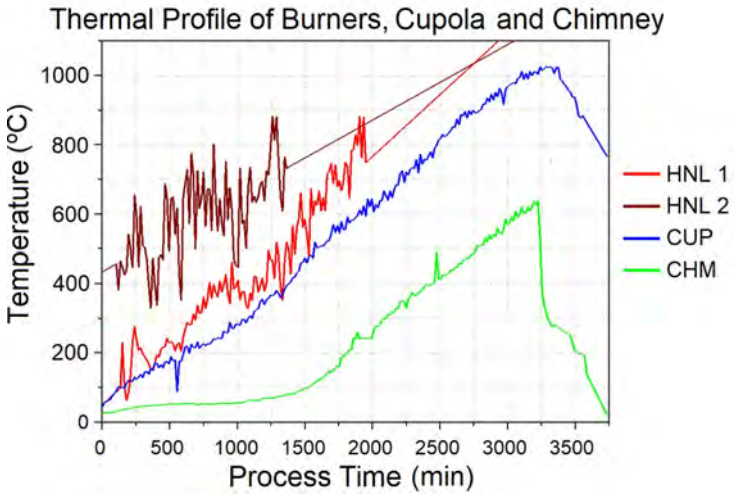

Figure 8. Thermal profile of the ceramic firing process in the beehive kiln

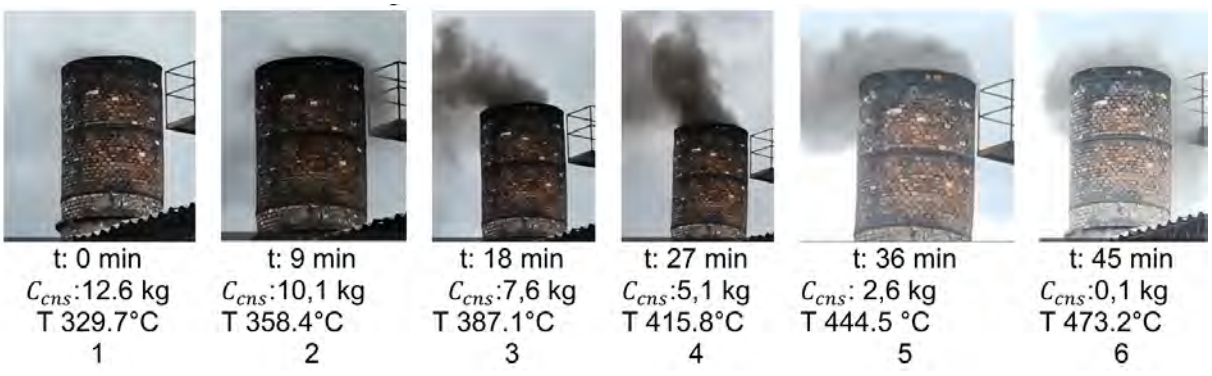

Figure 9. Photographic sequence of chimney emissions for a single loading cycle

contrast with the descending trajectories of O_2. At the end of the process, the reduction in the coal fed to the kiln correlates with the overall emissions reduction.

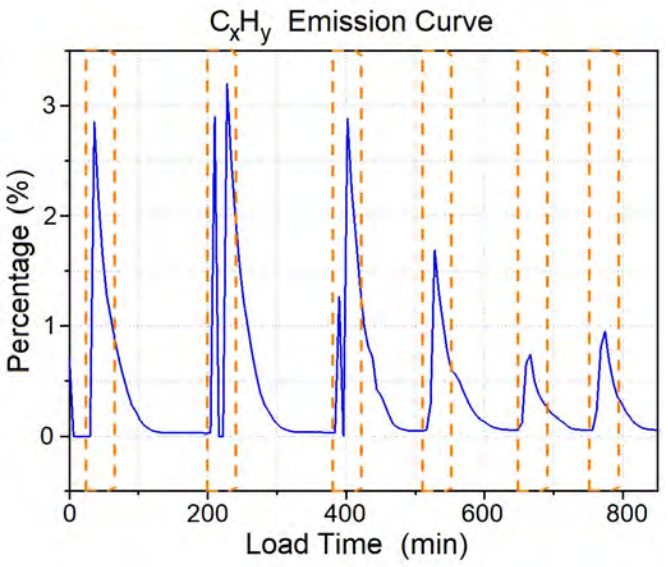

Figure 10. Hydrocarbon emissions plot

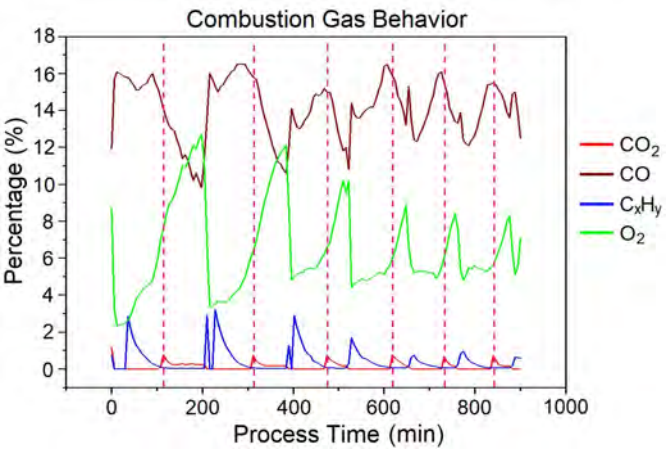

Figure 11. Plot of CO_2, CO, CXHY, and O_2 emissions

3.6. Thermodynamic modeling

As a result of the analysis and monitoring of the coal combustion process (12) on a fixed-bed grate (Fig. 2), a thermodynamic model was obtained for the SCMCS-PCV system (Fig. 12). This system consists of a fixed grate equipped with ducts for convective air pre-heating (18), utilizing the heat generated from the exothermic chemical reactions. This mechanism not only recovers heat; it also cools the grate tubes, thereby improving their service life.

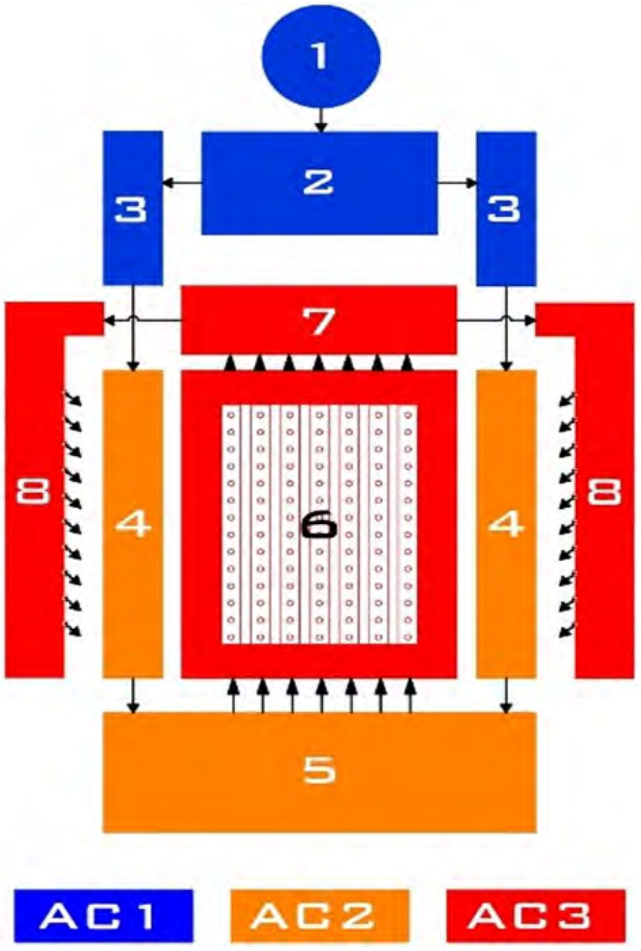

Figure 12. Flowchart of the SCMCS-VPC's thermodynamic model

Conventions

1. Controlled air supply source
2. Air distribution chamber
3. Air distribution ducts
4. Air preheating ducts
5. Pre-heated air distribution chamber
6. Grate for coal combustion with pre-heated air
7. Pre-heated air collector
8. Pre-heated secondary air injector for volatile port- combustion

AC1: Air condition 1 (25 °C)
AC2: Air condition 2 (250 °C)
AC3: Air condition 3 (400 °C)

The thermodynamic model operates as follows. Controlled air is supplied (1) at ambient temperature, which then reaches the air distribution chamber (2), continuing through two conduction sets (3) and the preheating ducts (4) to fill the pre-heated air distribution chamber (5). From this chamber, the air passes through the perforated tubular bars of the fixed-bed grate (6), where part of the flow acts as primary air for coal combustion, while the remaining portion continues towards the pre-heated air collector (7) and is distributed via the injectors as secondary air for volatiles post-combustion (8). The 3D model of the SCMCS-VPC (Fig. 13), derived from thermodynamic modeling, contains a variable-speed fan that delivers the air in a controlled manner. This air is pre-heated in the corresponding chambers by thermo-regulated electric heaters and then supplied to the fixed-bed grate, which consists of the air distribution chamber, the combustion tubes with primary air, and the collector duct. From the collector, the air continues to the secondary air injectors, where it is blown across the fuel load, transversely to the secondary combustion gas stream, to induce the post-combustion of volatiles. The supply of solid carbonaceous material to the grate is managed from a hopper equipped with a dosing system.

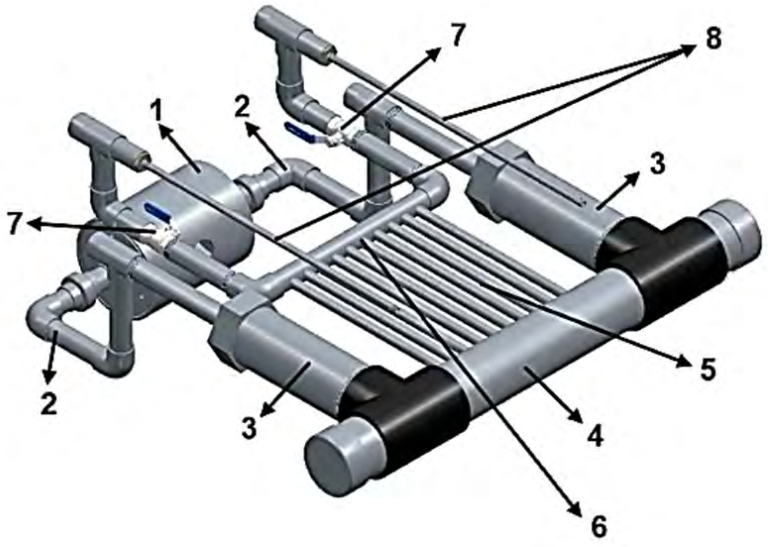

Figure 13. 3D design of the SCMCS-VPC and its components: 1) supply chamber, 2) duct, 3) assisted pre-heating chamber, 4) distribution chamber, 5) grate, 6) collector duct, 7) access ports, 8) secondary air injectors

4. Discussion

Based on the characterization results (Table I), and according to ASTM D388, the coal used can be classified as a low-rank, non-caking sub-bituminous type-A coal (19). This type of coal is also used in the brick industry of several Asian countries (8).

Factors such as the coal composition, the high volatile matter content (43.25 %), the coal particle size (+2 in), open-door combustion, the combustion temperature, air supply deficiency, and the lack

of operational control affected process efficiency and performance (20, 21), resulting in incomplete combustion and the emission of gases, smoke, and particulate matter (soot) through the chimney (Fig. 9), in addition to solid combustion residues (ashes and unburned carbon), which represent energy losses (4, 22).

Fig. **11** shows alternating cycles of maximum and minimum emissions with a decreasing trend as a function of process time. In the gas analysis, CO_2, the main product of combustion, exhibited concentrations between 10 and 16 %. In addition, CO reached 1 %, the C_XH_Y levels were less than 3 %, and no significant emissions of nitrogen oxides (NO_x) were detected, since high temperatures were not reached (17, 23).

According to the literature, at temperatures below 600 °C, alkenes (ethylene, propylene, butene) and aromatics (benzene, toluene, and naphthalene), can be formed, among others (23). These byproducts represent a significant risk to human health and the environment (24, 25).

According to Table I, the char (unburned material), the solid carbonaceous residue that remains after the release of volatile matter, formed due to oxygen deficiency, contains 52.44 % of fixed carbon and exhibits a higher calorific value (7269 kcal/kg), compared to the original coal (5850 kcal/kg), representing an increase of 19.52 %. This high energy value is explained by the fact that char is a carbon-rich matrix (1). Additionally, the mean char content in the ashes is higher than that reported for the boiler combustion process (up to 45 %) (27), which is consistent with a fixed-bed combustion configuration.

The results of the TGA (Fig. **7**) show a mass loss equivalent to 0.08705 mg (0.3979 %) within a temperature range of 25-600 °C. Water vaporization was recorded between 25 and 100 °C (28). Based on the proximate analysis of the coal and the XRF results of the ashes (Fig. **5**), the presence of S, Na, and Cl was inferred. These elements may be associated with the dehydration (100-200 °C) of sulfates and bicarbonates ($NaHCO_3.5H_2O$) (28). The mass losses between 200 and 400 °C indicate an exothermic behavior due to the combustion of the residual unburned carbon (29). Finally, the mass losses recorded between 400 and 900 °C suggest the fusion of chlorides and the decomposition of carbonates and sulfurates, corresponding to endothermic processes (29). In terms of energy analysis, the behavior between 200 and 400 °C may be due to oxygen absorption into the fuel's porous texture. Furthermore, the rapid mass loss beyond 400 °C indicates the onset of ignition and active combustion (29).

In the thermal profile (Fig. **8**), the temperature curves for HNL1 and HNL2 exhibit significant fluctuations, which are explained by the fact that the process involves open-door firebox combustion and is influenced by variable environmental conditions such as relative humidity, ambient temperature, and an irregular air inflow. The temperature profile in the dome (CUP) registers fewer variations, as this is the part of the kiln where heat generated in the fireboxes accumulates for distribution through the ceramic load. The chimney base (CHM) temperature curve reflects an average cooling of 380 °C compared to the maximum temperatures reached in the dome, which are associated with convective

and radiative heat transfer from the flue gases to the ceramic mass during firing. During the first 25 h (1500 min), the gas temperature at the CHM does not exceed 100 °C. After 29 h (1740 min), however, it decreases by approximately 30°C, which can be attributed to the thermal saturation of the firing material.

According to current and emerging trends, the objective is to reduce fuel consumption by up to 30 %, optimize firing times, and minimize pollutant emissions (30), (**?**). The design of the SCMCS-VPC (Fig. **13**) aims to enhance process efficiency and improve the quality of ceramic products (30, 31). The system integrates a coal feeding device and variable-speed blower as key components for animation and process control, along with preheated secondary air injectors to promote volatiles post-combustion.

At the industrial level and in mass production scales, coal combustion systems employing fixed-beds, moving grates, and upward-moving fixed-grates are utilized, wherein the combustion air is preheated to achieve a high-temperature operation. This approach involves the burning of solid fuel with particle sizes between 6 and 50 mm along with the released volatiles (**?**, 16). These design and operation principles were considered as references in the development of the SCMCS-VPC, aiming for improved energy efficiency and reduced environmental impacts.

5. Conclusions

This article presented the design of a 3D model for a solid carbonaceous material combustion system with volatiles post-combustion (SCMCS-PCV) as a technological conversion alternative for beehive kilns equipped with fixed-bed grates.

The monitoring of the ceramic product firing process, conducted at the Maguncia brick industry and the artisan factories in the municipality of Ráquira (Boyacá, Colombia), made it possible to identify the factors affecting the energy efficiency of the sub-bituminous coal used (volatile matter emissions and unburned material), as well as its environmental performance.

The 3D model, derived from the geometric and thermal design, improves the conventional fixed-bed grate combustion process by incorporating a primary air pre- heating system to increase the combustion temperature, as well as a secondary air injection system for volatiles post-combustion. Additionally, the system includes an ash evacuation control mechanism to minimize unburned carbon generation. Thus, the proposed model achieves an increase in energy efficiency and a reduction in the environmental impacts associated with coal combustion.

6. Author contributions

Marco Antonio Ardila-Barragán: project administration, methodology, formal analysis, investigation, writing (review and editing)

María del Pilar Triviño-Restrepo: methodology, investigation, writing (review and editing)
Luis Fernando Lozano-Gómez: investigation, writing (review and editing)
Naren Natalia Ardila-Otálora: methodology, investigation, visualization, writing (review and editing)
Brigith Daniela Cruz-Molina: methodology, investigation, visualization, writing (review and editing)
Fabián Rolando Jiménez-López: methodology, formal analysis, investigation, writing (review and editing)
Alfonso López-Díaz: investigation, conceptualization, funding acquisition
Jaime Alberto Riaño-Villamizar: investigation, funding acquisition, resources

7. Acknowledgments

The authors express their gratitude to the Vice-Principalship and Research Directorate of Universidad Pedagógica y Tecnológica de Colombia (UPTC), to Industria Ladrillera Maguncia, to the artisan factories of the municipality of Ráquira (Boyacá), and to INCITEMA for their valuable participation and support throughout this research.

8. Funding

This research received no external funding.

9. Data availability

The data will be made available upon request.

10. Conflicts of interest

The authors declare no conflict of interest.

11. Use of artificial intelligence

During this work, the authors did not employ any technologies associated with artificial intelligence.

References

[1] S. Jain, "Development of UNfiRED BRICKS USING INDUSTRIAL WASTE," 2016. [Online]. Available: https://doi.org/10.13140/RG.2.2.23905.51047 ↑3, 15

[2] A. Eser, "Essential brick industry statistics in 2023," ZipDo, 2023. [Online]. Available: https://zipdo.co/statistics/brick-industry/ ↑3

[3] Dirección de Asuntos Ambientales Sectorial y Urbana., L. F. González Herrera, J. I. Pedraza Vega, M. Gaitán Varón, and Corporación Ambiental Empresarial (CAEM), *Portafolio de mejores técnicas*

disponibles y mejores prácticas ambientales para el sector alfarero y de producción de ladrillo en Colombia. Bogotá DC, Colombia: Ministerio de Ambiente y Desarrollo Sostenible, 2021. ↑3

[4] C. David and M. Cabeza, "Panorama sobre modelado de eficiencia energética en hornos ladrilleros colombianos", 2023. [Online]. Available: https://www.cdtdegas.com/images/Descargas/Nuestra_revista/MetFlu16/1_Modelado_eficiencia_hornos.pdf ↑3, 15

[5] I. M. Guerrero, E. A. Goldstein, J. H. Stein, H. Acquay, and M. Sarraf, "Introducing energy-efficient clean technologies in the brick sector of Bangladesh," World Bank, 2011. [Online]. Available: https://documents.worldbank.org/en/publication/documents-reports/documentdetail/770271468212375012 ↑3

[6] C. W. Schmidt, "Modernizing artisanal brick kilns: A global need," *Environ. Health Perspect.*, vol. 121, no. 8, pp. A244–A 246, Aug. 2013, https://doi.org/10.1289/ehp.121-A242 ↑3

[7] M. Zavala *et al.*, "Black carbon, organic carbon, and co-pollutant emissions and energy efficiency from artisanal brick production in Mexico," *Atmos. Chem. Phys.*, vol. 18, no. 8, pp. 6023–6037, Apr. 2018. https://doi.org/10.5194/acp-18-6023-2018 ↑3

[8] K. M. ud Darain *et al.*, "Energy efficient brick kilns for sustainable environment," *Desalin. Water Treat.*, vol. 57, no. 1, pp. 105–114, Jan. 2016. https://doi.org/10.1080/19443994.2015.1012335 ↑3, 14

[9] M. R. Riazi and R. Gupta, *Coal Production and Processing Technology*. Boca Ratón, Florida, USA: CRC Press, 2016. ↑3, 6

[10] C. Weyant *et al.*, "Brick kiln measurement guidelines: Emissions and energy performance," Aug. 2016. [Online]. Available: https://www.ccacoalition.org/sites/default/files/resources/BC_BrickKilns_GuidanceDocument_Final.pdf ↑3

[11] I. Blasco, J. Ferrero, C. García, and R. González, "Análisis y descripción gráfica del funcionamiento de los hornos cerámicos," 2015. [Online]. Available: https://ceramica.name/img/descargas/Hornos%20ceramicos.pdf ↑3

[12] A. W. Date, *Analytic combustion: With thermodynamics, chemical kinetics, and mass transfer.* Bombay, India: Cambridge University Press, 2011. ↑6, 12

[13] J. M. Samet, "Introduction," in *Air pollution and cancer*, K. Straif, A. Cohen, and J. Samet, Eds. Lyon, France: International Agency for Research on Cancer (IARC), World Health Organization, 2013 ↑6

[14] N. Cross, *Métodos de diseño: estrategias para el diseño de productos*, F. R. Pérez Vázquez, Trad. México DF, Mexico: Limusa Wiley, Grupo Noriega Editores, 2002. ↑6

[15] K.-C. Xie, *Structure and reactivity of coal. A survey of selected Chinese coals*, Beijing, China: SpringerLink, 2015. https://doi.org/10.1007-978-3-662-47337-5 ↑6

[16] V. Raghavan, *Combustion technology: Essentials of flames and burners*. London, UK: John Wiley & Sons Ltd, 2016. ↑6, 16

[17] D. A. Bell, B. F. Towler, and M. Fan, *Coal gasification and its applications.* Oxford, UK: Elsevier, 2011. https://doi.org/10.1016/b978-0-8155-2049-8.10015-4 ↑9, 15

[18] Y. Cengel, *Transferencia de calor y masa: un enfoque práctico*, 3rd ed. México DF, Mexico: McGraw-Hill Interamericana, 2007. ↑12

[19] Servicio Geológico Colombiano, *El carbón colombiano. Recursos, reservas y calidad*, 2nd ed., vol. 32. Bogotá DC, Colombia: Libros del Servicio Geológico Colombiano, 2012. ↑14

[20] Y. Han *et al.*, "Different formation mechanisms of PAH during wood and coal combustion under different temperatures," *Atmos. Environ.*, vol. 222, art. 117084, 2020. https://doi.org/10.1016/j.atmosenv.2019.117084 ↑15

[21] T. G. Bridgeman, J. M. Jones, and A. Williams, "Overview of solid fuels, characteristics and origin," in *Handbook of Combustion*, Vol. 4: Solid Fuels, M. Lackner, F. Winter, and A. K. Agarwal, Eds. Weinheim, Germany: Wiley-VCH, 2010, ch. 1, pp. 1-30. https://doi.org/10.1002/9783527628148.hoc055 ↑15

[22] L. F. Velásquez Vallejo, J. F. D. L. C. Morales, J. F. Sánchez Morales, and M. A. Marín Laverde, "Remoción de carbón inquemado de las cenizas volantes producidas en el proceso de combustión de carbón," *Rev. Energ.*, vol. 38, pp. 107–112, Dec. 2007. ↑15

[23] J.-J. Weng, Z.-Y. Tian, Y.-X. Liu, Y. Pan, and Y.-N. Zhu, "Investigation on the co- combustion mechanism of coal and biomass on a fixed-bed reactor with advanced mass spectrometry," *Renew. Energy*, vol. 149, pp. 1068–1076, 2020. https://doi.org/10.1016/j.renene.2019.10.110 ↑15

[24] C. Chen, Q. Yang, R. Zhang, and D. Liu, "Assessment on combustion chemistry of coal volatiles for various pyrolysis temperatures," *J. Energy Inst.*, vol. 104, pp. 22–34, Oct. 2022. https://doi.org/10.1016/j.joei.2022.07.001 ↑15

[25] A. Abbas *et al.*, "Assessment of long-term energy and environmental impacts of the cleaner technologies for brick production," *Energy Rep.*, vol. 7, pp. 7157–7169, Nov. 2021. https://doi.org/10.1016/j.egyr.2021.10.072 ↑15

[26] J. G. Speight, *The chemistry and technology of coal*, 3rd ed. Abingdon, Oxfordshire, UK: Taylor & Francis Group, 2013. ↑

[27] S. V. Vassilev, C. G. Vassileva, and N. L. Petrova, "Thermal behaviour of biomass ashes in air and inert atmosphere with respect to their decarbonation," *Fuel*, vol. 314, art. 122766, Apr. 2022. https://doi.org/10.1016/J.FUEL.2021.122766 ↑15

[28] P. Kumar and B. K. Nandi, "Assessment of combustion characteristics of high ash Indian coal, petroleum coke and their blends for cement industry using TGA," *Cleaner Chem. Eng.*, vol. 5, art. 100091, 2023. https:/doi.org/10.1016/j.clce.2022.100091 ↑15

[29] H. Valdes, J. Vilches, G. Felmer, M. Hurtado, and J. Figueroa, "Artisan brick kilns: State-of-the-art and future trends," *Sustainabilty*, vol. 12, no. 18, art. 7724, 2020. https://doi.org/10.3390/su12187724 ↑15

[30] S. M. K. S. Rahman, "Assessment of brick kiln technologies of Bangladesh," MS thesis, Inst. Approp. Tech. (IAT), Bangladesh Univ. Eng. Tech. (BUET), Dhaka, Bangladesh, 2019. ↑16

[31] K. W. Ragland and K. M. Bryden, *Combustion engineering*, 2nd ed. Boca Raton, FL, USA: CRC Press, 2010. ↑16